ABSTRACT

Title of Document:	YEAST PSEUDO-HAPLOINSUFFICIENCY AS A MODEL SYSTEM FOR HUMAN RIBOSOMOPATHIES
	Ryan C. Kobylarz, Doctor of Philosophy, 2015
Directed By:	Dr. Jonathan D. Dinman, Department of Cell Biology and Molecular Genetics

Ribosomopathies belong to a class of human diseases caused by mutations in genes that encode ribosomal proteins, ribosomal biogenesis factors, ribosomal RNA (rRNA) or rRNA post-transcriptional modifying factors. Ribosomal Protein S19 (RPS19) is the gene linked to Diamond Blackfan Anemia, the first identified ribosomopathy. Paradoxically, patients suffering from this disorder initially present with insufficient blood cells but later exhibit a proclivity toward developing hyper-proliferative blood cell formation. The other two most common ribosomopathies include Isolated Congenital Asplenia (linked to mutations in the gene encoding for RPS0) and 5q- syndrome (a somatically acquired haploinsufficiency of RPS14). Despite originating in the ribosome, the unique phenotypes that are symptomatic of under-developed cells and the tissue specificity of ribosomopathies are not compatible with ribosomal biogenesis defect etiologies. The unique clinical

presentations of each of these diseases are consistent with the presence of “specialized” ribosomes, where each tissue type may require a certain subset of ribosomes. Recent studies into another ribosomopathy, X-linked dyskeratosis congenita (X-DC), revealed that defects in rRNA pseudouridylation patterns result in defects in translational fidelity. In order to study the translational effects of ribosomal protein haploinsufficient ribosomes, we used the *Saccharomyces cerevisiae* yeast as model for human ribosomopathies. Haploid yeast cells harbor two functional paralogs of RPS0, RPS14 and RPS19, in addition to other ribosomal proteins, due to an ancient whole genome duplication event. The yeast model enables the generation of single knockout of either the A or B paralogous ribosomal protein gene. Yeas also provides the ability to monitor gene specific differences in translational fidelity relative to isogenic wild-type cells. Ribosomal protein gene haploinsufficiency confers gene-specific translational fidelity defects. In assays that monitor recoding event frequencies, the most notable result was an increase in stop codon readthrough for all haploinsufficient strains. -1 or +1 Programmed Ribosomal Frameshift (PRF) recoding events were shown to exhibit isoform and sequence specific events, e.g. one isoform of RPS0 exhibits an increased -1 PRF recoding efficiency while the other demonstrates a decreased -1 PRF efficiency. Steady state mRNA abundance measurements reveals that RPS19 gene pseudo-haploinsufficiency confers a global decrease in mRNA abundance. In steady state mRNA abundance measurements of genes involved in telomere length

maintenance, RPS0 and RPS14 were shown to exhibit sequence specific effects, only presenting an increase in mRNA abundance for CDC13 while exhibiting a decrease for others. These idiosyncratic results challenge the prevailing notion of the “monolithic ribosome”. Here, we present a novel model whereby the transcriptome is translated and regulated by a heterogeneous population of ribosomes.

YEAST PSEUDO-HAPLOINSUFFICIENCY AS A MODEL SYSTEM FOR HUMAN RIBOSOMOPATHIES

By

Ryan C. Kobylarz

Dissertation submitted to the Faculty of the Graduate School of the
University of Maryland, College Park, in partial fulfillment
of the requirements for the degree of
Doctor of Philosophy
2015

Advisory Committee:
Professor Jonathan Dinman, Chair
Professor Douglas Julin
Professor Jason Kahn

Professor George Lorimer
Professor Eric Haag

Preface

The most exciting phrase to hear in science, the one that heralds new discoveries, is not 'Eureka!' but 'That's funny...'
-Isaac Asimov

Dedication

This is dedicated to my family and friends for their unconditional support and unwavering belief in me.

Acknowledgements

I would like to thank Dr. Jonathan Dinman for saying “yes” to me, the years of mentorship, support and reminding me that research laboratories are exciting places to work in. All members of the Dinman lab, past and present, have my gratitude for putting up with my questions and making this adventure an enjoyable experience. I want to especially thank my parents for instilling the belief that I can do anything I set my mind to and for supporting me as I chased my dreams.

Table of Contents

List of Abbreviations

aa-tRNA	Aminoacyl tRNA
ATP	Adenosine triphosphate
CP	Central protuberance
DBA	Diamond-Blackfan Anemia
DC	Decoding center
DNA	Deoxyribonucleic Acids
DXC	Dyskeratis Congenita
EF	Elongation factor
eEF	Eukaryotic elongation factor
eIF	Eukaryotic initiation factor
eRF	Eukaryotic release factor
GDP	Guanosine diphosphate
GTP	Guanosine triphosphate
HIV-1	Human immunodeficiency virus type 1
ICA	Isolated Congenital Asplenia
IF	Initiation factor
IL7	Interleukin 7 receptor
IRES	Internal ribosomal entry site
LSU	Large ribosomal subunit
mRNA	Messenger RNA
NGD	No-go decay
NMD	Nonsense mediated decay
NSD	Non-stop decay
ORF	Open reading frame
PABP	Poly-A binding protein
Pol	Polymerase
Poly A	Poly-adenosine
PRF	Programmed ribosomal frameshifting
PTC	Premature termination codon
RF	Release factor
RNA	Ribonucleic Acids
RP	Ribosomal protein
RRF	Ribosomal recycling factor
rRNA	Ribosomal RNA
snoRNAs	Small nucleolar RNAs
SSU	Small ribosomal subunit
tRNA	Transfer RNA

List of Tables

List of Figures

Chapter 1: Introduction

Central Dogma

The faithful conversion of genetic information into functional proteins responsible for sustaining life is an involved, complex, and multi-step process. Deoxyribonucleic acid (DNA) sequences are copied by ribonucleic acid (RNA) polymerases into complementary RNA sequences called messenger RNAs (mRNA). These mRNAs contain the genetic information that codes for proteins. Translation from mRNA into functional proteins is an essential process which is accomplished by the largest RNA-protein complex in the cell, the ribosome. Ribosomes, in concert with certain trans-acting factors, translate mRNA sequences from initiation to termination codons into proteins. Ribosomes are continuously engaged in translating mRNAs with high speed and accuracy, bridging the genetic information and functional protein worlds. While ribosomes are present in cells of all kingdoms, their assembly and structures vary among *Bacteria*, *Archaea,* and *Eukarya*. These differences effectively gave rise to the development and use of many antibiotics. However, with the emergence of increasingly antibiotic resistant *Bacteria* and the discovery of viruses that manipulate the host ribosome to translate the viral genome, it has become critical to improve our understanding of ribosome mechanisms. From an engineering perspective, the ribosome can be perceived as a model nanomachine. Despite the differences in ribosome structure, the ribosome is an evolutionarily conserved nanomachine with

homologous components that are preserved in many species. Studies of the inner workings of this nanomachine provide a platform for increasing our understanding of the roles and functions of each component in ribosomal assembly and function. Defects of the ribosome and canonical translation have broad implications in human health including birth defects, cancer, neurological diseases and blood disorders. Additionally, the combination of the rise of bioinformatics with the increasing computational power driving this field and the decreasing costs of genomic sequencing has revealed a new class of genetic diseases: ribosomopathies. Ribosomopathies are defined as a class of disease in which genetic abnormalities of either ribosomal protein or ribosomal RNA lead to impaired ribosomal function. By studying genetically-linked ribosomal diseases, we can obtain a deeper understanding of the chemistry, structure and mechanisms of ribosomes which may result in more effective treatments.

Ribosomal Anatomy

The ribosome is universally comprised of two subunits that are defined by their sedimentation coefficients, S: the large subunit (LSU, 50S in prokaryotes and 60S in eukaryotes) and the small subunit (SSU, 30S in prokaryotes and 40S in eukaryotes). The complete ribosome is defined as 70S in prokaryotes and 80S in eukaryotes. Each subunit has its distinct functions but both must coordinate together with the help of *trans*-acting factors to synthesize the proteins encoded within mRNA sequences. The secondary and tertiary structures that form the ribosomal core, which includes

the decoding center (DC) and the peptidyltransferase center, are conserved across all kingdoms of life. However, eukaryotic ribosomes are larger and more complex than their prokaryotic counterparts. Eukaryotic ribosomes possess additional rRNA segments, known as expansion segments (ES), and have a greater number of ribosomal proteins (79 compared to the 54 in prokaryotes). These increase the complexity of the ribosome and change the landscape of our understanding of how the ribosome works.

The yeast 80S ribosome has four ribosomal RNAs (rRNA) (LSU, 25S, 5.8S and 5S rRNA; SSU, 18S rRNA) and 79 ribosomal proteins (LSU, with 47 proteins; SSU, with 32 proteins). These rRNAs and RPs are essential for successful ribosomal functions (1, 2). The yeast *Saccharomyces cerevisiae* 80S ribosome crystal structure is shown in Figure 3. Each of the subunits contains an active region essential to the ribosome's function; the SSU contains the decoding center (DC) which is responsible for decoding the mRNA sequence and accepting the transfer RNA (tRNA) only after ensuring the complementarity of the codon sequence on the mRNA to the anti-codon of the tRNA molecule. The LSU contains the peptidyltransferase center, a catalytically active region in which the amino acid of the incoming aminoacyl-tRNA (aa-tRNA) is linked by a peptide bond to the elongating polypeptide chain. In addition, the LSU also contains the exit tunnel for the elongating polypeptide chain; three tRNA binding cavities; and the Sarcin-Ricin Loop (SRL) which is a rRNA region on the 25S that is responsible for interacting with either elongation (EF) or release factors (RF) during translation. All of

the aforementioned components are essential. When they coordinate with each other in addition to *trans*-acting factors, the ribosome is able to faithfully translate mRNAs with high speed and accuracy. This utilizes the kinetics and thermodynamics of these cofactors to ensure translational fidelity.

The ribosome is a RNA-based enzyme. Ribosomal RNA has over 100 base modifications, e.g. methylation and pseudo-uridylation (3). Ribosomal RNAs also utilize critical structural motifs. These include 20 of the 25 non-canonical base-pairing motifs (4), structural motifs including tetraloops, E-loops, U- and K- turns, purine stacks, coaxial stacking, ribose zippers, and A-minor motifs (5). Ribosomal proteins, for the most part, contain solvent-side globular regions and nonsolvent-side non-globular and flexible regions that interact with rRNA. Originally, it was believed that ribosomal proteins were essential to maintain the enzymatic functions of the ribosome, and the role of rRNA was limited to support and structural scaffolding roles. However, more detailed research revealed that all catalytic activity takes place in an RNA based environment. Many ribosomal proteins are essential and mutations can be lethal or have deleterious effects to health (6, 7).

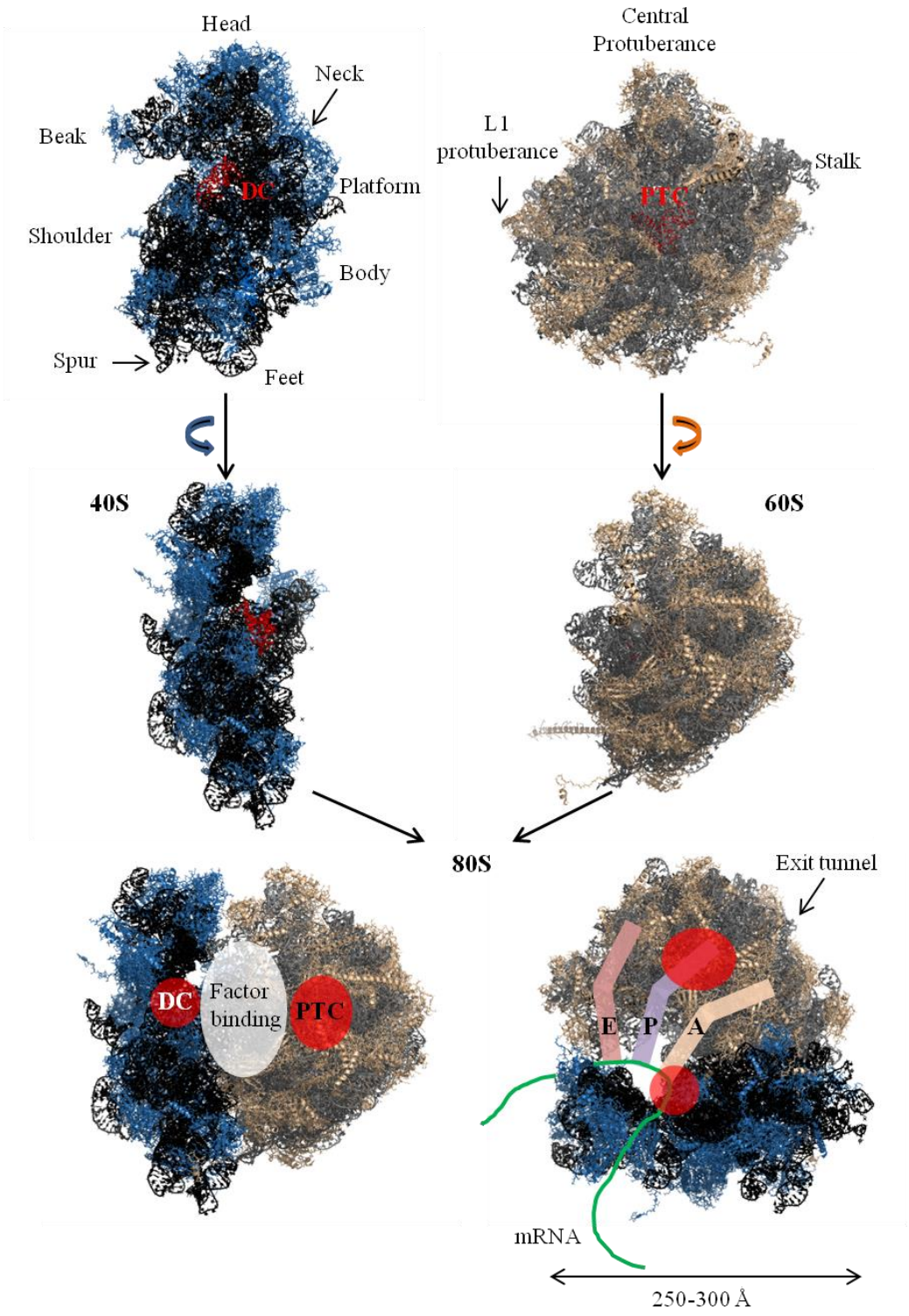

Figure 1. Yeast ribosome structure.
Both subunits are shown from the intersubunit face view (top), side view (middle) and in the 80S context (bottom). Images generated from 3Å crystallography structures using PyMOL (8, 9).

Efficient translation requires the active regions of structurally complex subunits to coordinate together. This is achieved via allosteric communication pathways through the 17 contact points between the LSU and the SSU, which are known as the intersubunit bridges (9). These intersubunit bridges are formed through RNA:RNA interactions, RNA:protein interactions, or a protein:protein interaction which known the B1b/c intersubunit bridge (9). The locations and points of contact of these intersubunit bridges are presented in Figure 4. The translating ribosome undergoes large structural and conformational changes. The nature of these intersubunit bridges are variable; some bridges remain intact, e.g. (B3), while others, e.g. (B7a) and (B1a – B1b/c) can break and form new connections between subunits.

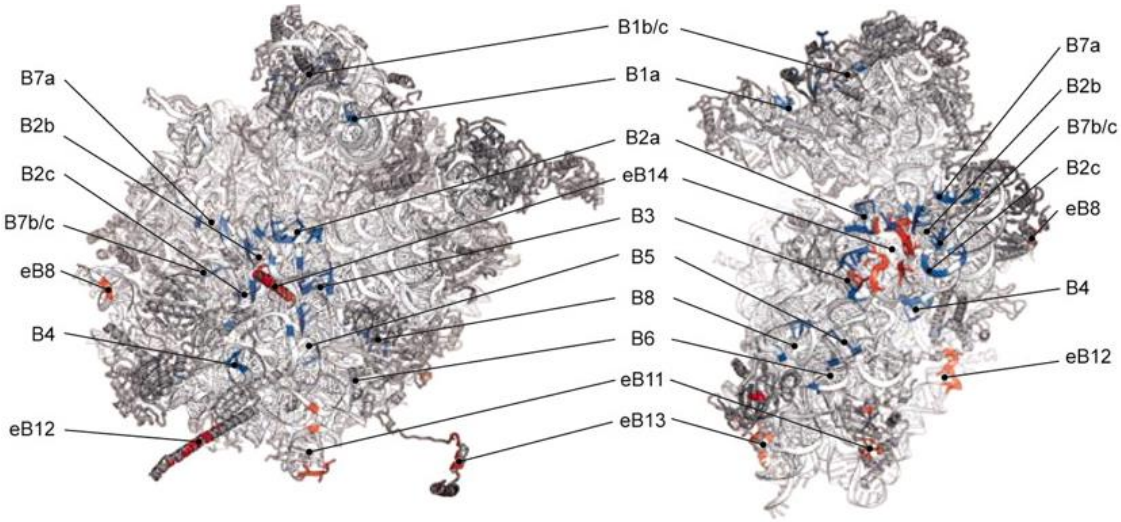

Figure 2. Location of ribosomal inter-subunit bridges.
Of the 17 inter-subunit bridges, B1b/c is the only protein:protein bridge, while all others are RNA:protein or RNA:RNA. Image from Ben-Shem (9).

These structural reconfigurations are essential for ushering transfer RNA (tRNA) through the translating ribosome. tRNAs are L shaped RNA molecules with 5 secondary and tertiary regions as shown in Figure 5. tRNAs harbor 4 loops: D-loop, T-loop, the anticodon loop with a variable “extra arm”, and an acceptor stem with one of the 20 amino acid attached at its 3’ CCA end. These structural elements enable the tRNA to interact with the mRNA in the SSU through the anticodon loop and the peptidyltransferase center in the LSU through 3’-CCA end of the acceptor stem. During translation, tRNA will travel through the ribosome and bind/interact with three distinct regions; the A-site, P-site and the E-site. Aminoacyl-tRNAs are tRNAs located in the “acceptor” A-site while peptidyl-tRNAs reside in the “peptidyl transfer” P-site and deaminoacylated tRNAs leave the ribosome through the “exit” E-site during peptide bond formation.

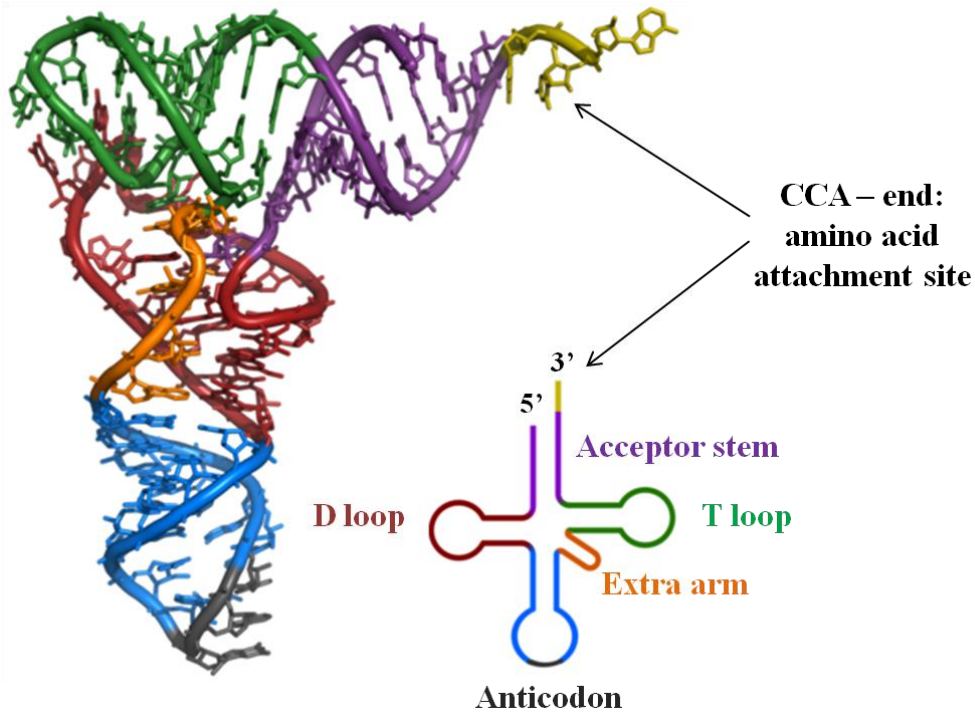

Figure 3. tRNA structure.
Non base-paired regions form the 4 shown loops. The anticodon interacts with the decoding center in the SSU, while the acceptor stem is covalently linked to the appropriate amino acid and interacts with the peptidyltransferase center in the LSU. Image modified from Griffiths-Jones (10).

Ribosome Biogenesis Overview

A single S*accharomyces cerevisiae* yeast cell can contain up to 200,000 ribosomes distributed throughout the cytoplasm and on the rough endoplasmic reticulum (11). To meet the needs of an actively growing cell, up to 2000 ribosomes can be assembled per minute (12). In order to ensure production of viable and fully functional ribosomes, the biogenesis of healthy ribosomes must follow a stringent and sequential assembly mechanism that incorporates multiple quality checkpoints. Impairment or defects in ribosomal assembly may lead to defective ribosomes, which can result in pathological conditions that are generally classified as ribosomopathies (see Ribosomopathies: An Overview of Ribosomal Dysfunction).

Most of our knowledge of the eukaryotic ribosome biogenesis pathway comes from the extensive studies of the yeast *Saccharomyces cerevisiae*. Yeast ribosomal biogenesis involves ~200 essential accessory proteins and *trans*-acting factors (13, 14). The process begins in the nucleolus, a specialized compartment within the nucleus (15, 16) where a 35S precursor ribosomal RNA (rRNA) is transcribed by RNA polymerase I. The 35S precursor rRNA is subjected to a series of exonucleolytic and endonucleolytic cleavages and base modifications, such as pseudo-uridylation and methylation (17), resulting in mature 5.8S, 18S and 25S rRNAs. The 5S rRNA is transcribed by RNA polymerase III in the nucleus, undergoes maturation in the cytoplasm and is transported to the nucleolus in complex with L5 and L11 (18). RNA polymerase II is responsible for transcribing the 79 ribosomal

protein mRNAs in the nucleus. The RP mRNAs transported to the cytoplasm for translation into mature RPs and then transported into the nucleus or the nucleolus for incorporation into the ribosome (12). In the nucleolus, the ribosomal proteins are processed and assembled with rRNA, in a stoichiometric manner that promotes equimolar assembly into ribosomes (19), to form the 43S and 66S preribosomal particles. They are then transported into the cytoplasm by non-ribosomal *trans*-acting factors that prevent any premature ribosomal subunit interactions. In the cytoplasm, after the final processing and maturation steps of ribosomal biogenesis (12), the fully matured and assembled subunits are able to interact and form a translationally-capable 80S ribosome.

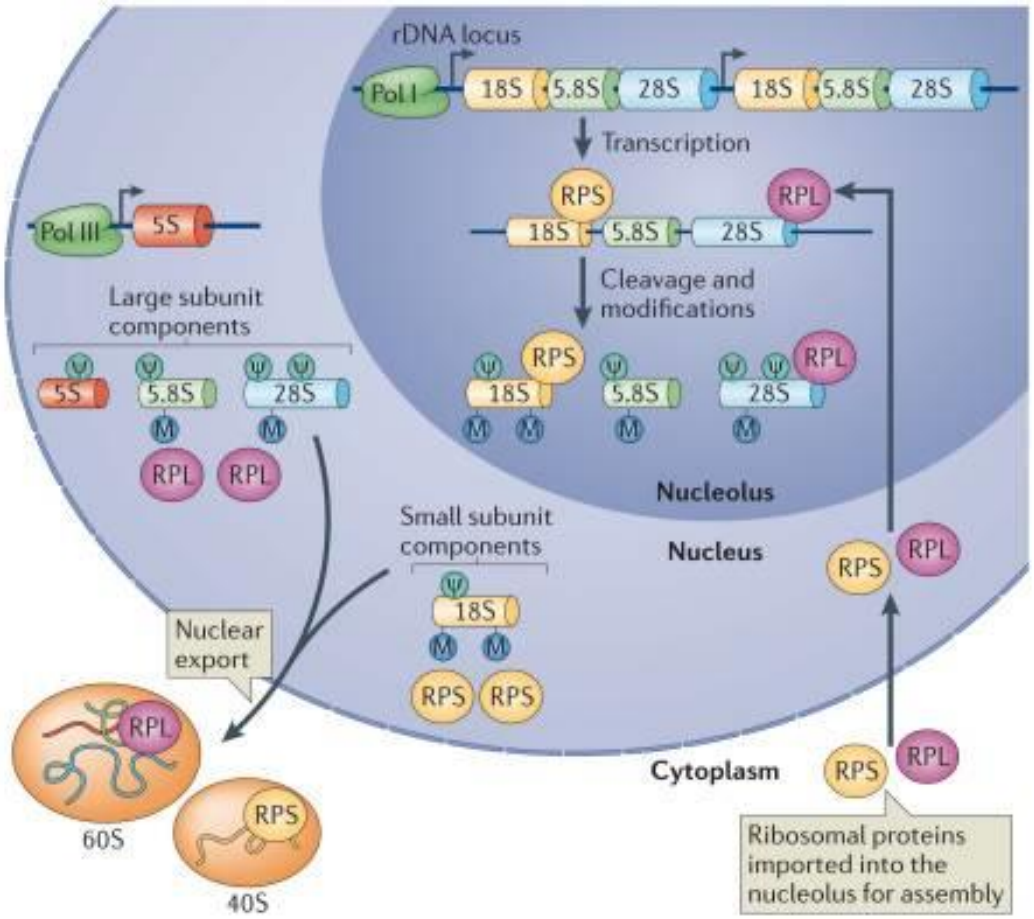

Figure 4. General Model of the Ribosomal Biogenesis Pathway
Pathway for the maturation of preribosomes to form 40S and 60S ribosomal subunits. Sequential assembly intermediates are shown, distinguished by the pre-rRNA processing intermediates contained within them. Image is from Xue and Barna (20).

Ribosome Function

Translation

Life requires rapid and accurate protein synthesis. The ribosome is capable of meeting the following criteria: it synthesizes new polypeptides, increasing the polypeptide length by one amino acid in approximately 60 ms with an error rate of 1 in every 10^3 – 10^4 codon reads (21). In addition to the efficiency of a single ribosome, a single mRNA can contain several translating ribosomes, called polysomes. The translation process is divided into 4 phases: initiation, elongation, termination and ribosome recycling; each phase is assisted by *trans*-acting factors. The initiation phase begins by assembling the 80S ribosome onto an mRNA strand at the appropriate start codon (AUG). Initiation is followed by the elongation phase, which is comprised of multiple elongation cycle. Each elongation cycle adds a new amino acid that corresponds to the codon on the mRNA to the nascent polypeptide. Between each elongation cycle, the ribosome will translocate along the mRNA in a 3' – 5' direction. The elongation phase ends when the ribosome encounters a stop codon (UAA, UAG, or UGA). This triggers the termination phase and releases the fully formed polypeptide chain with the assistance of release factors. After termination, the ribosome can either reinitiate at the start of the mRNA for another round of translation or dissociate to be used to translate another mRNA.

Initiation

Translational initiation is a multi-step process that involves several *trans*-acting eukaryotic initiation factors (eIF). This process imposes a significant rate-limiting step in translation. (22). First, a mature small ribosomal 40S subunit (SSU) is recruited to the mRNA. Once the intermediary complex is localized at the appropriate start codon, the complex will then recruit a mature large ribosomal 60S subunit (LSU) to form a translationally-capable 80S ribosome. The initiation process in eukaryotic ribosomes is shown in Figure 7 below.

Initiation begins with the assembly of 40S SSU, eIF1A and eIF3 to form a complex that will prevent any premature binding of the 60S LSU (23). The binding of eIF3 and eIF5 to the previously mentioned complex is required to recruit the eIF2:GTP:Met-tRNA^{iMet} ternary complex to form what is known as the 43S pre-initiation complex (24). However, before the 43S pre-initiation complex can bind to the mRNA, the mRNA must undergo an independent process that primes the message for initiation. The mRNA interacts with several factors, the poly adenosine binding protein (PABP) that interacts with both the 3' end poly-adenosine (polyA) tail of the message and the eIF4F complex. The eIF4F complex interacts with the 5' end 7-methylguanosine (m^7G) cap. The eIF4F complex is composed of eIF4A, eIF4B, eIF4E, and eIF4G. This complex binds to the m^7G cap via interactions with eIF4E. The eIF4G factor is a scaffolding factor within the eIF4 complex that interacts with the PABP that is attached to the 3' poly-A tail of the mRNA. This results in the

linkage of the two ends of the message, ie. circularizing the mRNA (25). This closed loop provides an additional translational expression control mechanism via any translational regulation feature contained within the untranslated regions (UTRs) of the mRNA.

The closed mRNA loop is now capable of interacting with the 43S pre-initiation complex. The initiation factors eIF1 and eIF1A which are bound to the 43S pre-initiation complex, will linearize the closed mRNA loop. The eIF4G which is bound to the 5' end m^7G cap of the open mRNA, facilitates binding to the eIF3 resulting in the formation of the 48S pre-initiation complex. Upon binding, the initiation factors eIF1 and eIF1A, in an ATP dependent manner, powers the 48S pre-initiation complex to begin scanning the mRNA for the AUG start codon in a 5' to 3' direction (26). The cognate binding of the anticodon of Met-tRNA^{iMet} to the AUG start codon triggers GTP hydrolysis by eIF2 and eIF5. This concurrently dissociates eIF2:GDP and subsequently dissociates all remaining initiation factors except eIF1A. This allows eIF5B:GTP to recruit the 60S LSUto the SSU to form a mature 80S ribosome with the stable Met-tRNAi^{Met} occupying the P-site bound to the AUG of the mRNA (27–29). The dissociated eIF2:GDP is then recycled by the guanine exchange factor (GEF) eIF2B into eIF2:GTP, reassembling the ternary complex for the next round of initiation.

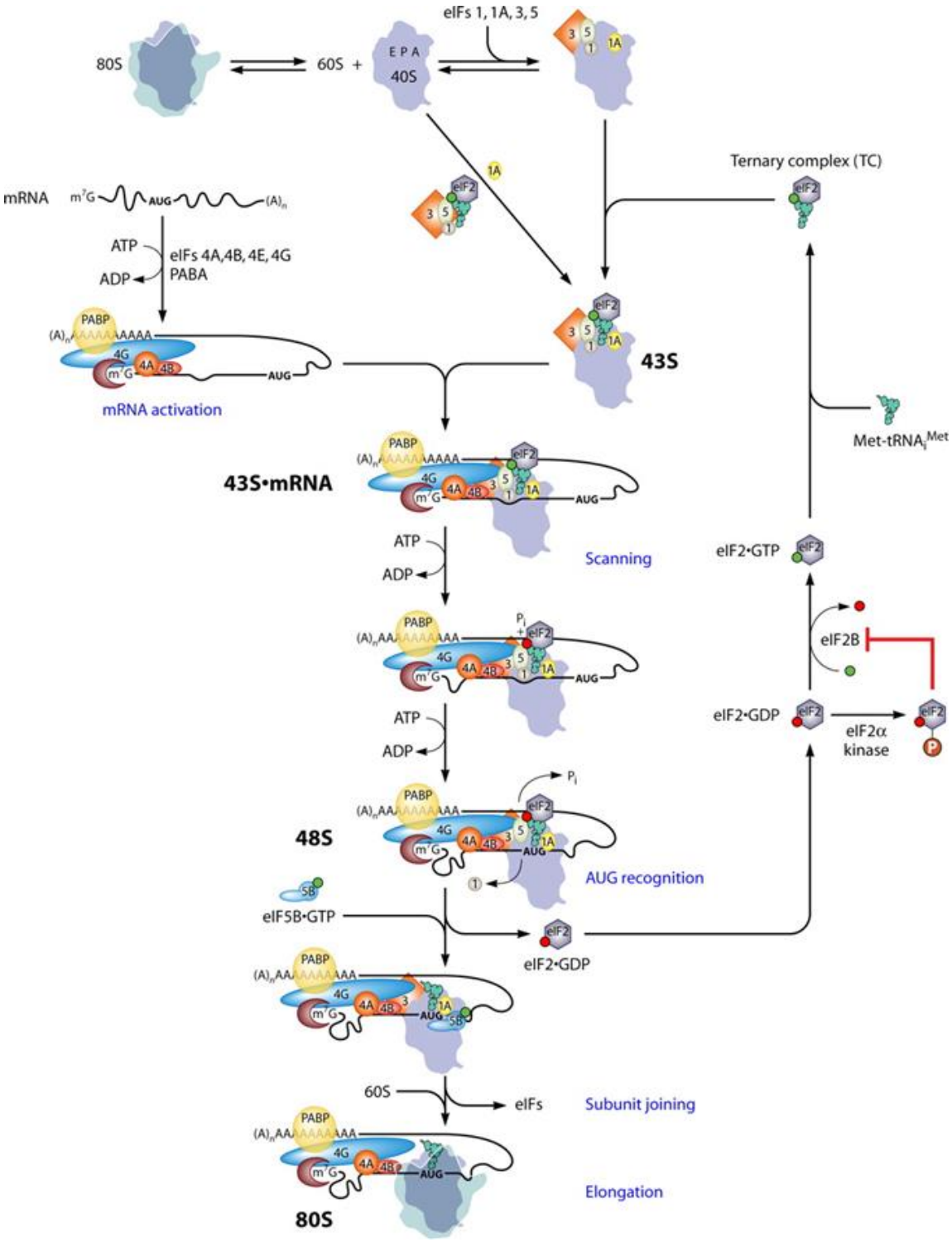

Figure 5. Summary of the Eukaryotic Initiation.
Known steps and factors are indicated. The GEF eIF2B is inhibited by the phosphorylation of eIF2 of its α subunit by various kinases, activated by different kinds of stress. Image from Hinnenbusch (30).

The 5'- m^7G cap and the 3' poly-A tail were thought to be essential structural components to successfully initiate translation. This is not the case as studies have detected the translation of cap-free viral mRNAs. Viruses have evolved cap-independent initiation mechanisms in order to become translationally competent. Some viruses have evolved mechanisms that "steal" the m^7G cap (flu viruses via cap-snatching endonucleases (31)), or m^7G cap mimics, eg. picornaviruses with VPg protein attached to the 5' end of the mRNA (32, 33). Internal Ribosomal Entry Sites (IRES) represent another method viruses employ to initiate translation that enables the viral mRNA to become translationally competent without the 5' m^7G cap(34, 35). IRES-containing mRNA possess stable secondary structures located in their 5'-UTR region which in some cases mimic the structure of tRNAs. These mimicked structures can interact with eIFs which makes them capable of recruiting ribosomes and initiating translation internally. IRES elements are structurally variable and these elements enable viruses to bypass the rate-limiting step of initiation which serves as a translational regulatory step. Recently, IRES elements have been discovered and characterized in eukaryotes (36–38). Cap dependent translation is compromised when the cell is under stress conditions. In a response to the stress condition, the ribosome will encourage a shift in translational initiation toward IRES-mediated cap independent translation (39).

Elongation

Elongation is an iterative process that begins once the 80S ribosome is stabilized after initiation. During elongation, the ribosome will read the mRNA in the 5’ to 3’ direction, one codon at a time. With each codon, the ribosome must simultaneously and rapidly decode the codon, screen for and select the cognate tRNA, and undergo peptidyltransfer. This transfers amino acid of the incoming tRNA onto the growing nascent polypeptide chain. The ribosome will continue to elongate until it encounters a stop codon. Ribosomes must rely on aa-tRNAs and elongation factors (EFs) to supply the ribosome with the appropriate amino acid for each codon read per elongation cycle. An elongation cycle has 4 major stages: aa-tRNA selection, accommodation, peptidyl transfer and translocation.

Amino-acyl tRNA selection

At the beginning of every elongation cycle, charged tRNAs must be brought to the elongating ribosome. These amino-acyl tRNAs (aa-tRNA) are bound with eEF1A and GTP, a complex known as the Ternary Complex (TC), and are delivered to the A-site of the ribosome. The interaction between the anticodon on the aa-tRNA of the TC and the mRNA codon, shown in Figure 8, determines whether the aa-tRNA is accepted (accommodation) or rejected (40–42). This process has several distinct steps. During the initial binding, the ternary complex forms an internal unstable interaction between the anticodon loop of aa-tRNA in the A-site of the decoding center. The rest of the tRNA is in a distorted conformation and positioned outside of the A-site of the LSU.

This adopted but distorted conformation is conserved between cognate and near-cognate tRNAs which enables the second step. The next step is the codon recognition step, which regulates and stabilizes cognate and near cognate TCs according to their codon-anticodon Watson-Crick base-pairing efficiencies. Non-cognate TCs are efficiently and quickly rejected at this step, the first of two proofreading steps.

After tRNA selection, the SSU 18S rRNA flips three bases (A1755, A1756, and G577) from a *syn* to *anti* conformation, stabilizing the aa-tRNA (43, 44). This stabilization induces conformational changes promoting the GTPase activity of eEF1A (45–47). The conversion from GTP to GDP causes eEF1A to undergo a conformational change, decreasing the TC's affinity to the aa-tRNA. This triggers a dissociation of aa-tRNA from eEF1A:GDP complex and allows the accommodation of the entire aa-tRNA into the A-site of the ribosome.

The conserved torsional distortion of the aa-tRNAs and codon and anti-codon Watson-Crick base-pairing efficiencies differences are insufficient for distinguishing between cognate and near-cognate ternary complexes. This is evident in the kinetic schematic in Figure 8 which shows that the difference in the reverse rate of codon recognition (k_{-2}) and the forward rate of activation of GTPase (k_3) is not large enough. However, due to decreased eEF1A activation and GTP hydrolysis rates, near-cognate aa-tRNAs dissociate at a much faster rate during the initial codon recognition step relative to those cognate aa-tRNAs, promoting translational fidelity (48–51). This allows

discrimination between cognate and near-cognate tRNAs in the second stage of accommodation, known as “proofreading”.

The process of the second stage is not fully understood. However, recent evidence suggests that the stabilization of the anticodon stem loop (ASL) by rRNA in both subunits is due to the recognition of the geometry of canonical Watson-Crick base-pairing of the codon-anticodon helix in the DC (51). This stabilization creates a relative fixed orientation of the anticodon stem loop as it traverses through the accommodation corridor through a cascade of structural rearrangements of the LSU rRNA and ribosomal proteins. This induced fit mechanism promotes the binding of cognate tRNAs to their corresponding codons on the mRNA enabling successful movement through the accommodation corridor. Near-cognate tRNAs lack this stabilization required to traverse the accommodation corridor, resulting in the dissociation of the near-cognate tRNA from the ribosome (52). Kinetic studies show that cognate tRNAs have quicker A-site accommodation and peptidyl transfer rates than near-cognate tRNAs. These studies support the induced fit mechanism model (53). This presents the second proofreading step as a “kinetic filter”. The two proofreading strategies ensure the accommodation of correct aa-tRNAs to ribosomes through increased binding stability and increased efficiency during A-site accommodation and GTP hydrolysis than their near and non-cognate counterparts.

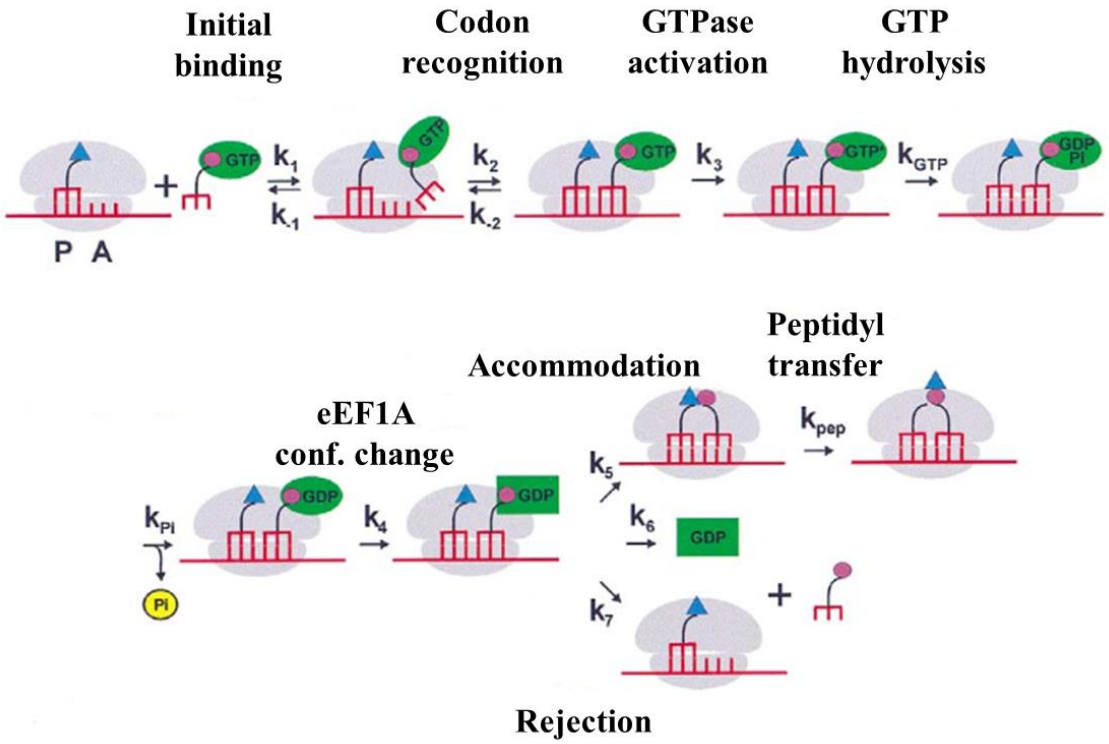

Figure 6. Scheme of tRNA selection at the ribosomal A-site

The initial binding step in tRNA selection, governed by the rate constants k_1 and k_{-1}, is a codon-independent reaction between the ternary complex and the ribosome, while the following codon-recognition step is codon dependent. The active site of the elongation factor undergoes a conformational change during GTPase activation. This step is pivotal for establishing the irreversible step essential to proofreading and appears to limit the rate of GTP hydrolysis. During the proofreading stage after factor dissociation the tRNA either moves into the A-site (accommodation) for peptidyltransfer or dissociates from the ribosome (rejection). Accommodation is regulated by the rate constant k_5 and depends on codon-anticodon interactions (48).

Peptidyl Transfer

Peptidyl transfer occurs after accommodation. It occurs in the peptidyltransferase center of the LSU which is solely responsible for peptide bond synthesis. The peptidyltransferase center is the catalytic core of the ribosome and is comprised entirely of rRNA. The nearest ribosomal protein is 13 angstroms away (9). Upon accommodation, the aa-tRNA is stabilized within the ribosome, with the 3'-CCA end in the peptidyltransferase center of the A-site of the LSU and the anticodon loop in the DC of the A-site of the SSU, as shown in Figure 9. Once properly positioned, the 3'-CCA end of the aa-tRNA is stabilized by the 25S rRNA into the peptidyltransferase center. The peptidyl transfer reaction between the α-amino group of the aa-tRNA and the ester linkage of the peptidyl-tRNA is then catalyzed. During the peptidyl transfer, the α-amino group of the A-site aa-tRNA carries out a nucleophilic attack on the carbonyl carbon of the ester bond that links the peptide chain to the P-site peptidyl-tRNA (54). This results in the deacylation of the P-site peptidyl-tRNA and transfers the nascent peptide to the A-site aa-tRNA. The peptidyl transfer reaction occurs nearly instantaneously; less than 50 ms (46). This speed is due the ability of amines intrinsically linking esters to form peptide bonds at rates of $\sim 10^{-4}$ M^{-1} s^{-1} at room temperature in addition to the ribosome being able to enhance this reaction by $\sim 10^{6}$ -to 10^{7} fold (55).

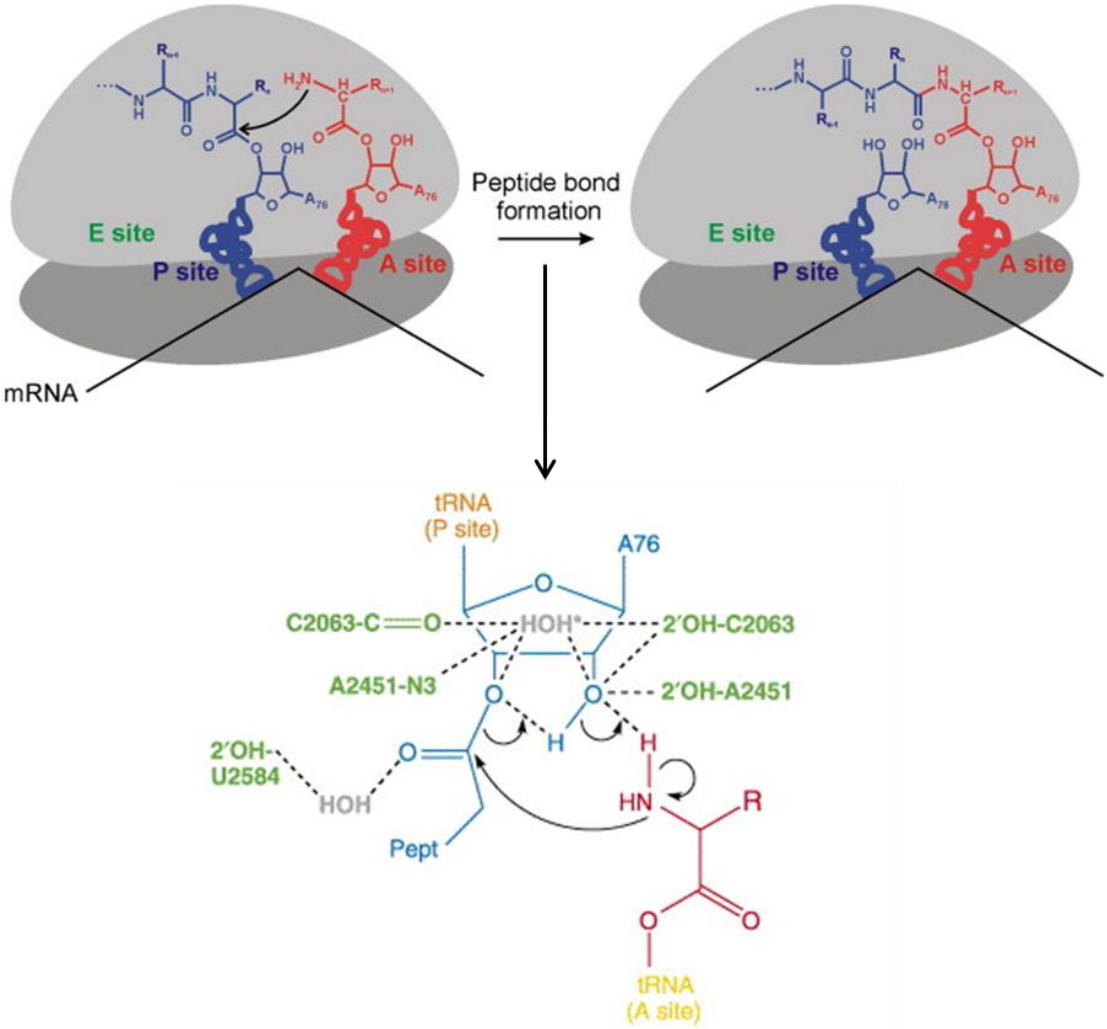

Figure 7 Mechanism of peptidyltransfer.
The α-amino group of the aminoacyl tRNA in the A site attacks the carbonyl carbon of the peptidyl-tRNA in the P site. The universally conserved bases in green, among others, promote electrostatic shielding and a concerted proton-shuttle mechanism resulting in stabilization of a six-membered transition state and facilitating catalysis. Figure modified from Rodnina (56, 57).

Translocation

After peptidyl transfer, the ribosome must translocate in order to prime for the next elongation cycle. During the translocation process, the A-site is vacated to prepare for the next ternary complex and the ribosome moves downstream the mRNA strand to the next codon. In order to vacate the A-site, the bound aa-tRNA and deacylated tRNA ligands in the A- and P-sites must be shifted into the P- and E-sites, respectively. This shift from one site to another is driven by the GTP hydrolysis of the eEF2:GTP complex. The tRNAs that undergo translocation will adopt specific ligand repositioning conformations which are known as classical and hybrid states as shown in Figure 10. The aa-tRNA and deacylated tRNA are in the classical A/A and P/P states (nomenclature refers to the tRNA position in the SSU/LSU) which shifts into the hybrid A/P and P/E states (58–60). This hybrid configuration is only possible after the deacylation of the peptidyl tRNA, likely due to the anchoring effect of the attachment of the peptidyl tRNA to the polypeptide chain in the exit tunnel (61). The repositioning of tRNA from the classical into the hybrid state requires movements of tRNAs. Unlike the P-site tRNA which has large movements of the D-loop, T-loop, and the CCA end; the A-site tRNA only has its CCA end repositioned into the P-site of the LSU (62). The ternary complex mimic, eEF2, binds to both subunits and through GTP hydrolysis, drives translocation. After translocation, the ribosome returns to the classical state and in the process, simultaneously shifts one codon

downstream and transfers the tRNAs bound to the SSU A- and P- sites to their P- and E-sites (63, 64).

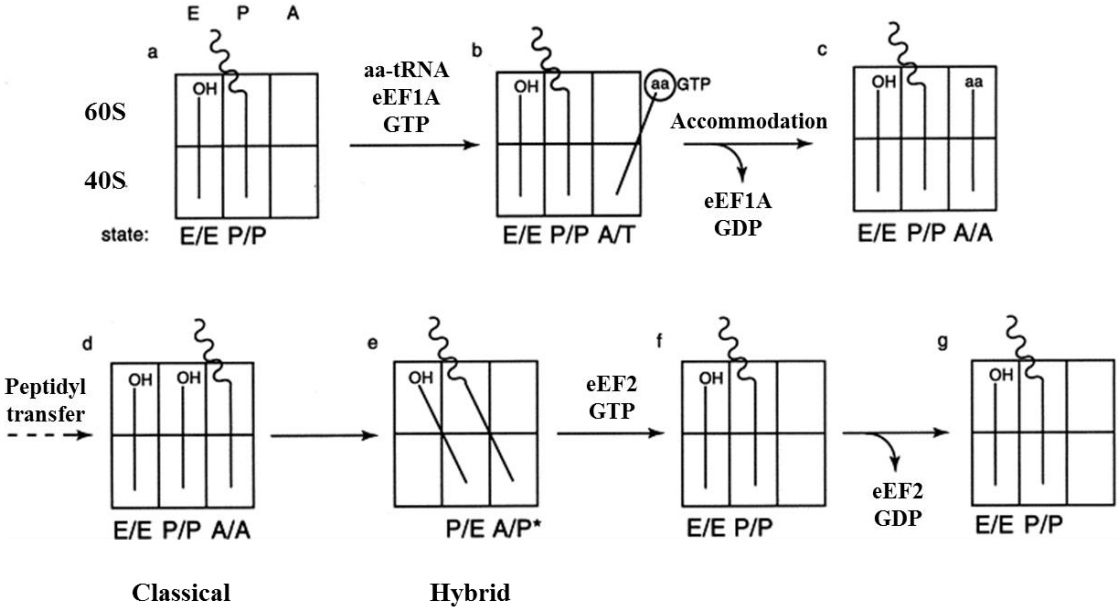

Figure 8. Positions of tRNAs transitioning between the classical and hybrid states during translation.
The relative position of tRNAs during classical, hybrid, and pre-accommodation states. Figure modified from Noller (65).

The transition between the classical and hybrid states is only accomplished through a dynamic structural rearrangement of the ribosome. This dynamic movement, once referred as “ratcheting”, is now considered a “rotation” due to the 6º rotation of the SSU in a counterclockwise direction relative to the LSU as shown in Figure 11 (66–69). The ribosomal conformation due to rotation determines the state of the ribosome, i.e. unrotated ribosomes exist in the classical state while rotated ribosomes exist in the hybrid state.

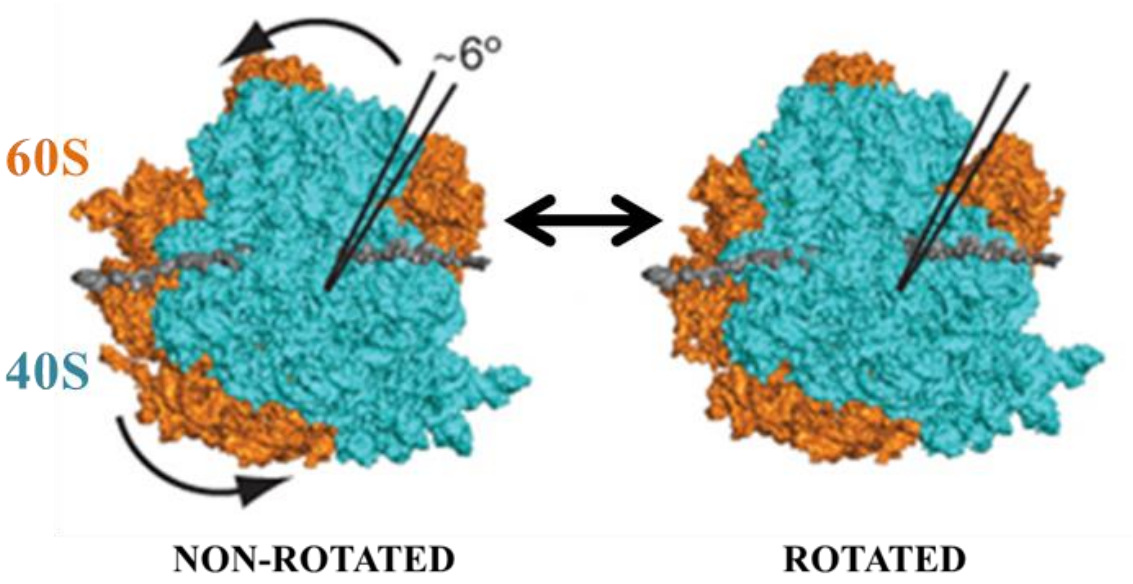

Figure 9. Ribosomal intersubunit rotation.
Subtle rotation of the SSU relative to the LSU during translation. Image modified from Schmeing (44).

Termination

When the DC of the elongating ribosome encounters one of the three stop codons (UAA, UAG, UGA) signifying the end of the ORF of the gene, it then enters the termination stage. These codons are also known as nonsense codons and do not have a correlating cognate tRNA (70). Instead, these codons are recognized and bind to eukaryotic release factors (eRFs) when the A-site of the ribosome is positioned in-frame to one of the stop codons and triggers a hydrolysis reaction which results in the release of the polypeptide chain from the tRNA in P-site of the ribosome. In eukaryotes, an omnipotent class I eRF (eRF1) can recognize all three stop codons and will bind to the stop codon in the A-site. Prior to binding to the ribosome, eRF1 will form a complex with class II RF (eRF3) and GTP (71–74). This eRF1:eRF3:GTP complex is a molecular mimic of the aa-tRNA Ternary Complex as shown in Figure 12. The structural mimicry also suggests that the two complexes employ similar mechanisms to bind to the ribosome (67). Binding of these RFs induces similar conformational changes of the ribosome as those during peptidyl transfer in the elongation stage. The only difference between the two stages is that during elongation, the ribosomal peptidyltransferase center is constructed in a conformation that precludes the presence of water in the peptidyltransferase center. This serves to reduce the possibility of premature polypeptide hydrolysis. The second difference occurs during termination, in which the GQQ motif of the eRF1 will induce structural rearrangements that enables appropriate hydrolysis and release the peptide (59, 60, 75) .

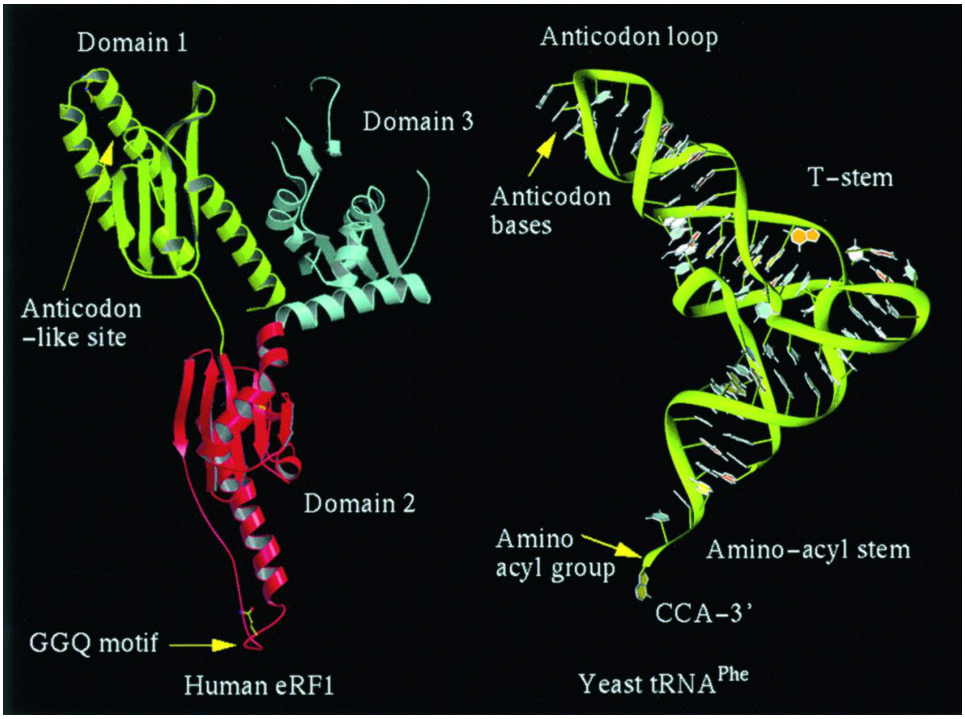

Figure 10. Molecular Mimicry of tRNA: structures of yeast eRF1 and tRNA^{Phe}. Eukaryotic release factors are biological mimics of tRNAs, structurally and functionally. Image from (69).

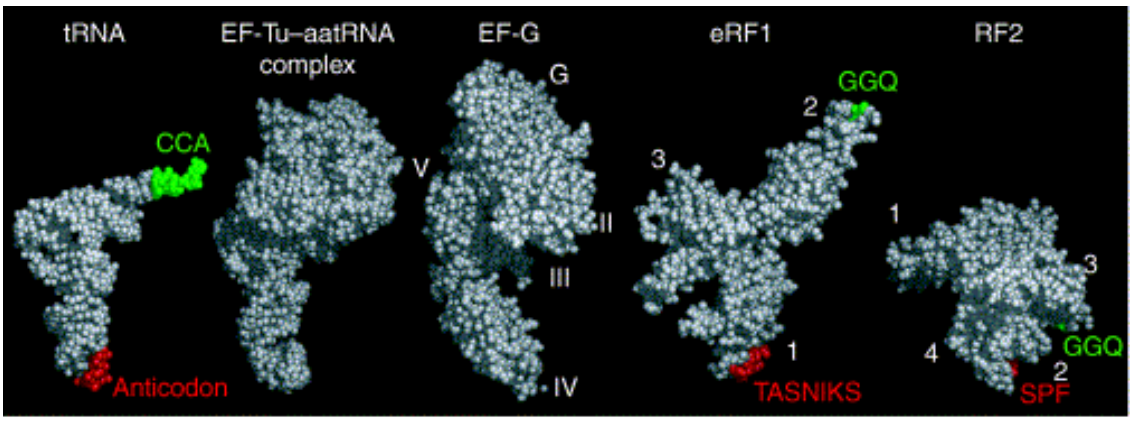

Figure 11. Crystal Structures of translational factors that mimic tRNA
Several examples of how ribosomal factors are biological mimics of each other, suggests that translation is a kinetic partitioning process where side reactions can compete during altered kinetic rates in any of the steps of translation. Image from (76).

As peptide release occurs, the ribosome is still bound to the mRNA with an deacylated tRNA and eRF in the P- and A-sites, respectively. Recent studies suggest that ABCE1 (an ATPase) promotes ribosomal subunits release and ribosomal recycling (77).

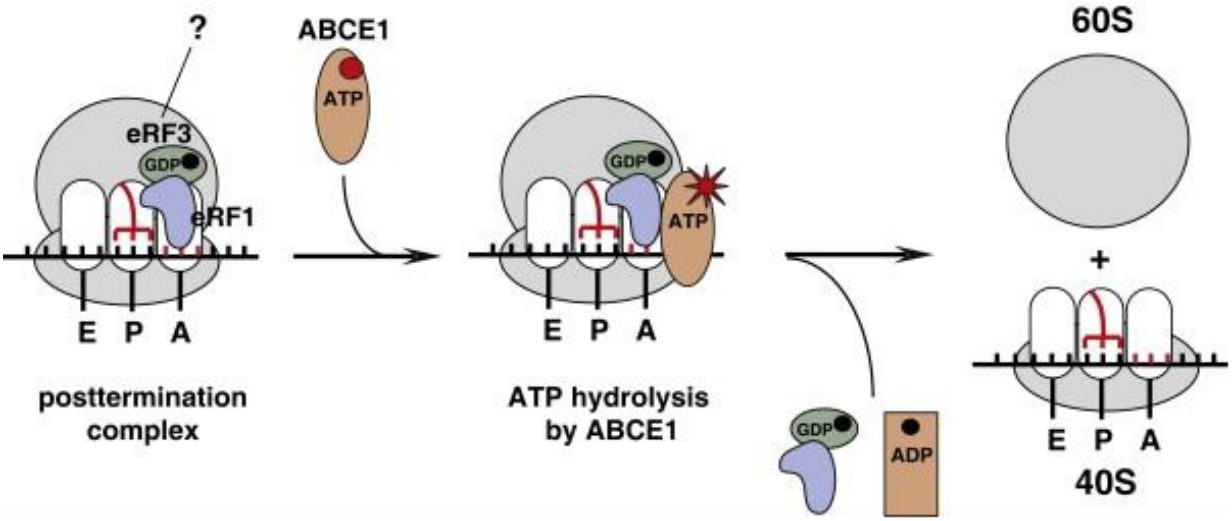

Figure 12. Model of the eukaryotic translation termination
Recognition of the stop codon recruits the eRF1:eRF3:GTP complex to the ribosomal A-site. eRF3 is a G-protein. This is followed by the binding of ABCE-ATP to the release factor complex. Subsequent GTP and ATP hydrolysis results in release of the ribosomal subunits from the mRNA and the consequent recycling (77).

Translational Recoding

Canonical protein synthesis begins at the AUG start codon and continues in-frame through the open reading frame (ORF) one codon at a time until terminating at a stop codon which results in a single protein product. The ribosome can also take other non-canonical translational pathways which are generally known as “translational recoding events”. These result in alternative protein products due to the alteration of the open reading frame post initiation or suppression of termination codons. While changes in translational reading frame maintenance and termination codon redefinition are intrinsically rare, occurring at a rate of 10^{-4} to 10^{-6} (78) recoding events occur at 10 – 100 fold greater frequencies through stimulation by mRNA *cis*-acting elements. Historically, such recoding events were first identified in viruses which have a demonstrated need for increased information content in a condensed genetic space. However, these recoding events have been identified in prokaryote and eukaryotic organisms (79). These discoveries demonstrate a need for greater understanding of the translational machinery which will lead to insights into how defective ribosomes differ from healthy ribosomes in maintaining translational fidelity.

Programmed -1 Frameshifting

Programmed -1 Ribosomal Frameshifting (-1 PRF) is a non-random recoding event that induces the elongating ribosome to shift “backwards” (in the 3’ direction) by one nucleotide on an mRNA, directing the ribosome to a new open reading frame (ORF). The elongating ribosome continues in this ORF to generate an alternate protein product. This type of recoding event allows the synthesis of multiple protein products from a single message; a genomic condensation strategy that is employed by viruses that have a need to maximize their genomic informational content because their genomic sizes are limited by the volumes of their nucleocapsids. The first -1 PRF recoding event was discovered in the Rous Sarcoma Virus (RSV), a retrovirus (80). Subsequently, -1 PRF signals have been identified in other retroviruses, alphaviruses (81), astroviruses (82), coronaviruses (83, 84), luteoviruses and totiviruses, (reviewed in database(85)). The large number of viruses employing -1 PRF has allowed elucidation of the parameters and rules governing this recoding event.

A -1 PRF signal requires three important mRNA elements: a heptameric slippery site, a spacer region of 0 to 12 nucleotides, and a downstream stimulatory mRNA tertiary structure, e.g. a pseudoknot or a stem loop (86–90). Figure 15 shows a model of the mechanism of the -1 PRF recoding event. The heptameric slippery sequence follows the 5’-XXXYYYZ-3’ format where X can be any three identical bases, Y is any three identical weak base and Z can be any base except guanine (91). The frameshift

stimulating structure is thought to cause the ribosome to stall upon encounter. If the ribosome stalls when positioned at the slippery site, a where the P- and A-site tRNAs are matched in the 0-frame with the XXY and YYZ codons respectively (92). This positioning increases “slippage” due to the sequence enabling re-positioning/re-pairing of the non-wobble base pairs of the aa-tRNA and peptidyl-tRNAs with the -1 frame codons. The frequency of “slippage” is primarily determined by the number of A/U nucleotides within the heptameric slip site. A/U nucleotides form weaker Watson-Crick base-pairs strength relative to G/C nucleotides. If there are more A/U nucleotides than G/C nucleotides in the slip site, the ribosome will slip more frequently. The slippery site alone does not confer biologically relevant -1PRF recoding, only occurring at a rate of approximately 0.1 – 0.2% in mammals (93, 94). However, the combination of the slippery site and the downstream tertiary structure (e.g. a pseudoknot) increases -1 PRF recoding rates to biologically significant rates due to the stalling of the ribosome as it attempts to resolve the obstructing structure upon encounter (95). Concurrently, the energetic barrier of the pseudoknot can be overcome and as the ribosome shifts in the -1 ORF, the tertiary structure is resolved and the ribosome resumes elongating in the new -1 reading frame. RNA structural elements that attenuate frameshifting/recoding events are also known (96). The molecular mechanism of -1 PRF is not just one particular mechanism. While several competing models attempted to pinpoint the exact time and mechanism for the shift out of frame, it has become clear that -1 PRF is merely an endpoint that can be

achieved through several different kinetic pathways. This is known as the "many pathways model" (97).

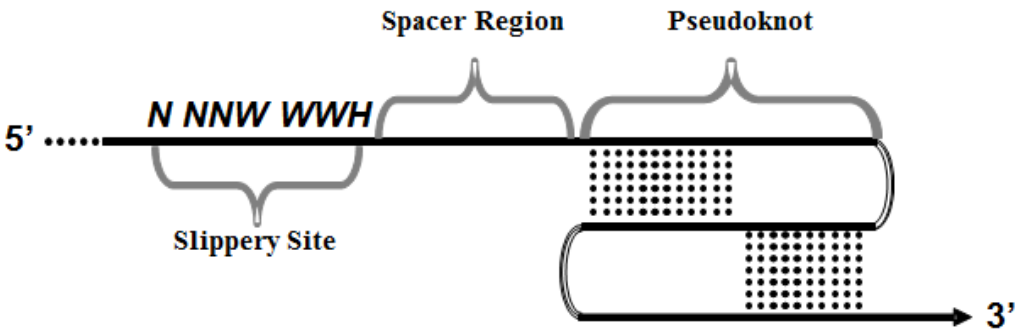

Figure 13. Structure of a -1 PRF signal on an mRNA.
The slippery site, where the A- and P-site tRNAs are positioned and the shift in frame occurs, is denoted by IUPAC notation (*N* = any 3 identical nucleotides, *W*=AAA or UUU, and *N*≠G). 22 functional slippery sites are known. While a pseudoknot is the most common type of stimulatory element, other mRNA structures are capable of filling that role as well (91).

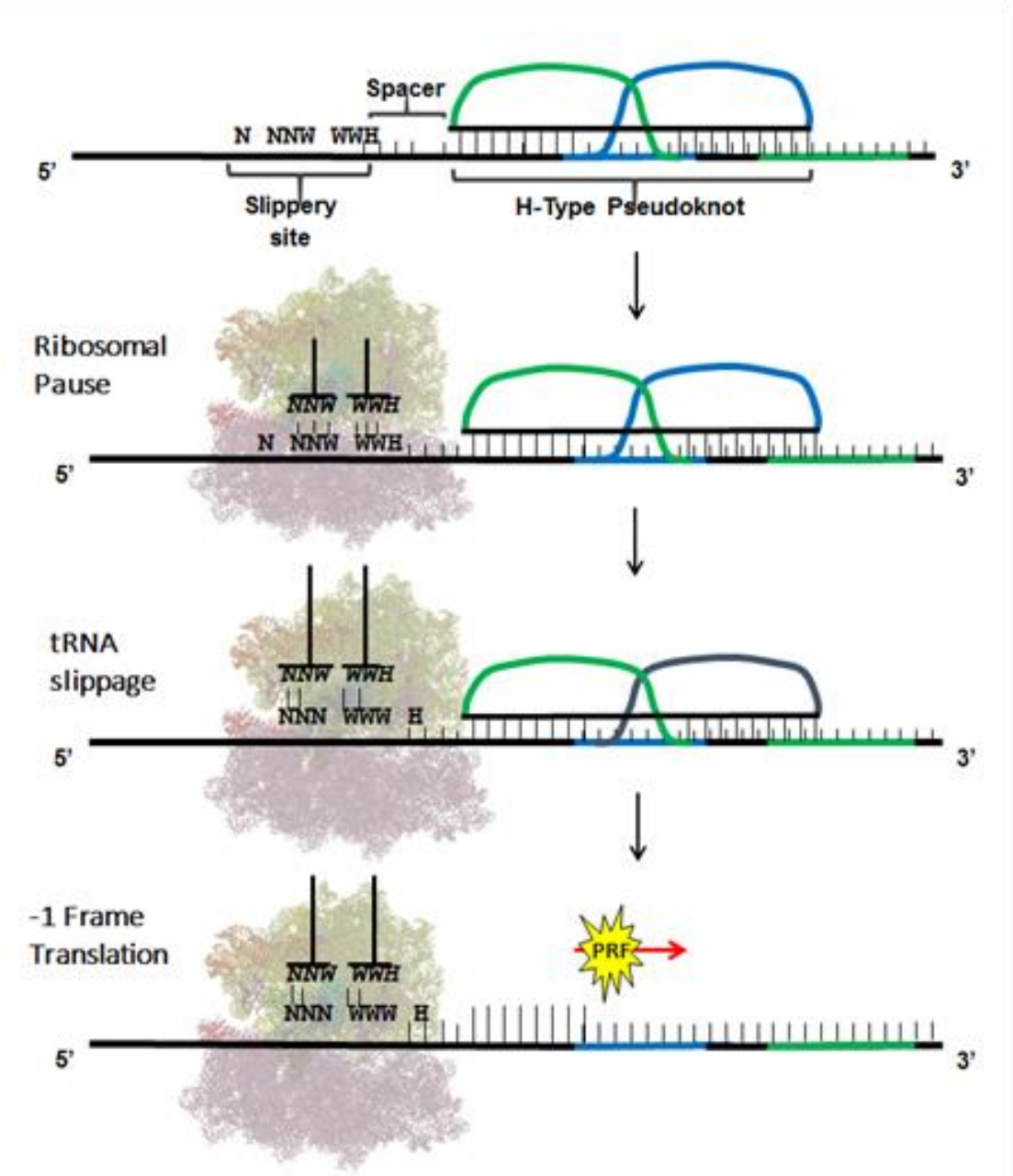

Figure 14. Structure and Mechanism of a -1 PRF.
The elements of a -1 PRF signal include a slippery heptamer of the form NNNWWWH (IUPAC notation), a spacer and a downstream mRNA tertiary structure which is usually an H-type pseudoknot. A frameshift event occurs during the ribosomal pause when a translating ribosome encounters downstream tertiary structure, usually a pseudoknot. This creates tension along the spacer which is relieved by a shift of one base, where by the P- and A- site codons at the slippery site repair in the -1 frame and translation continues (98).

In addition to enhancing genomic content, -1 PRF recoding events also serve to control the relative stoichiometric ratios of gene products. The L-A virus, as shown in Figure 17, depends on the stoichiometry of two products in a 60:1 ratio: Gag and Gag-Pol. Gag codes the viral capsid and Gag-Pol codes for the viral replicase. The stoichiometric ratio is essential for efficient proliferation of the virus (84, 99). Disrupting the -1 PRF recoding signal by mutation or any other means leads to inefficient viral proliferation due to the deviation from the stoichiometric ratio of Gag and Gag-Pol (91). Discoveries in yeast have further supported the premise that -1 PRF recoding events, via regulation through stoichiometry of gene products, can have biological implications. In the case of *Saccharomyces cerevisiae*, the function of the telomere length maintenance complex is regulated by the stoichiometry of the products of *CDC13*, *EST1*, *EST2*, *EST3* and *STN1*. All of the aforementioned genes, except for *EST3*, the mRNA of which contains a +1 PRF signal, are encoded by messages that contain -1 PRF signals. Studies in which the -1 PRF recoding rates are altered via mutations in either the slippery site or tertiary structure lead to rapid shortening of the yeast telomere length (100).

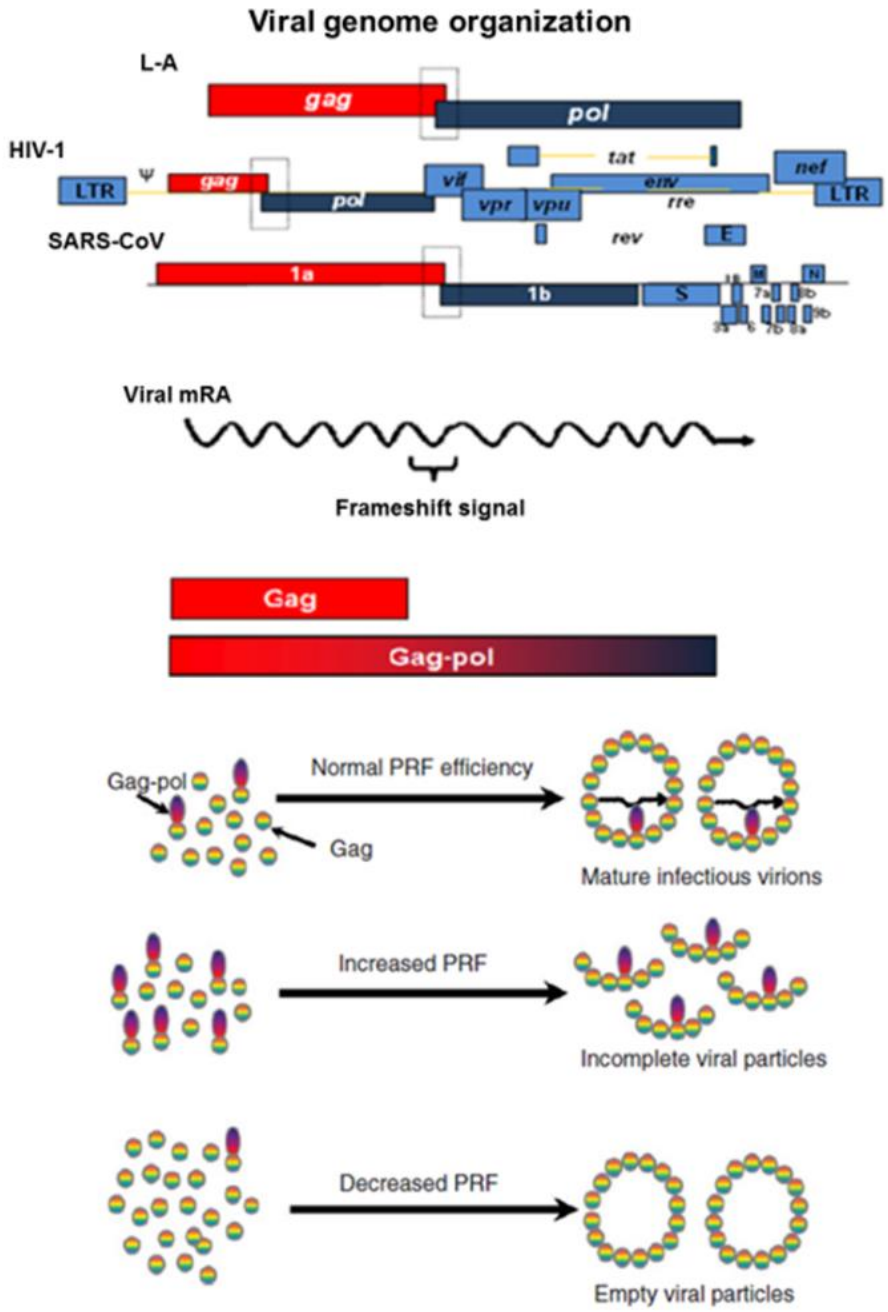

Figure 15. Viral genomic organization and gene expression regulation via -1 PRF

The figure shows a schematic of -1 PRF signals in L-A, HIV-1 and SARS genomes. The overlap regions highlighted by the rectangles harbors the -1 PRF signals. These sequences on the mRNA stochastically shift reading frame of the elongating ribosome and translate a fusion protein. Thus we have a scenario where the virus is able to coopt the host's translational machinery to get a specific ratio of two protein products from a single transcript. An increase or decrease in the frameshifting rate results in improper virion assembly and generates a non-functional virus (91).

A growing number of eukaryotic mRNAs have been identified that contain functional -1 PRF signals that serve as a means to regulate gene expression (101–104). Nearly all known cellular -1 PRF recoding events shift the elongating ribosome into -1 ORFs that contain premature termination codons (PTC). Studies using endogenous -1 PRF signals from yeast show that -1 PRF signals function as mRNA destabilizing elements through Nonsense Mediated Decay (NMD), and No-Go Decay (NGD) pathway (105, 106). As -1 PRF directs the ribosome to a PTC and stimulate NMD, this mechanism leads to an inverse correlation between -1 PRF recoding efficiency and mRNA abundance.

Programmed +1 Frameshifting

Programmed +1 Ribosomal Frameshifting (+1 PRF) is another mode of recoding that functions biologically similarly to -1 PRF by directing ribosomes to shift the translational frame, but by 1 nucleotide forward, i.e. in the 3' direction. This class of recoding event can result in either a premature termination or synthesis of a larger fusion protein due to the bypassing of the 0-frame stop codon. There are fewer known signals that induce a +1 PRF recoding event relative to the number of signals known to induce -1 PRF. +1 PRF signals are employed by viruses and transposable elements in a variety of organisms' genomes (ie. human, mouse, yeast, bacteria) to synthesize structural and enzymatic proteins (28, 107–109). In order for a +1 PRF recoding event to occur, it requires the presence of a heptameric slippery site. The downstream RNA tertiary structure is optional for +1 PRF recoding events.

Ty*1* and EST3 are both mRNAs that contain known +1 PRF signals and lack a downstream RNA tertiary structure. Ty*1* is a retroviral like retrotransposon in yeast where a +1 PRF recoding event results in synthesis of a Gag-pol fusion protein. A *Ty*1 +1 PRF recoding event requires the following: a heptameric slippery site, a near-cognate aa-tRNA bound to the P-site, an empty A-site where the mRNA 0 frame codon encodes for a rare tRNA and the codon in the +1 frame of the mRNA encodes for an abundant tRNA (110). In this circumstance, in lieu of a downstream stimulatory structure, the codon encoding for the rare tRNA in the A-site pauses the

elongating ribosome due the inherent low abundance of the rare tRNA in the cell (111). If the ribosome pauses on the requisite heptameric slippery site, it will result in weak Watson-Crick base pairing of the tRNA in the P-site. Should the codon in the +1 frame specify for a tRNA species that is in greater abundance than the 0 frame codon, the P-site tRNA will then reform stable base pairing in the +1 frame with assistance from the accommodation of the abundant tRNA species. At this point, the ribosome resumes elongating in the +1 frame. EST3 is a gene that encodes for a component of the yeast telomere telomerase holoenzyme complex. EST3 also contains a +1 PRF signal between its two open reading frames (ORF1 and ORF2). When a +1 PRF recoding event occurs, in a manner similar to that of Ty1, it results in the translation of the full length EST3p (112, 113).

OAZ1 is an example of a message that utilizes a downstream RNA tertiary structure to induce a +1 PRF recoding event. OAZ1 is a yeast gene that encodes for an ornithine decarboxylase antizyme that regulates polyamine biosynthesis by degrading ornithine decarboxylases. The elements required to induce a +1 PRF recoding event in OAZ1 are high levels of polyamines, a heptameric slippery site ‘UCC UGA U’ and a downstream tertiary structure to induce a ribosomal pause. These factors will stimulate the +1 PRF event that consequently results in the synthesis of the full length OAZ1 antizyme (114–116).

Missense and Nonsense Suppression

As the ribosome has evolved to rapidly and accurately decode mRNAs, translational fidelity is not only defined by the frequency of frameshifting recoding events but also by the intrinsic incorporation of missense and nonsense codons. Thus, we have addressed two additional aspects of translational fidelity utilized in this work; missense incorporation (the rate at which near or non-cognate tRNAs are erroneously accommodated and their amino acids incorporated in the growing nascent peptide chain); and nonsense suppression (the rate at which stop codons are not recognized or are translated using a suppressor tRNA). Both recoding events undermine the accuracy of the ribosome and, in the case of nonsense suppression, have a significant impact on protein synthesis.

Nonsense suppression (also called stop codon readthrough), refers to the rate at which suppressor tRNAs are incorporated at stop codons. *Cis*-acting elements such as mRNA pseudoknots and the identity of the nucleotide immediately downstream of the stop codon can also affect the accuracy of stop codon decoding (117–119). Selenocysteine incorporation at a UGA codon is a well-studied mechanism of programmed stop codon redefinition. This programmed event requires a selenocysteine incorporation signal (SECIS) downstream of the UGA stop codon, in the 3'-UTR region (120) . The SECIS is recognized by a specialized elongation factor SelB that delivers the $tRNA^{Sec}$ to the A-site and in the case of eukaryotes requires adaptor protein SBP2 (121, 122).

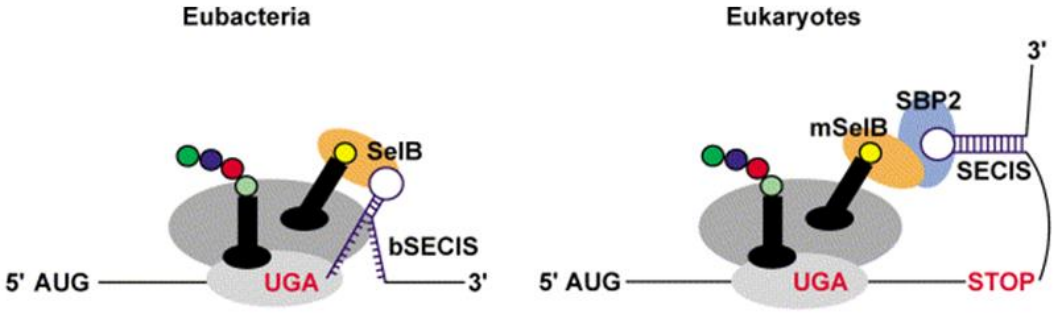

Figure 16. Mechanism of Selenocysteine incorporation.
The diagram shows the general mechanism of selenocysteine incorporation at UGA in both prokaryotes and eukaryotes. Selenocysteine incorporation in prokaryotes requires specialized elongation factor SelB and selenocysteine incorporation signals (SECIS) immediately after the stop codon. In eukaryotes the SECIS is located in the 3' UTR and the selenocysteine incorporation requires an additional accessory protein SBP2. This figure is from (113).

Programmed nonsense suppression is another method used in both viruses and eukaryotes to regulate gene expression. The murine leukemia virus (MuLV) utilizes a ribosomal pause induced by a strong pseudoknot which enables the reverse transcriptase to interact with eRF1. This reduces its availability to be used during ribosomal termination (123, 124). The reduced availability of eRF1 promotes an increase in frequency of stop codon readthrough (125). Recent studies in angiogenesis show the expression of an anti-angiogenesis factor, VEGF-Ax, is regulated through programmed stop codon readthrough in human endothelial cells (126).

Translational Recoding and mRNA abundance

Quality assurance is an important component of translation. If a message should contain defects, it could result in the translation of a protein that may have deleterious downstream biological effects. Recoding events often lead the ribosome to an aberrant message scenario, e.g. a -1 PRF may direct the ribosome to an alternate reading frame which contains a premature termination codon (PTC) prior to the *bona fide* 0 frame stop codon. Messages that contain recoding elements can be intentional, functioning as a mechanism to maintain cellular homeostasis by regulating gene expression. However, translating ribosomes must have the ability to identify aberrant messages and efficiently eliminate them from the transcriptome. There are mechanisms in place so that when aberrant messages are identified, they are directed to one of the three decay pathway that will eliminate the message from the transcriptome. The three known mRNA surveillance/decay pathways that have evolved to monitor mRNA quality are: the Nonsense Mediated Decay (NMD), No-Go Decay (NGD) and Non-Stop Decay (NSD).

Nonsense Mediated Decay (NMD) Pathway

The NMD surveillance pathway primarily monitors and degrades messages that harbor premature termination codons (PTC) (127–130). In addition to -1 PRF recoding elements, the NMD surveillance pathway can be triggered by transcripts that contain nucleotide mutations, splicing errors, and long 3’-UTRs (131–133).

Upf1, Upf2 Upf3 are proteins that form a complex that is essential for the NMD pathway of the yeast *Saccharomyces cerevisiae* (134). The Upf complex interacts with the release factors that are drawn to the ribosome as it recognizes a stop codon distal from the polyA tail. In this distal location, the release factors are able to associate in the absence of Pab1. This absence enhances recruitment of Upf1 to the eRF1-eRF3 complex (135). Upf2 and Upf3 then bind to Upf1 forming the Upf1:Upf2:Upf3 complex which is bound to the ribosome through the interactions between Upf1 and RPS26 (136). Activation of Upf1 is triggered by the formation of the Upf complex which then causes the release and degradation of the nascent polypeptide. eRF3 is dissociated from the termination complex (Figure 19). The large subunit then dissociates from the small subunit which remains associated with the mRNA. At this point, Upf1 recruits the decapping enzyme complex which destabilizes the closed loop structure and initiates mRNA decay (137, 138).

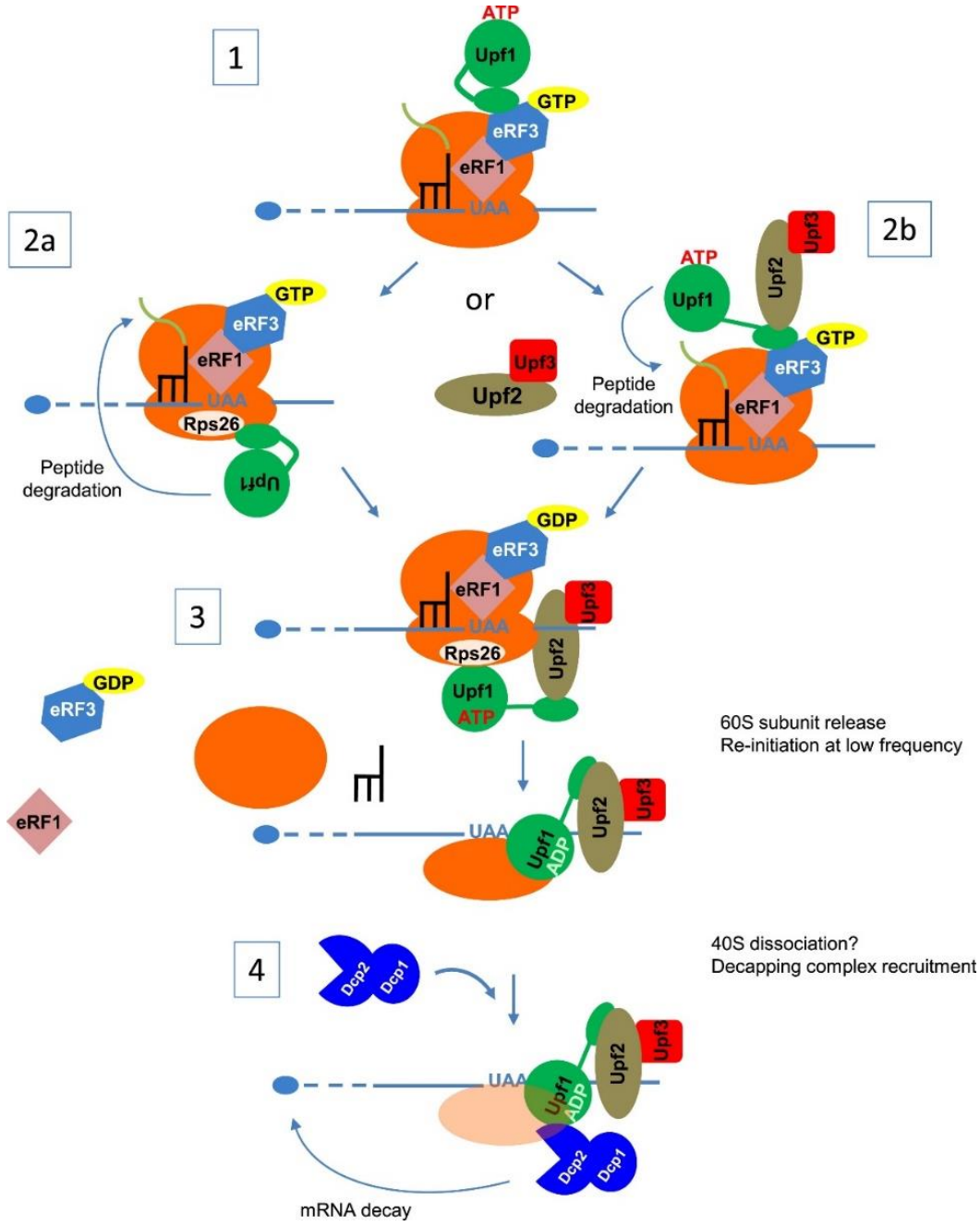

Figure 17. General model of NMD in yeast.
NMD is triggered by the recognition of the premature termination codon by the termination complex in yeast and binding of Upf1. In context of PTC the absence of Pab1p in the vicinity promotes the association of Upf1 with the termination complex. Subsequent activation of Upf1 causes peptide release, ribosomal subunit dissociation and activation of downstream mRNA decay complexes. This figure is from (137).

The relationship between -1 PRF and NMD in Cellular Gene Expression

Only 0.07% of the messages in the human genome that contain a predicted -1 PRF signal are able to extend beyond 30 codons (98). This indicates that >99% of predicted -1PRF events of human mRNAs will direct ribosomes to PTCs and initiate NMD. Prior studies have shown an inverse correlation between -1 PRF efficiencies and mRNA abundances and that ablation of a component of the NMD pathway stabilizes mRNA abundances in yeast (106), as shown in Figure 17. The induction of factors that alter frameshifting by reducing -1 PRF efficiencies stabilizes the mRNA abundance in both yeast and humans (100, 139). This highlights the relationship between frameshifting/NMD efficiencies and mRNA abundances. Mutations that affect the translational fidelity of the ribosome, thus altering the frequency by which the ribosome undergoes a recoding event can have biological implications. These have been exemplified in the translation of yeast telomere maintenance genes which require a stochastic ratio to maintain telomere length. Altered -1 PRF efficiencies due to mutations of the ribosome, have altered the mRNA abundances resulting in short telomere lengths (100).

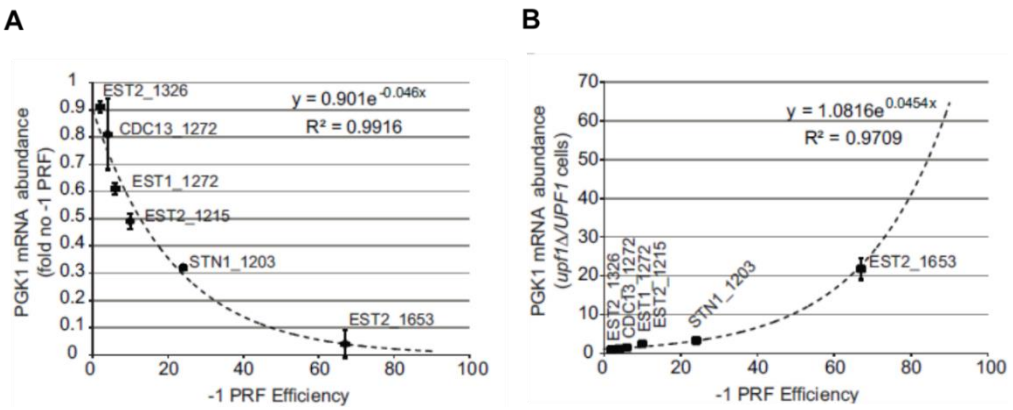

Figure 18. Delineation of mathematical relationships between -1 PRF and mRNA abundance in wild-type (panel A) and NMD-deficient cells (panel B)

Panel A demonstrates that the mRNA abundance of a transcript containing a -1 PRF signal is inversely correlated to the efficiency of -1 PRF due to redirecting the ribosome to a premature termination codon in the -1 frame, eliciting the NMD pathway. Panel B exhibits a comparision of the mRNA abundance of messages containing -1 PRF signals between NMD-deficient yeast cells to wild-type yeast cells. Image from (100).

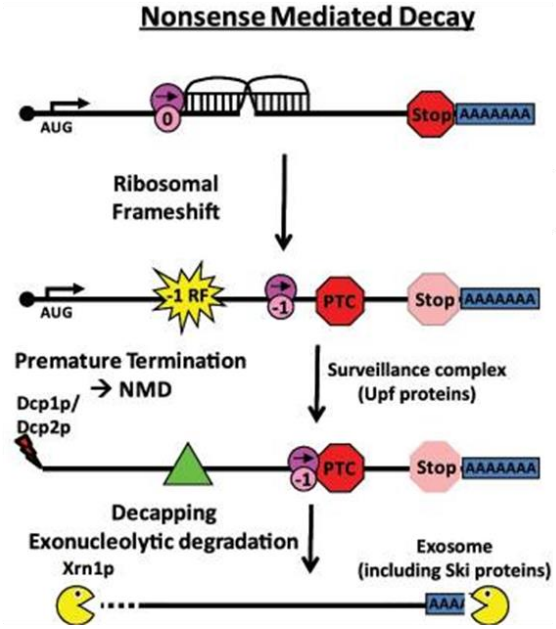

Figure 19. Model of -1 PRF dependence on NMD.

For genomic frameshift signals an elongating ribosome is directed to a -1 frame premature termination codon after as frameshift event. The recognition of the PTC by the ribosome results in activation of NMD and subsequent degradation of the frameshift signal containing mRNA. Image is modified from (106)

No-Go Decay (NGD) Pathway

The NGD pathway degrades messages that cause ribosomes to stall. Ribosomal stalling can be induced by RNA tertiary structures, rare codons or poly-lysine sequences (140, 141). The mechanism of NGD is not fully understood for ribosomes that stall mid-message. Once the ribosome stalls, the NGD pathway begins with an endonucleolytic activity near the stalled site by the Dom34/Hbs1 complex (140, 142, 143). The complex then dissociates from the stalled ribosome on the 3' end of the mRNA and stimulates the 3'-to-5' mRNA degradation by exosomes. The mechanism of NGD for ribosomes that stall at the 3' end of messages at the polyA tail is indistinguishable from the mechanism of NSD and is described in the section below.

Non-Stop Decay (NSD) Pathway

The NSD pathway monitors and degrades messages that lack stop codons. The NSD pathway is triggered once the ribosome reaches and stalls at the 3' end of the mRNA without encountering a stop codon. Substrates of NSD may contain processing errors where polyadenylation occurs prematurely within the mRNA coding region or mRNAs with truncated 3' UTRs (144, 145). The mechanism by which transcripts that lack stop codons are degraded is not fully understood. It is thought that as the ribosome continues to translate to the 3' polyA tail of the mRNA and that the ribosome stalls due to the multiple lysines encoded by the AAA codon. The stalled ribosome is recognized and associates to the C-terminus domain of the Ski7p which shares structural similarities to eRF3, a ribosomal termination factor

(145). The bound Ski7p then recruits the exosome and Ski2p, Ski3p, and Ski8p, which forms the Ski complex. This triggers a 3'-to-5' degradation of the nonstop transcript (145, 146). However, mRNA degradation by endonuclease activity alone was shown to be insufficient to inhibit protein synthesis. Nonstop mRNAs can contain polyribosomes on the message, and studies show that the presence of these polyribosomes can inhibit ribosomal translation (147). In support of the endonucleolytic degradation of the mRNA, the proteasome has been implicated in assisting the degradation of the resulting proteins translated by nonstop transcripts (148).

Ribosomopathies: An Overview of Ribosomal Dysfunction

Substandard cellular functions are caused by abnormal protein synthesis. Defective protein synthesis can be due to either ribosomal translational fidelity defects or altered gene expression. Deficient cellular homeostasis due to aberrant protein translation highlights the need to understand the source of these deleterious proteins: the ribosome. This class of disorders is categorized as ribosomopathies. They are rare diseases characterized by hypo-proliferative phenotypes, e.g. bone marrow failure, anemia, dystosis. Recently, they have been associated with the tumor suppressor protein p53 pathway (149). Table 1 lists several recognized ribosomopathies and their causative genetic defects.

DISEASE	GENE DEFECT	CLINICAL FEATURES	TREATMENT
Diamond-Blackfan anemia (DBA)	10–15 ribosomal proteins (eg. *RPS19, RPS26, RPL5, RPL11*) (mutations)	Anemia Growth retardation Congenital (craniofacial and thumb) abnormalities	Corticosteroids Blood transfusions Hematopoietic stem cell transplantation (HSCT) Leucine
5q-syndrome	*RPS14* (Deletion)	Anemia	Lenalidomide
Isolated Congential Asplenia (ICA)	*RPSA* (*RPS0* in yeast) (mutations)	Absence of Spleen	Antibiotic prophylaxis and pneumococcal vaccination
Schwachman-Diamond syndrome (SDS)	*SBDS*	Exocrine pancreatic insufficiency Hematologic abnormalities (esp. neutropenia) Neurocognitive impairment Gl (esp. liver) abnormalities	Pancreatic enzyme supplementation HSCT
X-linked dyskeratosis congenita (DC)	*DKC1*	Mucocutaneous abnormalities (e.g. skin pigmentation and nail changes) Pulmonary fibrosis Bone marrow failure	Oxymetholone HSCT
Cartilage-hair hypoplasia (CHH)	*RMRP*	Short stature Bone deformities Hair growth abnormalities	Symptomatic
Treacher-Collins syndrome (TCS)	*TCOF1*	Craniofacial abnormalities	Symptomatic

Table 1: Clinical characteristics of different ribosomopathies
This table is adapted from (149, 150).

Are ribosomopathies just a ribosomal biogenesis problem?

Ribosomopathies are a class of congenital diseases caused by ribosomal dysfunction due to functional and structural defects within the ribosome. Studies have attempted to probe and understand the underlying causes of the ribosomal dysfunction. At a first glance, ribosomopathies appear to present a direct causal link between mutations in a gene encoding for a ribosomal factor and haploinsufficiency of the factor leading to ribosomal dysfunction. Haploinsufficiency is a state in which a diploid organism has a single functional copy of a gene while the other is inactivated by a mutation, and the organism does not produce enough of the gene product to maintain the wild-type condition. Ribosomopathies caused by haploinsufficiency for ribosomal factors are often deficient in factors involved with ribosomal biogenesis. For example, X-linked dyskeratosis congenita (X-DC) is caused by a mutation in the DKC1 gene which encodes dyskerin, a protein involved with post-transcriptional pseudouridylation of uridines present in ribosomal RNA (151). Diamond-Blackfan Anemia (DBA) Isolated Congenital Asplenia (ICA) and 5q- syndrome (5q-) are all caused by mutations in genes that encodes for ribosomal proteins (RP) S19, S0 and S14 respectively. RPS19, RPS0 and RPS14 are all involved in rRNA processing (152). DBA, ICA and 5q- are all considered to be haploinsufficiency-caused ribosomopathes since all exhibit decreased amounts of their respective ribosomal protein.

Attributing defects in ribosomal biogenesis as the underlying pathology of ribosomopathies is an insufficient answer. The decreased ribosomal

quantity does not account for the tissue specificity of ICA (spleen) or DBA and 5q- syndrome (bone marrow). In the case of congenital ribosomopathies, every cell of the body contains the same genetic mutation and not all tissues exhibit symptoms of ribosomal dysfunction. It is worthy to note that some of these ribosomopathy disorders are symptomatic of tissue developmental defects, e.g. a lack or severely underdeveloped spleen in ICA patients and defects in the development of progenitor red blood cells in the bone marrow of DBA and 5q- patients. A recent study has shown that hematopoiesis of stem/precursor cells are regulated by Nonsense Mediated Decay (NMD), (106, 153). NMD is a mRNA decay pathway triggered by recoding events that redirect the ribosome to alternate reading frames, resulting in the translation of an alternate protein. NMD is a process that relies on the translational fidelity of the ribosome which, if altered, can up or down regulate gene expression (154, 155). If the maturation of red blood cells is dependent on a process that is regulated by translational fidelity, then “dysfunctional” ribosomes with altered translational fidelities will hinder the development of mature red blood cell. Studies in the structure and function of yeast RPs have shown that mutations in genes encoding for RPs exhibit translational fidelity defects (156–158). Mutations of Cbf5, the yeast homolog of DKC1, are known to cause ribosomal translational fidelity defects (159). The tissue specificity of ribosomopathies may be linked to the responsible ribosomal factor having tissue specific roles, whether by influencing translational fidelity or possessing

an extra-ribosomal function, e.g. regulating transcription or enzymatic activity (160).

Ribosomopathies can present paradoxical effects, e.g. ribosomopathic patients that exhibit opposing phenotypes: several disorders are characterized by a hypo-proliferative phenotype, e.g. anemia, which then converts to a hyper-proliferative phenotype, i.e. cancer. This transition from hypo-proliferative to hyper-proliferative phenotype is not well understood. However, the current hypothesis is that these ribosomopathic ribosomes are still capable of translating messages, to a degree, but are dysfunctional enough that translational fidelity is affected which alters gene expression and in a domino-like manner, generates an accumulative effect. This accumulation invariably cumulates in the phenotype associated with the ribosomopathy. Cancerous tumors are associated with enhanced ribosomal biogenesis, increased translation rates, and in some cases, the overexpression of RPs (161). However, due to the nature of haploinsufficient ribosomopathies, RPs are underexpressed.

The preponderance of evidence indicating defects in translation and the subsequently altered gene expression in ribosomopathies is suggestive of specialized ribosomes. It is hypothesized that specialized ribosomes are the result of heterogeneity in ribosome composition. The variation in ribosomal composition may be a consequence of differential expression and post-translational modifications of RPs, rRNA base modification and the activity of ribosome-associated factors (20). Heterogeneity in ribosomal composition

may affect the translation of genetic material. As studies in ribosomopathies continue to reveal translational fidelity defects that alter cellular gene expression, it becomes more important to understand what these ribosomes actually do, rather than attributing the pathogenesis of the disease simply to a lack of ribosomes. It stands to reason that the pathogenesis of ribosomopathies would be better understood by exploring and treating each ribosomal factor linked to their respective ribosomopathies as a unique set of circumstances that cumulatively presents a translational pattern that leads to the disease's phenotype.

Diamond-Blackfan Anemia: RPS19 Gene Haploinsufficiency

Diamond-Blackfan Anemia (DBA) is a rare genetic disorder that is identified primarily by hematological features. It is a congenital bone marrow failure syndrome that results in erythoid aplasia. However, DBA does exhibit non-hematological features in 20% of patients. These include defects in the cranio-facial region, eyes, neck, thumb, urogenital tract, heart, and musculoskeletal structures, in addition to increased incidences of acute myeloid leukemia (AML) and osteogenic sarcoma (162–165).

DBA was first reported to be associated with gene mutations in the ribosomal protein S19 (RPS19) gene locus on chromosome 19q13.2, which is mutated in about 25% of patients (166–168). Recently, mutations in other genes that encode for RPs in both the large and small ribosomal subunits have been linked to this disorder. (169–173) (Table 2). Genes associated to

DBA are not limited to ribosomal proteins but also include TSR2 (a protein involved in pre-rRNA processing) and GATA1 (an erythroid transcription factor) (174–176). A variety of RPS19 mutations, e.g. whole gene deletions and truncation mutations have been observed, all of which suggests that haploinsufficiency is the basis of DBA pathology (166). Haploinsufficiency of RPS19 as the pathogenesis of DBA was further supported by the introduction of RPS19 in $CD34^{+}$ bone marrow cells and in murine models (177, 178). Mutations in RPS19 are more often associated with bone marrow failure resulting in anemia. Mutations in other ribosomal protein genes are linked to other phenotypes, e.g. heart and craniofacial malformations are strongly associated to mutations in ribosomal proteins L5 and L11 (173). Clinically, RPS19 linked DBA exhibits a normochromic (normal concentration of hemoglobin within red blood cells) and macrocytic (enlarged red blood cells) anemia and a normocellular bone marrow but with decreased or absent erythoid precursor cells. DBA exhibits a relationship between ribosomal functions and erythroid aplasia. Its etiology is currently not well understood, however it is generally thought to be a biogenesis defect of the ribosome due to the basis that RP mutations lead to a decrease in functional ribosomes (179, 180).

Gene Associated to Diamond Blackfan Anemia	Percent Prevalence
RPS19	**~25%**
RPL5	7%
RPS10	3-6%
RPS26	3-6%
RPL11	5%
RPL35a	3%
RPS24	2%
RPS7	~1%
RPS17	~1%
TSR2	~1%
GATA1	~1%
Unknown	40-50%

Table 2: List of Ribosomal Proteins associated with Diamond Blackfan Anemia
Table adapted from (162).

Ribosomal protein S19 is one of the 33 ribosomal proteins in the 40S subunit of the ribosome. RPS19 is a 144 amino acid long protein (MW ~16 kDa) located at the head region of the small subunit of the ribosome, highlighted in yellow in Figure 2. RPS19 is encoded by two paralogous genes, RPS19A (YOL121C) and RPS19B (YNL302C). The two paralogous genes differ by a single amino acid (Figure 1)

Score	Expect	Method	Identities	Positives	Gaps
291 bits(745)	1e-106	Compositional matrix adjust.	144/145(99%)	144/145(99%)	0/145(0%)

```
Query  1    MPGVSVRDVAAQDFINAYASFLQRQGKLEVPGYVDIVKTSSGNEMPPQDAEGWFYKRAAS  60
            M GVSVRDVAAQDFINAYASFLQRQGKLEVPGYVDIVKTSSGNEMPPQDAEGWFYKRAAS
Sbjct  1    MAGVSVRDVAAQDFINAYASFLQRQGKLEVPGYVDIVKTSSGNEMPPQDAEGWFYKRAAS  60

Query  61   VARHIYMRKQVGVGKLNKLYGGAKSRGVRPYKHIDASGSINRKVLQALEKIGIVEISPKG  120
            VARHIYMRKQVGVGKLNKLYGGAKSRGVRPYKHIDASGSINRKVLQALEKIGIVEISPKG
Sbjct  61   VARHIYMRKQVGVGKLNKLYGGAKSRGVRPYKHIDASGSINRKVLQALEKIGIVEISPKG  120

Query  121  GRRISENGQRDLDRIAAQTLEEDE*  145
            GRRISENGQRDLDRIAAQTLEEDE*
Sbjct  121  GRRISENGQRDLDRIAAQTLEEDE*  145
```

Figure 20. Blast Alignment of Ribosomal Protein S19 paralog A (YOL121C) vs B (YNL302C).
Protein Alignment was obtained via Blast (181).

In addition to its role in improving translational efficiency, RPS19 has been linked to several steps in ribosomal biogenesis: rRNA processing, ribosomal assembly, and polypeptide assembly (182, 183). RPS19 is responsible for recruiting factors, Enp1, Tsr1, and Rio2 for pre-RNA processing. These recruited factors are essential in pre-RNA processing and maturation of the precursor 40S particle during the cleavage at site A_2 within ITS1 step (as shown in Figure 3) and the subsequent maturation of the 3' end of the 18S rRNA in yeast cells (152, 184–186). The diminished abundance of mature 18S rRNA leads to diminished levels of 40S and mature 80S ribosomes (187, 188). The diminished levels of 40S may also, in part, be due to RPS19 mutations promoting increased nucleolar mislocalization and defective in its' self-incorporation into the 40S subunit during ribosomal assembly (152, 189, 190). The failure to mature the 40S subunit may not be solely attributed to RPS19 haploinsufficiency of RPS19 but rather a loss of factor recruitment and/or interactions. Recent studies show that RPS19 may

interact with Pim1, an oncoprotein, suggesting a potential physical linkage between signal transduction pathways and the ribosome (191).

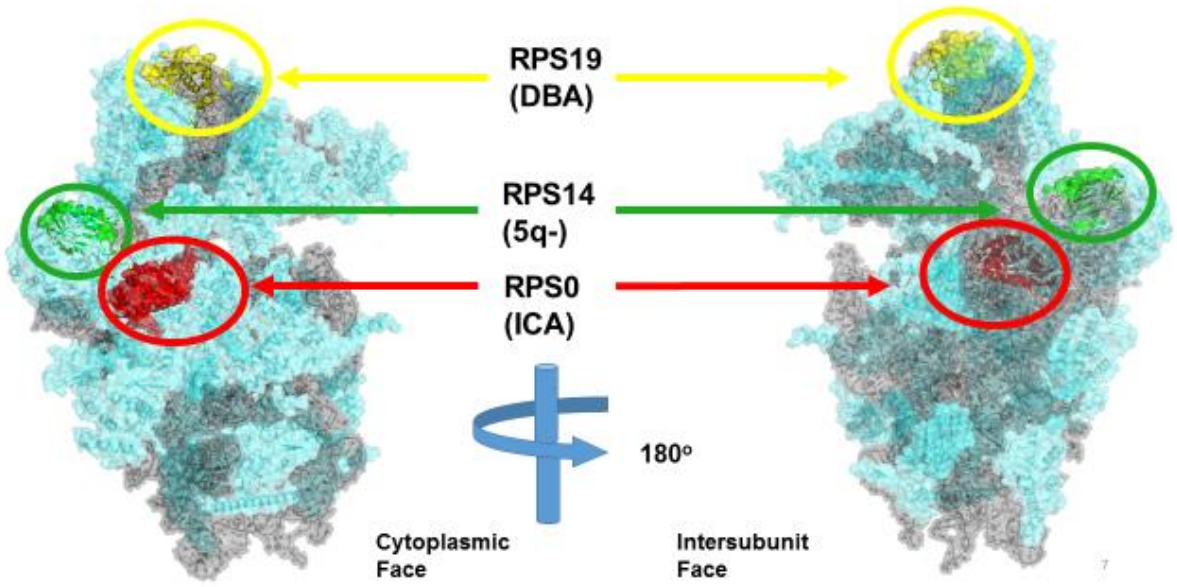

Figure 21. Locations of ribosomopathy associated ribosomal proteins in the Saccharomyces cerevisiae 40S subunit.
The left image shows the 40S subunit from the cytoplasmic face and the right image shows the 40S subunit in the intersubunit face. RPS19 is highlighted and circled in yellow, RPS14 in green and RPS0 in red. Image was modified from Ben-Shem using Pymol **(8, 9)**. PDB accession codes: 3U5B, 3U5C, 3U5D, 3U5E, 3U5F, 3U5G, 3U5H, and 3U5I.

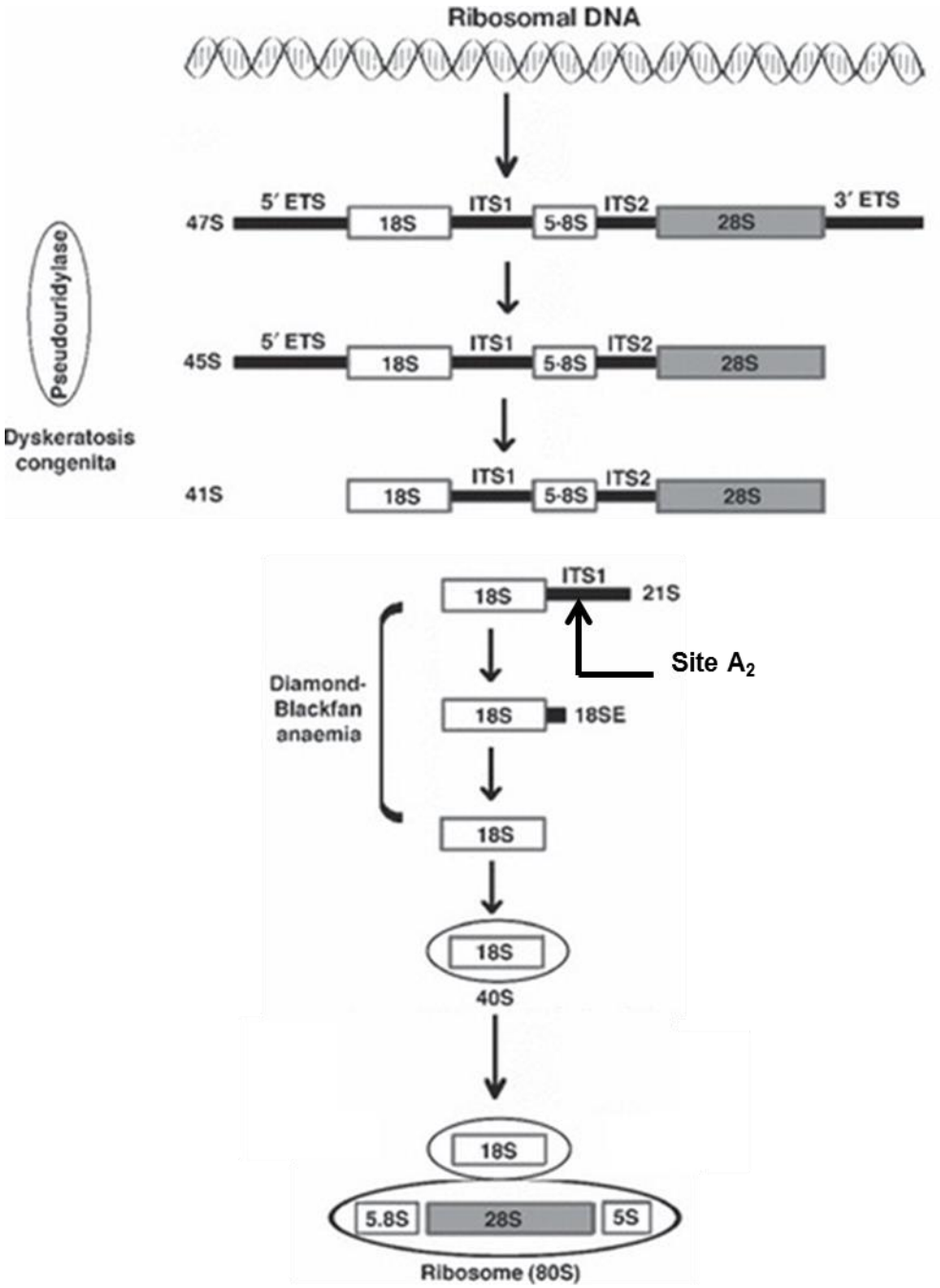

Figure 22. Ribosomal rRNA synthetic pathway in Humans
Image modified from from Ganapathi and Shimamura (180)

Isolated Congenital Asplenia: RPSA/yRPS0 Gene Haploinsufficiency

Isolated Congenital Asplenia (ICA) is a rare genetic disorder caused by mutations in human ribosomal protein SA (RPSA). This disease is characterized by a lack of or severely under developed spleen while demonstrating no other developmental defects (192, 193). However, defects in spleen development puts patients at high risk for pneumococcal sepsis (194, 195). While the pathogenesis of ICA is not fully understood, studies show that mutations in the RPSA gene that generate premature termination codons directs the message to the NMD pathway. This results in haploinsufficiency of the RPSA locus (193). It is interesting that haploinsufficiency of RPSA alone presents a defective spleen development phenotype, given that RPSA is not associated with spleen development. Spleen development, in murine models are regulated by a cascade of transcription factors (i.e. Tlx1 and Pbx1) (196, 197). RPSA has a role in the rRNA processing of the 18S precursor rRNA. Studies have shown that siRNA knockdown of RPSA correlates to diminished levels of mature 18S rRNA, demonstrating ITS1 cleavage/processing defects in humans (198). The processing of the 18S precursor rRNA by ITS1 cleavage at the A_2 site is conserved between RPSA (humans) and RPS0 (yeast) (199). While RPSA/RPS0 function of 18S rRNA processing may be conserved between humans and yeast, lymphocytes of ICA patients do not exhibit any pre-rRNA processing defects (193). Two models have been hypothesized for the

pathogenesis of ICA: (1) specialized ribosomes that have preferential translation of a certain set of transcripts which may be affected by mutations in RPSA or (2) RPSA that may have a yet to be discovered non-ribosomal function.

RPS0 is a 252 amino acid long protein (MW ~28 kDa), It is located at the lower periphery of the ribosomal small subunit near the head of the subunit, highlighted in red in Figure 2. RPS0 is encoded by two paralogous genes, RPS0A (YGR214W) and RPS0B (YLR048W). A protein blast alignment of the two proteins in Figure 4 shows that the paralogs are 95% identical (240 out of 253 amino acid residues). In the results section, we use yeast RPS0 gene pseudo-haploinsufficiency as a model for the ICA ribosomopathy to probe the correlation of translational fidelity and cellular gene expression.

Score	Expect	Method	Identities	Positives	Gaps
450 bits(1157)	2e-165	Compositional matrix adjust.	240/253(95%)	242/253(95%)	0/253(0%)

```
Query  1    MSLPATFDLTPEDAQLLLAANTHLGARNVQVHQEPYVFNARPDGVHVINVGKTWEKLVLA  60
            MSLPATFDLTPEDAQLLLAANTHLGARNVQVHQEPYVFNARPDGVHVINVGKTWEKLVLA
Sbjct  1    MSLPATFDLTPEDAQLLLAANTHLGARNVQVHQEPYVFNARPDGVHVINVGKTWEKLVLA  60

Query  61   ARIIAAIPNPEDVVAISSRTFGQRAVLKFAAHTGATPIAGRFTPGSFTNYITRSFKEPRL  120
            ARIIAAIPNPEDVVAISSRT+GQRAVLKFAAHTGATPIAGRFTPGSFTNYITRSFKEPRL
Sbjct  61   ARIIAAIPNPEDVVAISSRTYGQRAVLKFAAHTGATPIAGRFTPGSFTNYITRSFKEPRL  120

Query  121  VIVTDPRSDAQAIKEASYVNIPVIALTDLDSPSEFVDVAIPCNNRGKHSIGLIWYLLARE  180
            VIVTDPR DAQAIKEASYVNIPVIALTDLDSPSEFVDVAIPCNNRGKHSIGLIWYLLARE
Sbjct  121  VIVTDPRLDAQAIKEASYVNIPVIALTDLDSPSEFVDVAIPCNNRGKHSIGLIWYLLARE  180

Query  181  VLRLRGALVDRTQPWSIMPDLYFYRDPEEVEQQVAEEATTEEAGEEEAKEEVTEEQAEAT  240
            VLRLRGALVDRTQPWSIMPDLYFYR+PEEVEQ   E A  EE  EEE KEEVTE QAEAT
Sbjct  181  VLRLRGALVDRTQPWSIMPDLYFYRNPEEVEQVAEEAAAAEEGEEEEVKEEVTEGQAEAT  240

Query  241  EWAEENADNVEW*  253
            EWAEENADNVEW*
Sbjct  241  EWAEENADNVEW*  253
```

Figure 23. Blast Alignment of Ribosomal Protein S0 paralog A (YGR214W) vs B (YLR048W).
Protein Alignment was obtained via Blast (181).

5q- Syndrome: Somatically Acquired RPS14 Gene Haploinsufficiency

Somatically acquired 5q- syndrome, a subtype of myelodysplastic syndrome, is caused by haploinsufficiency for ribosomal protein S14 (RPS14) due to the deletion of the q arm of chromosome 5. In humans, 5q- syndrome presents an erythroid phenotype that is similar to DBA. The deletion of the 5q arm is the sole cytogenetic abnormality in 5q- patients. The disease is characterized by severe macrocytic anemia, elevated platelet count which are hypo-lobulated micro-megakaryocytes, and a predilection toward developing acute myeloid leukemia (AML) (200, 201). Haploinsufficiency of RPS14 via siRNA knockdown in CD34+ stem cells has been shown to exhibit similar erythroid phenotypes as those derived from 5q- syndrome patients.

Additionally, the forced overexpression of RPS14 in RPS14 deficient cells resulted in rescued erythroid phenotypes (200). Recent studies in RPS14 haploinsufficient mammalian cells have revealed both p53 independent and p53 dependent tumor suppressor effects (202–204).

RPS14 is a 137 amino acid long ribosomal protein (MW: ~15 kDA) located near the head of the 40S subunit of the ribosome, highlighted in green in Figure 2. RPS14 is encoded by two paralogous genes, RPS14A (YCR031C) and RPS14B (YJL191W). Figure 5 shows a protein blast alignment of the two RPS14 protein paralogs, revealing that the two proteins are 98% identical for amino acid residues and are 100% identical when one residue is substituted for a similar residue.

Deletions or mutations of RPS14 are strikingly similar to mutations of RPS19 in DBA and RPS0 in ICA. They have been linked to inhibition of the late stages in the maturation of the 43S pre-ribosome particle (205–208). RPS14 has also been shown to engage in a “test drive” quality control checkpoint during the maturation of the pre 40S subunit (209).

Score	Expect	Method	Identities	Positives	Gaps
269 bits(687)	4e-98	Compositional matrix adjust.	134/137(98%)	137/137(100%)	0/137(0%)

```
Query  2    SNVVQARDNSQVFGVARIYASFNDTFVHVTDLSGKETIARVTGGMKVKADRDESSPYAAM  61
            +++VQARDNSQVFGVARIYASFNDTFVHVTDLSGKETIARVTGGMKVKADRDESSPYAAM
Sbjct  3    NDLVQARDNSQVFGVARIYASFNDTFVHVTDLSGKETIARVTGGMKVKADRDESSPYAAM  62

Query  62   LAAQDVAAKCKEVGITAVHVKIRATGGTRTKTPGPGGQAALRALARSGLRIGRIEDVTPV  121
            LAAQDVAAKCKEVGITAVHVKIRATGGTRTKTPGPGGQAALRALARSGLRIGRIEDVTPV
Sbjct  63   LAAQDVAAKCKEVGITAVHVKIRATGGTRTKTPGPGGQAALRALARSGLRIGRIEDVTPV  122

Query  122  PSDSTRKKGGRRGRRL*  138
            PSDSTRKKGGRRGRRL*
Sbjct  123  PSDSTRKKGGRRGRRL*  139
```

Figure 24. Blast Alignment of Ribosomal Protein S14 paralog A (YCR031C) vs B (YJL191W) (YLR048W)
Protein Alignment was obtained via Blast (181).

Pseudo-haploinsufficiency in yeast as a model system for ribosomopathies

Saccharomyces cerevisiae yeast was selected as a model in order to further understand human ribosomopathies and haploinsufficiency of associated ribosomal factors. *Saccharomyces cerevisiae* underwent a genome duplication event that occurred approximately a hundred millions years ago (210–212). While most of the duplicated genes have been lost, we find that several paralogous RP genes have been selected for ongoing preservation. The presence of paralogous genes and the relative ease of generating single gene paralog knockouts in the yeast genome enable a haploinsufficient state to exist in the pseudo-diploid yeast model system. This state is a condition that we refer to as pseudo-haploinsufficiency. The existence of paralogous RP genes that are the yeast homologs of RP genes associated with human RP haploinsufficient ribosomopathies enables the yeast to be the ideal model system to study the effects of ribosomal protein

gene pseudo-haploinsufficiency and ribosomal protein heterogeneity (to an extent) on translational fidelity and cellular expression.

We hypothesized that ribosomopathies caused by ribosomal protein haploinsufficiency cause subtle changes in translational fidelity. This affects the mechanism of protein synthesis, which effectively modulates gene expression so that it results in the phenotype exhibited by the ribosomopathy. In the results, we show that using RP gene pseudo-haploinsufficient yeast is a valid model system to investigate and monitor the effects of translational fidelity defects and cellular gene expression.

Scope of Work and Thesis Summary

The project began with a question about a unique facet of ribosomopathies: why are they tissue specific? How can we better understand the nature of ribosomal dysfunction and which factors contribute to disease pathogenesis? At the very basic level, we understood that haploinsufficiency for ribosomal factors leads to ribosome dysfunction but how do we quantitatively assess the effects of haploinsufficiency? The presence of duplicated RP genes in yeast enabled us to generate a pseudo-diploid model system to assess the effects that ribosomal protein haploinsufficiency have on ribosomal function. We were able to improve our understanding of haploinsufficiency as it contributes to defects in ribosomal translational fidelity and hence, haploinsufficiency's effects on gene expression. This work has provided new insights in the nature of ribosomopathies as well as the nature of ribosomes.

The scope of the research focuses on the role played by ribosomal dysfunction in the yeast model ribosomopathies. Research has shown that factors that alter the translational fidelity of the ribosome can lead to ribosomal dysfunction during translation, altering gene expression which can have deleterious downstream biological effects. The fidelity of the ribosome during translation is critical for regulating gene expression which is essential in tissue development / cellular differentiation. Recent research in our lab has shown a relationship between translational recoding efficiencies and gene expression. As ribosomopathies are a class of disease associated with

ribosomal dysfunction, the primary objective of this work was to quantitatively measure translational recoding rates and the subsequent effects on gene expression. Chapter 2 will show the effects of ribosomal protein haploinsufficiency on translational fidelity and gene expression, the results of which are characteristic of specialized ribosomes. In the discussion section, we discuss the results and present a model for how ribosomal protein haploinsufficient ribosomopathies exhibit specialized ribosome behaviors that leads to the distinct phenotype of the ribosomopathy and how this challenges our current understanding of the ribosome.

Chapter 2: Results

Ribosomal protein gene pseudo-haploinsufficiency promotes decreased stop codon recognition

Ribosomal translational fidelity is not only measured by reading frame maintenance, but also by the interaction of codon:anti-codon interaction between the message and the tRNA that takes place in the decoding center of the small subunit. There are three possible outcomes that can occur when the anti-codon of the tRNA interacts with the triplet nucleotide codon of the message RNA; a cognate pair where the triplet nucleotides of the tRNA's anti-codon perfectly complements the codon of the mRNA, a near-cognate pair where the codon:anti-codon interaction only has two of three complementary pairs and a non-cognate pair where the codon:anti-codon interaction do not share any complementary pairs.

Ribosomal protein gene pseudo-haploinsufficient yeast were investigated whether pseudo-haploinsufficiency would exhibit any effect on an important aspect of translation; codon recognition. Stop codon recognition and missense incorporation, like -1 and +1 PRF, are two additional forms of translational recoding. Dual luciferase reporters containing these recoding events were assayed in yeast cells that were pseudo-haploinsufficient for *RPS0*, *RPS14* or *RPS19*. Dual luciferase reporters contain a recoding signal cloned in between the Renilla and Firefly Luciferase genes. The stop codon recognition reporters used one of the three canonical stop codons (UAA, UAG, UGA) inserted in-frame and downstream of the *Renilla* luciferase gene.

In addition to the canonical stop codons, *GCN4* was selected as a proxy to measure the potential cumulative effect of multiple upstream ORFs prior the Firefly luciferase gene due to the 5'- UTR region upstream of the *GCN4* gene containing 4 in-frame stop codons (213). The missense incorporation reporter assays utilized two different R218S inactivating mutations of the Firefly luciferase. One monitors the misreading of the non-cognate TCT mutation and the other monitors the misreading of a near-cognate AGC mutation.

Overall, the results of these assays revealed decreased in stop codon recognition. The magnitude of this effect appeared to be isoform specific. For example, the loss of *RPS0A* promoted a greater increase in Firefly luciferase activity which is a byproduct of the effect of decreased stop codon recognition, than the loss of *RPS0B* for the UAG stop codon (2.58 vs 1.49 of fold wild-type for RPS0AΔ and RPS0BΔ respectively). The increased Firefly activity and isoform specific trend repeated when assaying the UGA stop codon (3.03 vs 1.82 fold wild-type) and the UAA stop codon (1.55 and 1.99 fold wild-type read through rates for RPS0AΔ and RPS0BΔ respectively) (Figure 25A). The GCN4 reporter assay revealed that *RPS0* gene pseudo-haploinsufficiency promoted increased sequential stop codon readthrough (3.89 and 1.89 fold of wild-type for RPS0AΔ and RPS0BΔ respectively) (Figure 25A). The missense incorporation assay revealed that only the loss of *RPS0A* increased the incorporation of non-cognate (1.41 fold of wild-type) and near-cognate (1.29 fold wild-type) tRNAs (Figure 25A).

Stop codon recognition is inhibited by *RPS14* gene pseudo-haploinsufficiency. The translational fidelity reporter assays revealed the loss of either paralog of RPS14 inhibited stop codon recognition. UAA stop codon readthrough was found to be ~1.5 fold of wild-type, UAG stop codon readthrough was ~1.4 fold of wild-type and the UGA stop codon readthrough was 1.66 and 1.32 fold of wild-type for RPS14AΔ and RPS14BΔ respectively (Figure 25B). The GCN4 reporter assay exhibited the most pronounced effect, demonstrating that RPS14 gene pseudo-haploinsufficiency inhibited multiple, sequential stop codon recognition. As shown in Figure 25B, the GCN4 reporter assay revealed stop codon readthrough efficiencies that were 3.60 and 5.94 fold of wild-type for RPS14AΔ and RPS14BΔ respectively. Missense incorporation rates was not affected by RPS14 gene pseudo-haploinsufficiency.

The overall decrease in stop codon recognition held for *RPS19* gene pseudo-haploinsufficiency. RPS19 gene pseudo-haploinsufficiency demonstrated isoform specific effects in the three canonical stop codon recognition. The translational fidelity assay revealed that the RPS19 pseudo-haploinsufficient ribosome bypassed the UAA stop codon 2.82 and 4.06 fold of wild-type for RPS19AΔ and RPS19BΔ respectively. The UAG stop codon was bypassed 2.14 and 2.37 fold of wild-type and the UGA stop codon bypassed 1.41 and 5.41 fold of wild-type for RPS19AΔ and RPS19BΔ respectively (Figure 25C). The GCN4 reporter assay revealed that RPS19 gene pseudo-haploinsufficiency inhibited recognition of multiple, sequential

stop codons. RPS19 pseudo-haploinsufficient ribosome, as shown in Figure 25C, bypassed multiple sequential stop codons 5.52 and 2.39 fold of wild-type for RPS19AΔ and RPS19BΔ respectively. The missense incorporation effects were demonstrated to be paralog specific. Loss of the *RPS19A* paralog stimulated non-cognate missense incorporation by 1.87 fold of wild-type while the loss of the *RPS19B* paralog had no effect. In the case of near-cognate missense incorporation, the loss of the *RPS19B* paralog stimulated incorporation by 1.83 fold of wild-type while the loss of the *RPS19A* paralog had no effect (Figure 25C).

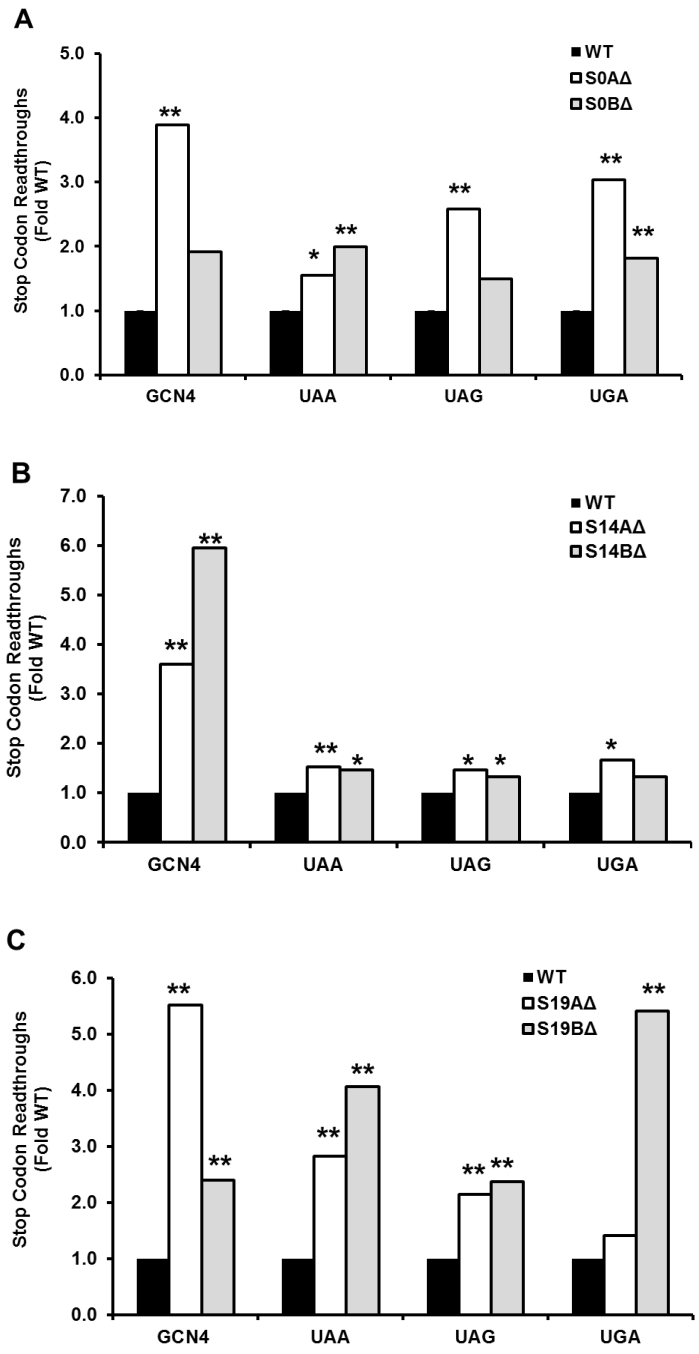

Figure 25. Dual Luciferase reporter assays to monitor in-frame stop codon recognition and missense incorporation rates in *Saccharomyces cerevisiae* yeast cells.

Stop codon read-through rates were measured in yeast strains using dual luciferase reporters containing in-frame stop codons; UAA, UAG, UGA. GCN4 dual luciferase reporter assay measured multiple in-frame upstream ORFs prior the luciferase gene (213). Error bars denote standard error. *P < 0.05, **P < 0.01. Raw values can be found in Supplementary Table 1.

Ribosomal protein gene pseudo-haploinsufficient yeast cells demonstrated a trend of decreased stop codon recognition. *RPS0* and *RPS19* gene pseudo-haploinsufficiency demonstrated paralog-specific decreased stop codon recognition for all canonical stop codons. All ribosomal protein gene pseudo-haploinsufficient yeast cells demonstrated an accumulative inhibitory effect when translating messages that contained multiple uORFs. These results suggesting that ribosomal protein composition of the ribosome may have a role in translational fidelity and/or codon recognition. Regardless of the mechanism that inhibited stop codon recognition, translational termination is vital to maintaining cellular homeostasis. These inhibitory effects demonstrated by ribosomal protein gene pseudo-haploinsufficiency may have deleterious downstream effects. Ultimately, these results suggest that decreased stop codon recognition may play an important role in the pathology of ribosomopathies.

Ribosomal protein gene pseudo-haploinsufficient yeast cells exhibit idiosyncratic effects during programmed translational recoding events

The effects of ribosomal protein gene haploinsufficiency on two aspects of translational recoding, -1 PRF and +1 PRF, were assayed in yeast cells that were pseudo-haploinsufficient for *RPS0*, *RPS14* or *RPS19.* A dual luciferase reporter assay that contained a recoding signal cloned in between the Renilla and Firefly Luciferase genes. The cloned recoding signals were derived from viral and cellular sources. One -1 PRF signals utilized here was derived from the yeast L-A virus (159, 214), and other -1 PRF signals were derived from yeast mRNAs encoding proteins involved in telomere maintenance (*CDC13, EST1, EST2, STN1*) (100). We employed two +1 PRF recoding signals, one derived from the yeast *OAZ1* mRNA and the other from the *Ty1* retrotransposable element (110, 116).

The results of these assays (Figure 26) revealed that the changes in -1 and +1 PRF recoding efficiencies are sequence and ribosomal protein gene paralog specific. For example, the loss of *RPS0A* (i.e. in RPS0AΔ cells) stimulated the -1 PRF recoding when directed by the CDC13 recoding element to 1.73 fold of wild-type. Conversely, the loss of *RPS0B* inhibited the -1 PRF recoding when directed by the CDC13 recoding element to 0.60 fold of wild-type (Figure 26A). When directed by the STN1 recoding element, the loss of *RPS0B* stimulated -1 PRF to 1.83 fold of wild-type and the loss of *RPS0A* had no effect. The deletion of either RPS0 paralog had no significant effect in -1 PRF recoding efficiencies when directed by the EST1 or EST2 -1

PRF recoding elements (Figure 26A). Only the loss of *RPS0A* exhibited any change in the translational recoding efficiency of the viral *LA* -1 PRF recoding signal, demonstrated in Figure 26A by a increase in -1 PRF recoding efficiency to 1.37 fold of wild-type. The deletion of *RPS0A* increased +1 PRF recoding efficiency when directed by either the *OAZ1* or *Ty1* recoding elements (2.20 and 1.46 fold wild-type, respectively). However, in yeast cells that lacked *RPS0B*, only the *OAZ1* recoding signal increased +1 PRF recoding efficiency to 1.68 fold of wild-type (Figure 26B).

RPS14 gene pseudo-haploinsufficiency exhibited idiosyncratic effects in -1 and +1 PRF recoding efficiencies. RPS14 gene pseudo-haploinsufficiency stimulated -1 PRF when directed by the EST1 recoding element to 3.65 and 2.21 fold of wild-type for RPS14AΔ and RPS14BΔ, respectively (Figure 26C). The loss of *RPS14A* paralog inhibited -1 PRF recoding to 0.46 and 0.58 fold of wild-type when directed by the CDC13 and EST2 recoding signals, respectively. Only the loss of *RPS14B* demonstrated a reduced -1 PRF, 0.62 fold wild-type, when directed by the STN1 recoding signal (Figure 26D). *RPS14* gene pseudo-haploinsufficiency exhibited no significant change in +1 PRF recoding efficiency whether directed by the *OAZ1* or the *Ty1* recoding element (Figure 26D).

RPS19 gene pseudo-haploinsufficiency revealed that the effects of programmed frameshift recoding to be paralog specific. *RPS19* gene pseudo-haploinsufficiency increased -1 PRF recoding efficiencies when directed by the STN1 recoding element to 1.51 and 3.06 fold of wild-type for RPS19AΔ

and RPS19BΔ, respectively (Figure 26E). The loss of *RPS19B* increased -1 PRF recoding efficiencies to 1.61 and 1.57 fold of wild type for the LA and EST1 recoding signals, respectively (Figure 26E). RPS19 gene pseudo-haploinsufficiency stimulated +1 PRF recoding when directed by the *Ty1* recoding signal to 1.35 and 1.76 fold of wild-type for RPS19AΔ and RPS19BΔ, respectively (Figure 26F). +1 PRF rates when directed by the *OAZ1* recoding element was shown to be unaffected by *RPS19* gene pseudo-haploinsufficiency (Figure 26F).

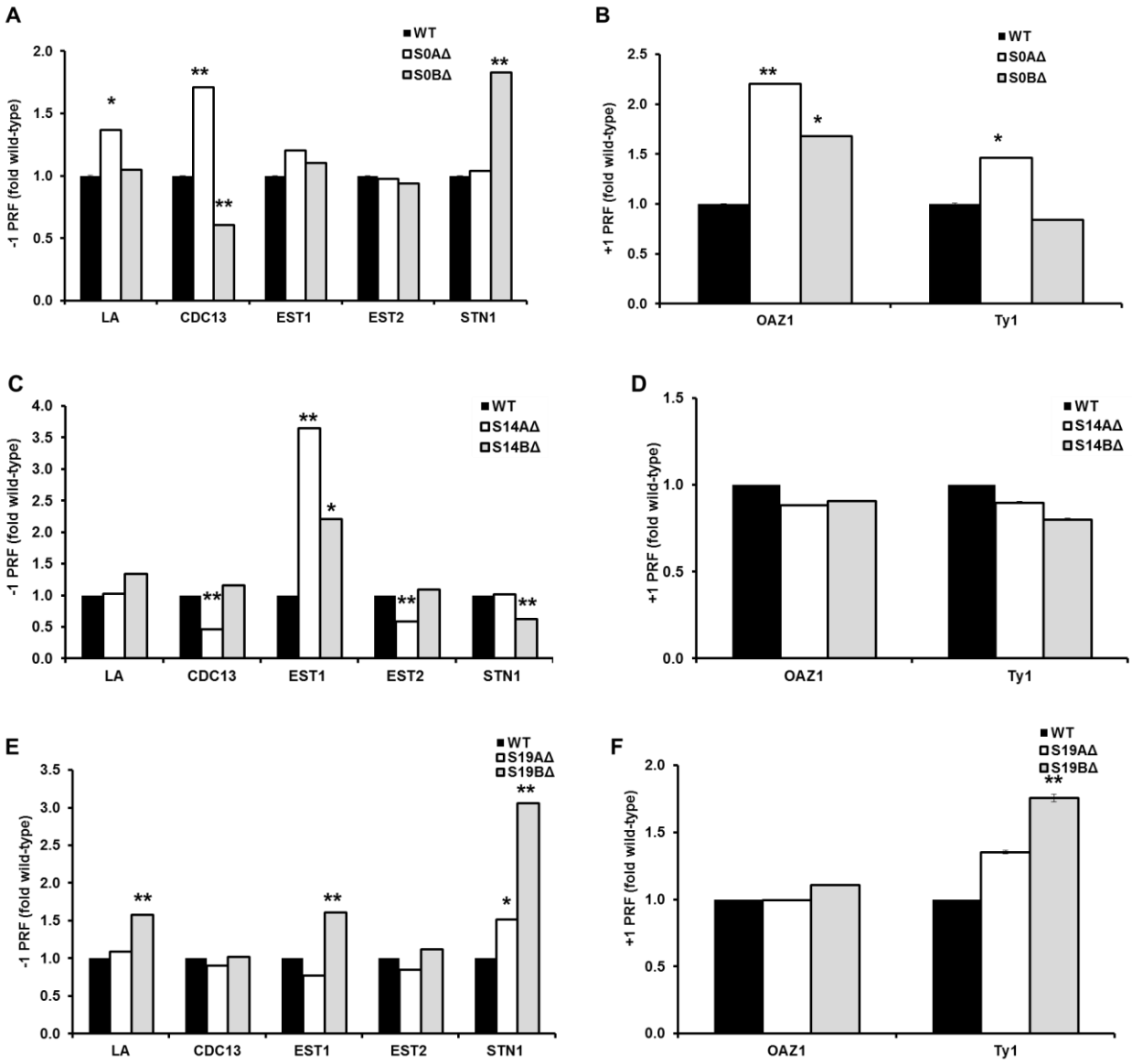

Figure 26. Dual Luciferase reporter assays to monitor -1 PRF and +1 PRF in single isoform knockout of RPS0, RPS14 and RPS19 *Saccharomyces cerevisiae* yeast cells.

-1 PRF was monitored using dual luciferase reporters (78) in isogenic *Saccharomyces cerevisiae* cells expressing the isogenic A gene deletion or the isogenic gene deletion. All assays were repeated to generate statistically meaningful results. +1 PRF rates were measured in yeast strains using frameshift signal derived from yeast Ty*1* retrotransposable element and *OAZ1*. Error bars denote standard error. All results are expressed as fold WT. *P < 0.05, **P < 0.01. Raw values can be found in Supplementary Table 1.

Ribosomal protein gene pseudo-haploinsufficiency exhibited idiosyncratic results when quantifying its effects on programmed frameshifting. The lack of any discernable trend suggested that changes in recoding efficiencies may be an effect of unique ribosomal composition interacting with specific recoding signals. The results did not offer any discernable mechanism but did suggest that ribosomal protein pseudo-haploinsufficient ribosomes may have downstream implications. The downstream effects would be due to the idiosyncratic responses to programmed frameshifting recoding signals which may alter gene expression.

Ribosomal protein gene pseudo-haploinsufficent yeast exhibit idiosyncratic effects in mRNA abundances of sequences that contain recoding elements

Recent studies revealed an inverse correlation between -1 PRF and steady state abundances of yeast telomere maintenance genes (100). A -1 PRF recoding event will direct the ribosome into an alternate reading frame and encounter a premature termination codon, triggering the nonsense mediated mRNA decay pathway (NMD). The nonsense mediated mRNA decay pathway functions to regulate the transcriptome by quickly degrading aberrant messages. The efficiency of the NMD surveillance pathway is highly contingent on translational termination or in other words, stop codon recognition (215, 216). The decreased stop codon results led to the hypothesis that the steady state mRNA abundances in ribosomal protein gene pseudo-haploinsufficient yeast would decrease global mRNA

abundance through Non-Stop Decay. This hypothesis would mean that this decreased stop codon recognition reduces the efficiency of NMD's role in regulating mRNA abundances.

Yeast telomere maintenance genes *CDC13*, *EST1*, *EST1* and *STN1* all contain bona fide -1 PRF signals. Recent studies of steady state mRNA abundances of these genes revealed a stochastic correlation to maintaining telomere length (100), linking recoding rates and biological function. Endogenous *EST3*, also a component of the telomere holoenzyme, and *OAZ1*, a ornithine decarboxylase antizyme, were probed to quantify the effects of ribosomal protein gene pseudo-haploinsufficiency on steady state mRNA abundances of messages containing +1 PRF recoding elements (112, 114, 116). The steady state mRNA abundances were then determined by qRT-PCR with U3 snoRNA as the loading control.

RPS0 gene pseudo-haploinsufficiency generally promoted decreased steady state mRNA abundances for messages that contained frameshift recoding signals. Quantitative Real Time PCR assays revealed that the loss of either paralog of RPS0 decreased mRNA abundance of messages that contained a -1 PRF recoding element to approximately half of wild-type. The mRNA abundance of EST1, EST2, and STN1 were decreased to 0.46, 0.48, 0.36 fold of wildtype for RPS0Δ yeast cells. In RPS0BΔ yeast cells, the mRNA abundance for EST1, EST2, and STN1 were decreased to 0.43, 0.47, 0.39 fold of wildtype, respectively. The exception to this trend was CDC13*,* a yeast telomere length maintenance gene that harbored a -1 PRF recoding element,

which exhibited an increase in mRNA abundance to 2.45 and 2.31 fold of wild-type for RPS0AΔ and RPS0BΔ respectively (Figure 27A). *RPS0* gene pseudo-haploinsufficiency decreased the steady state mRNA abundances of messages containing +1 PRF recoding elements to less than half of wild-type (Figure 27A). RPS0AΔ yeast cells exhibited a decreased mRNA abundance that were 0.22 and 0.48 fold of wildtype for EST3 and OAZ1 respectively. The loss of RPS0BΔ decreased mRNA abundance of EST3 and OAZ1 to 0.19 and 0.54 fold of wildtype, respectively.

RPS14 gene pseudo-haploinsufficiency demonstrated sequence and paralog specific effects in mRNA abundances of messages containing any frameshift-type recoding element. The most noticeable effect was the change in the steady state mRNA abundance of CDC13. *RPS14* gene pseudo-haploinsufficiency increased CDC13 mRNA abundance to 3.8 and 5.6 fold of wild-type for RPS14AΔ and RPS14BΔ, respectively (Figure 27B). Of the remaining -1 PRF probes, only STN1 exhibited significant decreased mRNA abundances (0.58 and 0.72 fold of wild-type for RPS14AΔ and RPS14BΔ respectively). Of the two +1 PRF probes, *RPS14* gene pseudo-haploinsufficiency demonstrated a significantly decreased mRNA abundance for the EST3 message, which was decreased to 0.34 and 0.43 fold of wild-type for RPS14AΔ and RPS14BΔ respectively. However, or the OAZ1 +1 PRF probe, only the loss of *RPS14A* resulted in a decrease in mRNA abundance to 0.69 fold of wild-type (Figure 27B).

RPS19 gene pseudo-haploinsufficiency revealed a global decrease in steady state mRNA abundances. The loss of either *RPS19* paralog decreased the steady state mRNA abundance to less than half of the wild-type control (Figure 27C). The mRNA abundances of CDC13, EST1, EST2 and STN1 were decreased to 0.40, 0.62, 0.51 and 0.48 fold of wild-type, respectively, for RPS19AΔ yeast cells. RPS19BΔ yeast cells exhibited a decrease in mRNA abundance to 0.16, 0.22, 0.17 and 0.20 fold of wild-type for CDC13, EST1, EST2 and STN1, respectively (Figure 27C). Messages that contained +1 PRF recoding signals demonstrated a global decrease of mRNA abundance in *RPS19* gene pseudo-haploinsufficient yeast cells. The loss of *RPS19A* decreased the mRNA abundance of EST3 and OAZ1 to 0.74 and 0.41 fold of wildtype, respectively. The loss of *RPS19B* decreased the mRNA abundance of EST3 and OAZ1 to 0.25 and 0.13 fold of wildtype, respectively (Figure 27C).

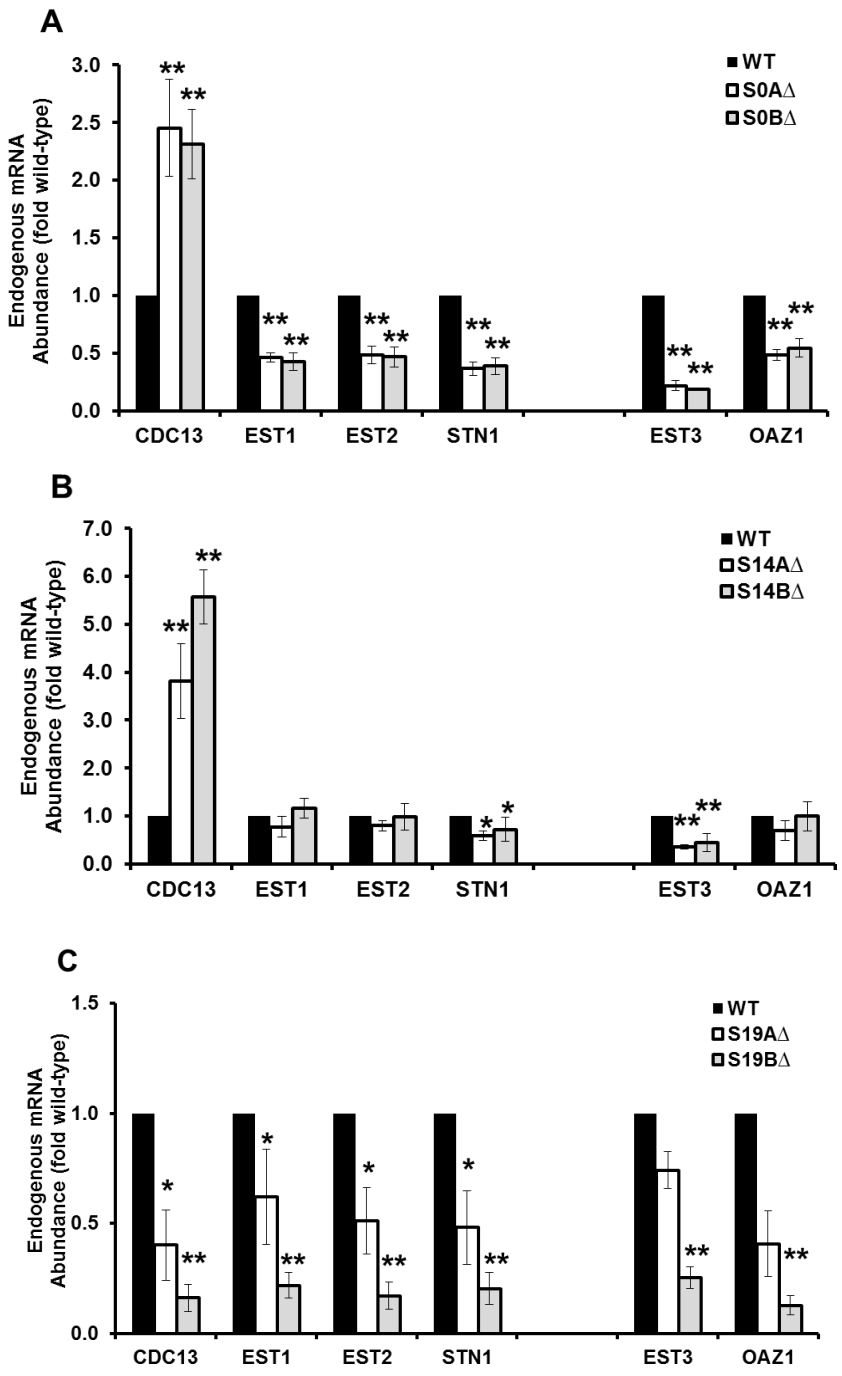

Figure 27. qualitative Real Time Polymerase Chain Reaction (qRT-PCR) to measure steady state mRNA abundances of yeast telomere length messages and messages containing translational recoding signals

Steady-state endogenous abundances of *CDC13, EST1*, *EST2*, *STN1*, *EST3* and *OAZ1* mRNAs were monitored using quantitative RT-PCR in yeast strains. Error bars denote standard error. *P < 0.05, **P < 0.01. Exact and student t-test values can be found in Supplementary Table 4-5.

The results did not support the original hypothesis. *RPS0* and *RPS14* gene pseudo-haploinsufficiency exhibited similar but idiosyncratic mRNA abundances while RPS19 gene pseudo-haploinsufficient yeast demonstrated a global decrease in mRNA abundance of messages that contain frameshift recoding signals. The absence of any discernable trend of frameshifting rates in Figure 26 and in conjunction with inhibited stop codon recognition rates as shown in Figure 25, lead to the question whether the efficiencies of mRNA decay mechanisms were altered by ribosomal protein gene pseudo-haploinsufficiency.

Ribosomal protein gene pseudo-haploinsufficiency decreases the mRNA abundances of sequences that are substrates for Nonsense Mediated Decay (NMD)

Saccharomyces cerevisiae yeast cells that are ribosomal protein gene pseudo-haploinsufficient do not follow the inverse correlation between -1 PRF efficiencies and mRNA abundance. The increased CDC13 mRNA abundance found in *RPS0* and *RPS14* gene pseudo-haploinsufficient yeast cells (Figure 27A and B) led to the question whether the Nonsense Mediated Decay pathway was affected. However, as the dual luciferase reporter assays revealed an overall decrease in stop codon recognition and the fact that the efficiency of the NMD surveillance pathway is highly contingent on translational termination or in other words, stop codon recognition (215, 216). We developed a hypothesis that the inhibited stop codon recognition directed the ribosome to bypass the premature termination codons, continue elongating to the 3’ end of the message and stall at the polyA tail. The stalled

ribosome at the polyA tail of the message would then elicit mRNA degradation via the NSD pathway instead of the NMD pathway. RPS19 gene pseudo-haploinsufficiency qRT-PCR results support this hypothesis.

Messages that were natural targets for decay via NMD were selected to test whether the NMD surveillance pathway was inhibited by ribosomal protein gene pseudo-haploinsufficiency. Messenger RNAs that contain uORFs are natural substrates for NMD. *GCN4* (a transcriptional activator (213)), *CPA1* (a component of the carbamoyl phosphatase synthetase (217)) and *NMD4* (a component of the NMD mechanism (218)) are known yeast NMD substrates due to their mRNAs containing uORFs which triggers the NMD surveillance pathway and regulates their mRNA abundances (219–222).

RPS0 gene pseudo-haploinsufficiency conferred a global decrease in mRNA abundances of messages that containing uORFs and are substrates for NMD. Multiple uORFs destabilize the GCN4 mRNA and decreased the steady state mRNA abundance to ~0.23 fold relative to wild-type. RPS0 gene pseudo-haploinsufficiency decreased the steady state mRNA abundances of messages containing a single uORF; CPA1 mRNA abundance was decreased to 0.31 and 0.43 fold of wild-type for RPS0AΔ and RPS0BΔ, respectively. The mRNA abundance of NMD4 was decreased to 0.30 and 0.35 fold of wild-type for RPS0AΔ and RPS0BΔ, respectively (Figure 28A).

RPS14 gene pseudo-haploinsufficient yeast cells exhibited similar steady state mRNA abundances patterns to RPS0 gene pseudo-

haploinsufficient yeast cells. The presence of multiple uORFs decreased the GCN4 message to 0.32 and 0.38 fold of wild-type for RPS14AΔ and RPS14BΔ, respectively (Figure 28B). Messages that contain single uORFs also exhibited decreased mRNA abundances; CPA1 mRNA abundance was decreased to 0.48 fold of wild-type for RPS14AΔ while RPS14BΔ exhibited a 0.87 fold of wildtype decrease. *RPS14* gene pseudo-haploinsufficiency decreased the mRNA abundance of NMD4 to 0.46 and 0.57 fold of wild-type for RPS14AΔ and RPS14BΔ, respectively (Figure 28B).

RPS19 gene pseudo-haploinsufficient yeast cells demonstrated a global decrease in mRNA abundance that was paralog specific. The loss of the *RPS19B* paralog resulted in an mRNA abundance that was half of that found in RPS19AΔ yeast cells (Figure 28C). The GCN4 message was decreased to 0.60 and 0.27 fold of wild-type for RPS19AΔ and RPS19BΔ, respectively (Figure 28C). Messages that contained single uORF exhibited similar mRNA abundance decreases in *RPS19* gene pseudo-haploinsufficient yeast. The mRNA abundance for CPA1 was decreased to 0.58 and 0.16 fold of wild-type for RPS19AΔ and RPS19BΔ, respectively. NMD4 mRNA abundance was decreased to 0.49 and 0.19 fold of wild-type for RPS19AΔ and RPS19BΔ, respectively (Figure 28C).

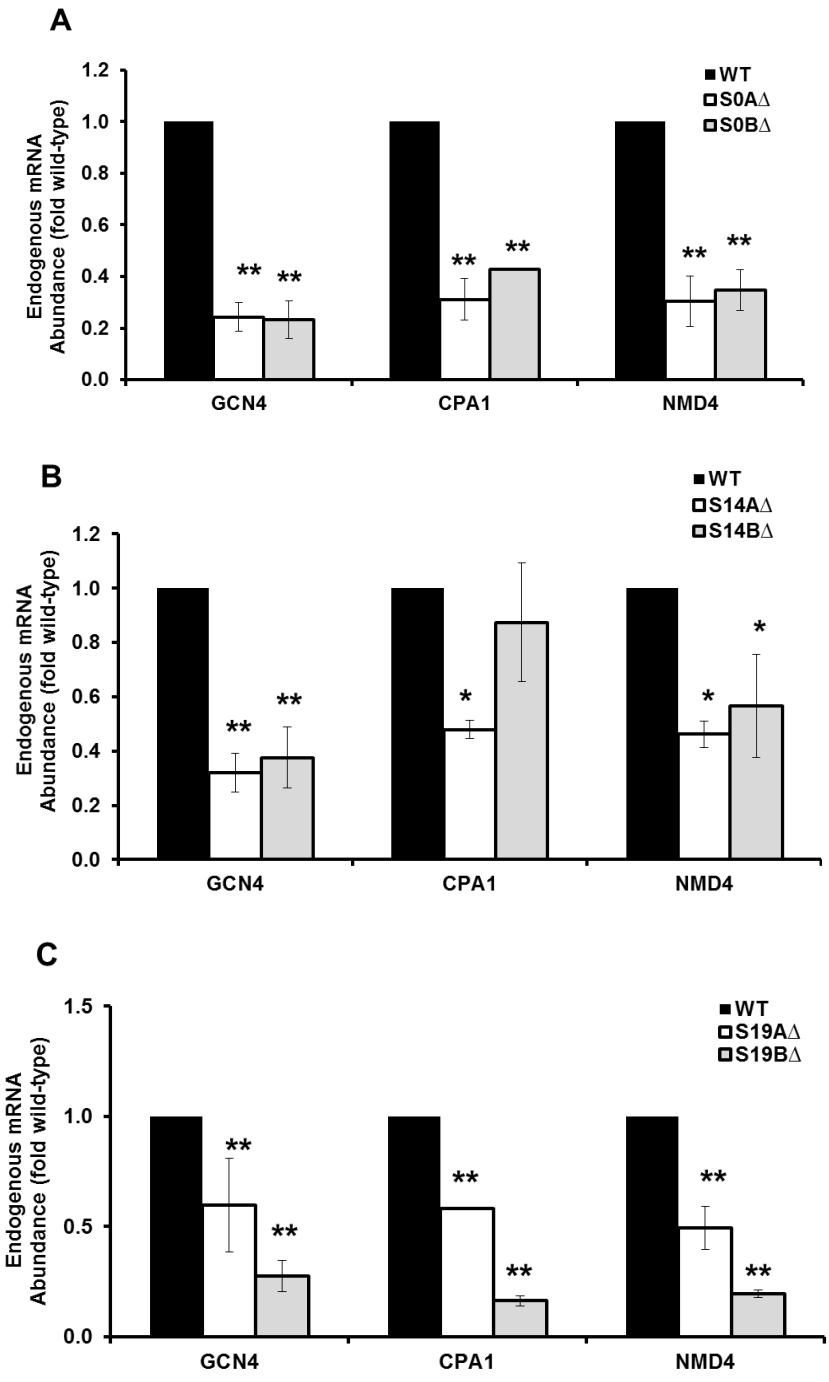

Figure 28. qualitative Real Time Polymerase Chain Reaction (qRT-PCR) to measure steady state mRNA abundances of substrates for NMD

Steady-state mRNA abundances of the endogenous messages containing elements that trigger the NMD surveillance pathway; *GCN4*, CPA1, and NMD4 were monitored using quantitative RT-PCR in yeast strains. Error bars denote standard error. *P < 0.05, **P < 0.01. Exact and student t-test values can be found in Supplementary Table 4-5.

All ribosomal protein gene pseudo-haploinsufficient yeast revealed a global decrease in mRNA abundance of messages that were substrates for NMD. Regardless of which paralog is deleted in *RPS0* and *RPS14* gene pseudo-haploinsufficient yeast cells, both exhibited similar decreases in mRNA abundances of messages that were substrates for NMD. Only RPS19 gene pseudo-haploinsufficient yeast exhibited paralog-specific decreases in these messages. These results are suggestive of either increased global mRNA decay activity or an increase in mRNA decay of specific messages, i.e. those that contain elements that are substrates for either NMD, NSD or NGD.

Ribosomal protein gene pseudo-haploinsufficiency confers sequence specific effects to mRNA abundances of housekeeping messages

The messages examined thus far all have elements that destabilize their mRNAs. Subsequently, the question became whether ribosomal protein pseudo-haploinsufficiency would affect the steady state mRNA abundances of messages that are inherently stable, i.e. transcripts that do not contain elements that direct the message to one of the three mRNA surveillance pathways. New targets were selected on the basis of their stability and "housekeeping" roles in the yeast cell; *ACT1* encodes for actin, an essential cytoskeletal element that is used in many cellular processes (223). *BRR6* encodes for an essential nuclear envelope integral membrane protein (224). *HOM3* encodes for an aspartate kinase (225). *PGK1* encodes for a

phosphoglycerate kinase, an enzyme used for glycolysis (226). *TUB1* encodes for alpha-tubulin which polymerizes to form microtubules (227).

RPS0 gene pseudo-haploinsufficiency continued to demonstrate message specific effects in mRNA abundances of messages lacking elements that trigger mRNA decay pathways. The mRNA abundance of ACT1 was decreased to 0.57 and 0.41 fold of wild-type for RPS0AΔ and RPS0BΔ, respectively (Figure 29A). *RPS0* gene pseudo-haploinsufficiency decreased the mRNA abundance of BRR6 to 0.50 fold of wild-type for both RPS0AΔ and RPS0BΔ. HOM3 was decreased to 0.43 and 0.67 fold of wild-type for RPS0AΔ and RPS0BΔ, respectively. The mRNA abundance of PGK1, a highly stable message, was decreased to 0.22 and 0.17 fold of wild-type for RPS0AΔ and RPS0BΔ, respectively. Unlike the other messages, *RPS0* gene pseudo-haploinsufficiency increased the mRNA abundances of TUB1 to 1.34 fold of wild-type for RPS0AΔ and exhibited no mRNA abundance change in RPS0BΔ yeast cells.

RPS14 gene pseudo-haploinsufficient yeast demonstrated sequence specific mRNA abundance effects. RPS0AΔ yeast did not cause any change in ACT1 mRNA abundance, but the loss of *RPS0B* decreased ACT1 mRNA abundance to 0.72 fold of wild-type (Figure 29B). The mRNA abundance of BRR6 was reduced to 0.60 and 0.70 fold of wild-type for RPS14AΔ and RPS14BΔ, respectively. *RPS14* gene pseudo-haploinsufficiency exhibited paralog specific effects on the mRNA abundances for HOM3; the loss of the *RPS14A* paralog decreased the mRNA abundance to 0.68 fold of wild-type

while the loss of *RPS14B* increased the mRNA abundance to 1.44 fold of wild-type (Figure 29B). The mRNA abundance of the stable PGK1 message was decreased to 0.48 and 0.56 fold of wild-type for RPS14AΔ and RPS14BΔ, respectively (Figure 29B). Unlike the other messages, *RPS14* gene pseudo-haploinsufficiency increased the mRNA abundance of TUB1 to 2.64 and 3.18 fold of wildtype for RPS14AΔ and RPS14BΔ, respectively (Figure 29B).

RPS19 gene pseudo-haploinsufficient continued to demonstrate a decreased steady-state mRNA abundances for all messages. RPS19 gene pseudo-haploinsufficiency decreased the mRNA abundances for all housekeeping messages (Figure 29C). The mRNA abundance of ACT1 was reduced to 0.50 and 0.19 fold wild-type for RPS19AΔ and RPS19BΔ, respectively. The mRNA abundance of BRR6 decreased to 0.58 and 0.27 fold of wild-type for RPS19AΔ and RPS19BΔ, respectively. The mRNA abundance of HOM3 decreased to 0.53 and 0.22 fold of wild-type for RPS19AΔ and RPS19BΔ, respectively. The stable PGK1 exhibited a decrease in mRNA abundance to 0.37 and 0.26 fold of wild-type for RPS19AΔ and RPS19BΔ, respectively. TUB1 mRNA abundances were reduced to 0.49 and 0.23 fold of wild-type for RPS19AΔ and RPS19BΔ, respectively.

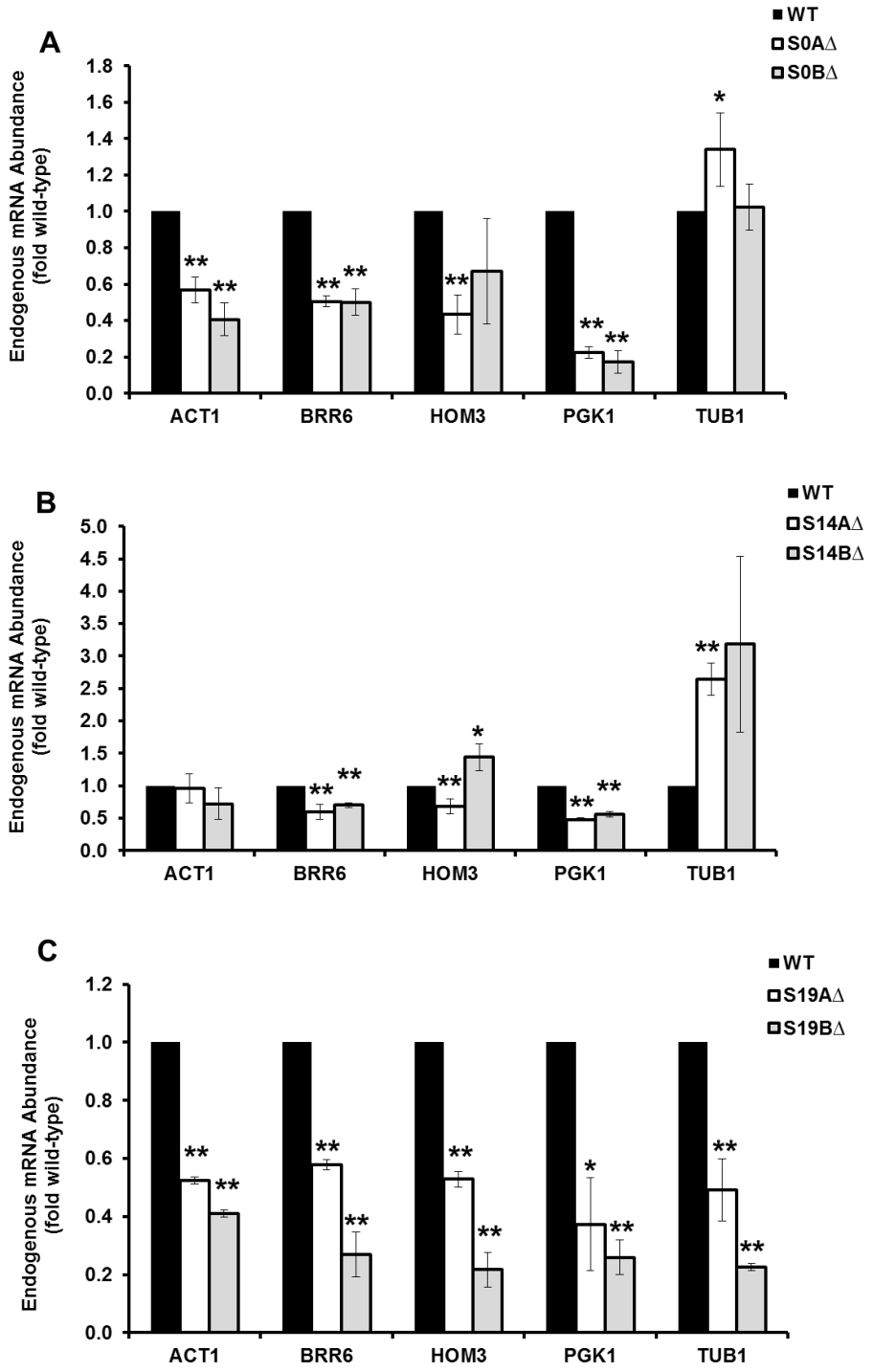

Figure 29. qualitative Real Time Polymerase Chain Reaction (qRT-PCR) to measure steady state mRNA abundances of housekeeping messages that are substrates for NMD and stable messages.

Steady-state mRNA abundances of endogenous *ACT1*, *BRR6*, *HOM3*, *PGK1*, and *TUB1* were monitored using quantitative RT-PCR in yeast strains. Error bars denote standard error. *P < 0.05, **P < 0.01. Exact and student t-test values can be found in Supplementary Table 4-5.

Ribosomal protein gene pseudo-haploinsufficiency decreases total mRNA abundances for sequences that code for ribosomal proteins

Ribosomal protein pseudo-haploinsufficient yeast demonstrate a general trend of decreased mRNA abundances globally. Only *RPS19* gene pseudo-haploinsufficiency exhibits a total global decrease in mRNA abundance of all messages probed via qRT-PCR. *RPS0* and *RPS14* gene pseudo-haploinsufficient yeast have exhibited increased mRNA abundances in specific messages. Expression of ribosomal proteins are coordinated in a stochastic ratio necessary for ribosomal assembly (19). This lead to the question whether RP pseudo-haploinsufficiency down regulated all messages or if pseudo-haploinsufficiency confers unique coordinated expression of proteins. Probes were designed to quantify total mRNA abundance of each of the three selected ribosomal proteins, while not differentiating between paralogs. The isogenic wild-type yeast cell was determined the norm control and the U3 snoRNA as the loading control. Each yeast strain was quantified for the total mRNA abundance for RPS0, RPS14 and RPS19 to determine if the change in mRNA abundance would consistent between paralogs and revealed demonstrated a coordinated effect.

RPS0 gene pseudo-haploinsufficient yeast cells revealed a similar decrease in mRNA abundance in all probed RP mRNAs. The mRNA abundance for RPS0 was decreased to 0.20 and 0.15 fold of wild-type for RPS0AΔ and RPS0BΔ, respectively. The mRNA abundance for RPS14 in *RPS0* gene pseudo-haploinsufficient yeast was decreased to 0.26 and 0.22

fold of wild-type. The mRNA abundance of RPS19 in *RPS0* gene pseudo-haploinsufficient yeast cells was decreased to 0.26 and 0.21 fold of wild-type (Figure 30A).

RPS14 gene pseudo-haploinsufficient yeast cells continued to demonstrate similar global decreased RP mRNA abundances. The mRNA abundance for RPS0 was decreased to 0.46 and 1.52 fold of wild-type for RPS14AΔ and RPS14BΔ, respectively. The mRNA abundance for RPS14 was found to be 0.22 and 0.36 fold of wild-type, and similar to the mRNA abundance of RPS0 and RPS14, RPS19 demonstrated a decrease to 0.36 and 0.35 fold of wild-type (Figure 30B).

Like *RPS0* and *RPS14* gene pseudo-haploinsufficiency, *RPS19* gene pseudo-haploinsufficient yeast cells demonstrated global decreased RP mRNA abundances. However, the extent of the decrease was paralog specific. Similar to previous qRT-PCR data, *RPS19* gene pseudo-haploinsufficient yeast cells continued to demonstrate a pattern where the loss of *RPS19B* resulted in a quantified mRNA abundance that would be roughly half to the mRNA abundance of the same message in *RPS19A* gene pseudo-haploinsufficient yeast cells. The mRNA abundance for RPS0 was found to be 0.82 and 0.42 fold of wild-type for RPS19AΔ and RPS19BΔ, respectively. The mRNA abundance of RPS14 decreased to 0.75 and 0.37 fold of wild-type for RPS19AΔ and RPS19BΔ, respectively. However, the mRNA abundance for RPS19 demonstrated a decrease that was 0.73 and 0.02 fold of wild-type for RPS19AΔ and RPS19BΔ, respectively (Figure 30C).

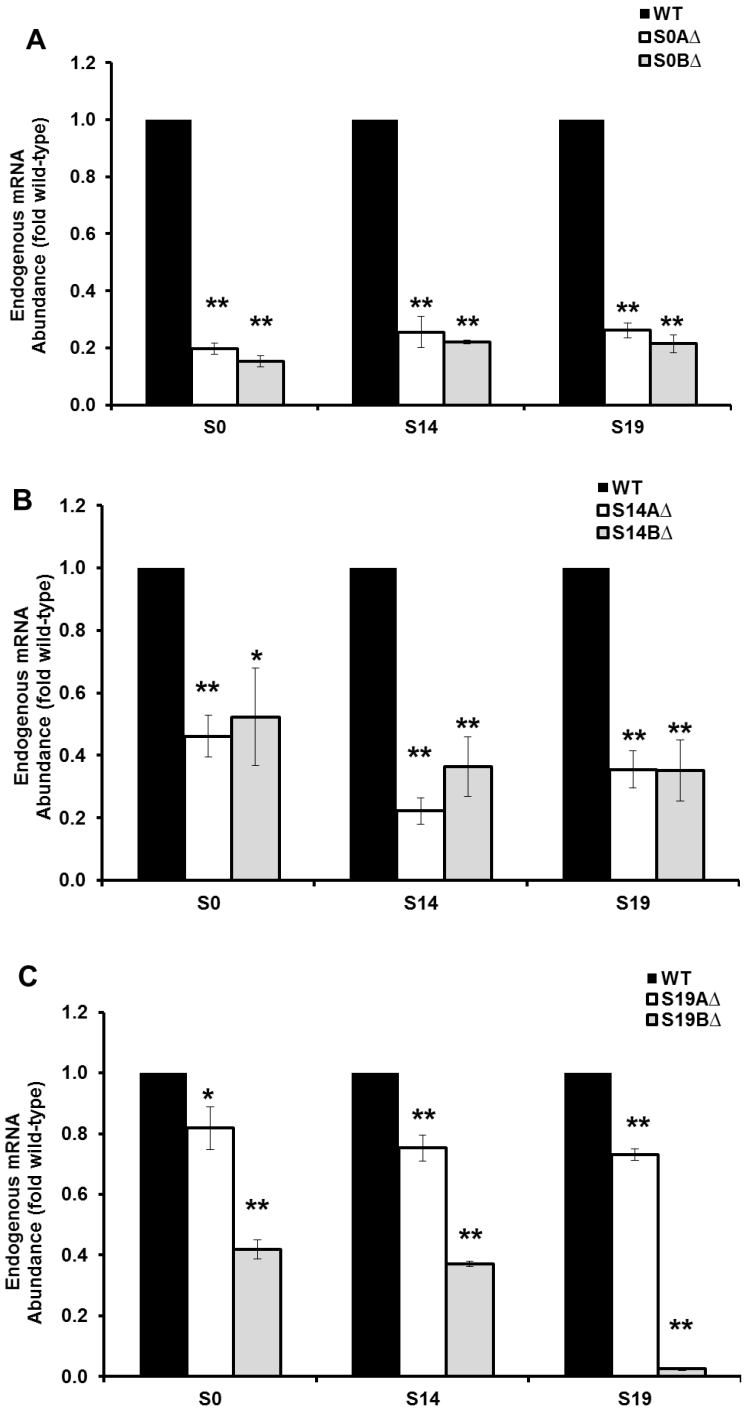

Figure 30. qualitative Real Time Polymerase Chain Reaction (qRT-PCR) to measure the global steady state mRNA abundances of ribosomal protein messages

Steady-state mRNA abundances of endogenous RPS0, RPS14 and RPS19 were monitored using quantitative RT-PCR in yeast strains. Error bars denote standard error. *P < 0.05, **P < 0.01. Exact and student t-test values can be found in Supplementary Table 4-5.

All ribosomal protein gene pseudo-haploinsufficient yeast cells demonstrated a decrease in global RP mRNA abundances. The results showed that, except for RPS19BΔ yeast, reduced ribosomal protein expression conferred a coordinated expression of other ribosomal proteins to similar mRNA abundances. This suggests that, at least in the yeast model, ribosomopathies may have a selective and coordinated expression of messages.

Ribosomal protein gene pseudo-haploinsufficient yeast cells present mRNA abundances characteristic of cellular stress and increased ribosomal turnover

The messages examined thus far all have elements that destabilize their mRNAs. Subsequently, the question became whether ribosomal protein pseudo-haploinsufficiency would affect the steady state mRNA abundances of messages that are inherently stable, i.e. transcripts that do not contain elements that direct the message to one of the three mRNA surveillance pathways. New targets were selected on the basis of being affected by cellular stress, high ribosomal turnover and increased ribosomal biogenesis. *ADE4* encodes for a protein that catalyzes first step of the 'de novo' purine nucleotide biosynthetic pathway (228) and would be upregulated in scenarios with high ribosomal turnover and increased ribosomal biogenesis. *CCR4* encodes for a dominant polydeadenylase, an essential component for mRNA degradation (229). *HAC1* encodes for a transcriptional activator that is involved in the unfolded protein response where ribosomes that are stalled in the 3’-UTR region of the mRNA trigger the No-Go Decay pathway (230).

LUC7 encodes for an essential protein associated with the U1 snRNP complex (231, 232), and *PRP8* encodes for an component of U4/U6-U5 snRNP complex (233–235).

RPS0 gene pseudo-haploinsufficiency continued to have message specific effects on mRNA abundances. *RPS0* gene pseudo-haploinsufficiency increased mRNA abundances for ADE4 to 3.69 and 2.38 fold of wild-type for RPS0AΔ and RPS0BΔ respectively. The mRNA abundance of CCR4 was increased to 4.84 and 4.19 fold wild-type for RPS0AΔ and RPS0BΔ respectively (Figure 31A). Only RPS0BΔ had a significant increase in the mRNA abundance of HAC1, 1.44 fold of wild-type, while RPS14AΔ exhibited an increase of 1.11 fold of wild-type. RPS0AΔ yeast cells revealed no change in mRNA abundance of LUC7 while RPS0BΔ yeast decreased the mRNA abundance of LUC7 to 0.83 fold of wild-type (Figure 31A). *RPS0* gene pseudo-haploinsufficiency increased the mRNA abundance of PRP8 to 4.15 and 3.69 fold of wild-type for RPS0AΔ and RPS0BΔ respectively.

RPS14 gene pseudo-haploinsufficient yeast demonstrated an overall increase in mRNA abundance. The extent of the increase in mRNA abundance were sequence specific. The mRNA abundance of ADE4 was increased to 7.79 and 6.64 fold of wild-type for RPS14AΔ and RPS14BΔ, respectively (Figure 31B). *RPS14* gene pseudo-haploinsufficiency increased the mRNA abundance of CCR4 to 5.47 and 6.49 fold of wild-type for RPS14AΔ and RPS14BΔ, respectively. The mRNA abundance of HAC1 was increased to 1.94 and 1.86 fold of wild-type for RPS14AΔ and RPS14BΔ,

respectively. LUC7 mRNA abundances were increased to 1.22 and 1.57 fold of wild-type for RPS14AΔ and RPS14BΔ, respectively. RPS14 gene pseudo-haploinsufficient yeast demonstrated a large increase in the mRNA abundance of PRP8, 7.32 and 8.02 fold of wild-type RPS14AΔ and RPS14BΔ, respectively.

RPS19 gene pseudo-haploinsufficient yeast cells continued to demonstrate a global decrease in mRNA abundances for all messages. The extent of this decrease in mRNA abundance also continued to be paralog-specific. *RPS19* gene pseudo-haploinsufficiency decreased the mRNA abundances of ADE4 to 0.50 and 0.19 fold of wild-type for RPS19AΔ and RPS19BΔ, respectively (Figure 31C). The mRNA abundance of CCR4 was decreased to 0.50 and 0.12 fold of wild-type for RPS19AΔ and RPS19BΔ, respectively. HAC1 mRNA abundances were reduced to 0.33 and 0.12 fold of wild-type in RPS19AΔ and RPS19BΔ yeast cells, respectively. The mRNA abundances of LUC7 decreased to 0.41 and 0.17 fold of wild-type for RPS19AΔ and RPS19BΔ, respectively. PRP8 mRNA abundances were decreased to 0.26 and 0.13 fold of wild-type in RPS19AΔ and RPS19BΔ yeast cells, respectively (Figure 31C).

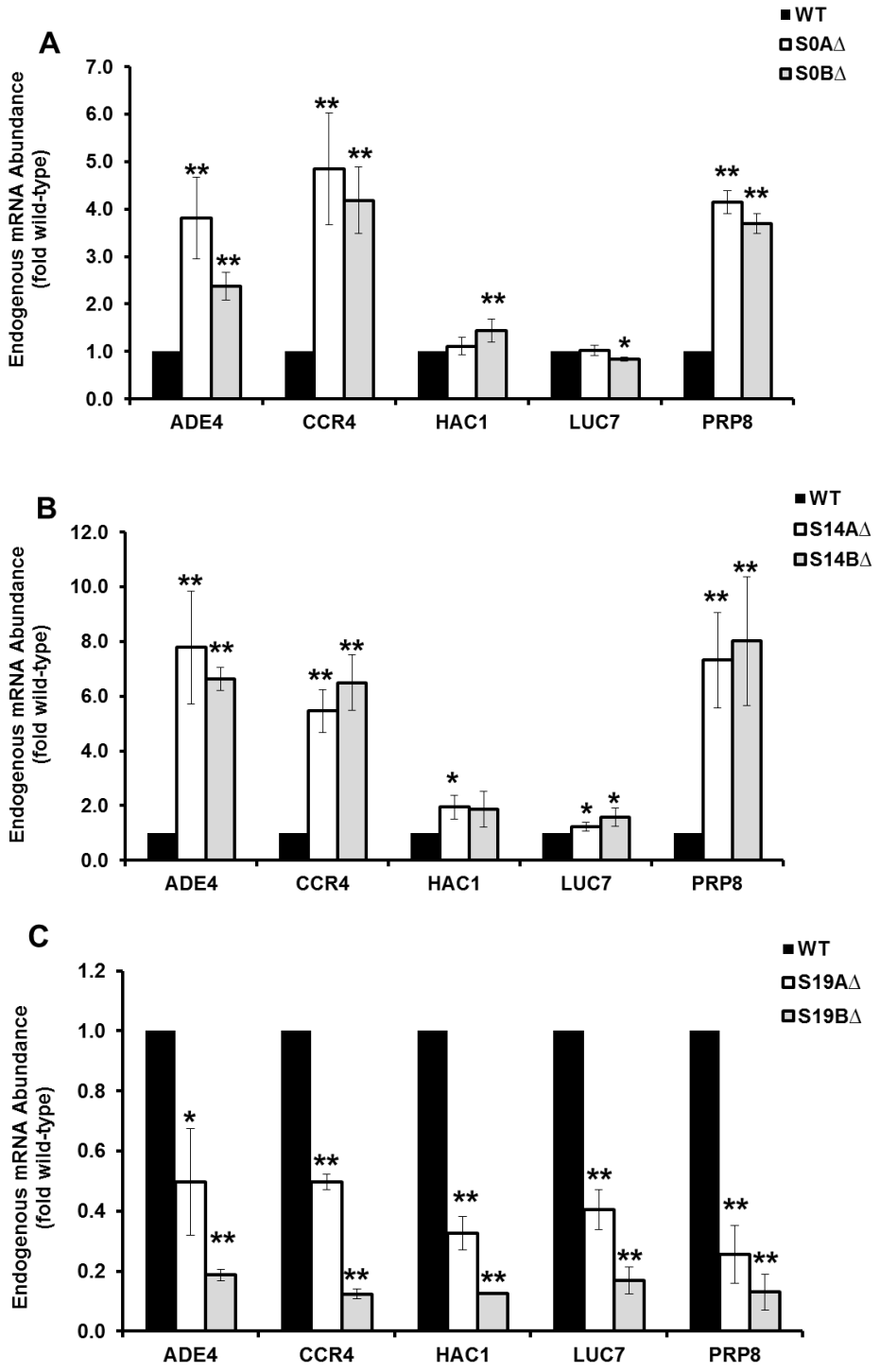

Figure 31. qualitative Real Time Polymerase Chain Reaction (qRT-PCR) to measure steady state mRNA abundances of messages associated to cellular stress and ribosomal turnover

Steady-state mRNA abundances of endogenous ADE4, CCR4, HAC1, LUC7, PRP8 were monitored using quantitative RT-PCR in yeast strains. Error bars denote standard error. *P < 0.05, **P < 0.01. Exact and student t-test values can be found in Supplementary Table 4-5.

RPS0 and *RPS14* gene pseudo-haploinsufficient yeast demonstrated strikingly similar effects on mRNA abundances. RPS0 and RPS14 gene pseudo-haploinsufficiency demonstrated an upregulation of messages associated to cellular stress and ribosomal turnover. These two RP gene pseudo-haploinsufficient yeast strains increased the mRNA abundance of ADE4, CCR4 and PRP8. The qRT-PCR studies revealed that CCR4 has an at least 4 fold increase in mRNA abundance relative to WT, this upregulation may be due to an elicited response to the need for an increased degradation of mRNAs. These messages could be upregulated during cellular stress conditions; where ribosomal turnover rates are high and messages are degraded rapidly. This would promote the need for increased transcription, i.e. increased adenine synthesis (ADE4), and increased splicing of messages (LUC7 and PRP8). The mRNA abundance of HAC1 was increased in RPS0 or RPS14 gene pseudo-haploinsufficient yeast. HAC1 is used as a proxy for NSD and the slight increase in mRNA abundance of this message relative to wild-type suggests that this upregulation is due to increased unfolded protein response. These results suggests that *RPS0* or *RPS14* pseudo-haploinsufficient ribosomes cannot terminate properly and the ribosome, along with the message, are rapidly degraded.

Chapter 3: Discussion/Conclusions and Future Directions

In the central dogma of molecular biology, translation is a late process that occurs between mRNA synthesis and protein degradation. Translation is a complex process which involves the rapid and high-fidelity interactions of the mRNA, the ribosome and complementary GTPases that deliver amino-acylated tRNAs to the ribosome and translocation along the message. Faithful translation of the mRNA ensures the proper propagation of genetic information essential to cellular homeostasis. Translation of genetic information can be influenced by rRNA post-transcriptional modifications that induce translational recoding events which modulates cellular gene expression (113, 155, 236). The translational apparatus has a system of checks and balances for regulating cellular homeostasis. The translational machinery has evolved mechanisms to ensure degradation of messages that harbor errors that may produce deleterious effects. In investigating translational recoding, e.g. -1 PRF, it was discovered these recoding events can be used as a means to regulate mRNA abundances and gene expression by directing the message to a nonsense codon that elicits the nonsense mediated decay mechanism to degrade the message (98).

A new class of diseases is now gaining attention. Ribosomopathies are characterized by congenital or somatically acquired mutations of a ribosomal factor that leads to ribosomal dysfunction. Studies show that altering the composition (both quantity and quality) of ribosomal factors affect the

recoding efficiencies that in turn dysregulates gene expression (100, 156, 157, 159). Warner's work shows that the stoichiometric relationship between the rRNAs and ribosomal proteins is regulated by the cell to promote their equimolar assembly into ribosomes (19). According to this study, insufficiency or excess of any component may result in aberrant ribosomal protein processing and the disruption of ribosome production. However, we argue in this thesis that the etiology of ribosomopathies, at least in those that are caused by ribosomal protein gene haploinsufficiency, are attributed to altered translational fidelity, and are not wholly attributed to the diminished quantity of mature ribosomes.

The yeast *Saccharomyces cerevisiae* is a robust model system to investigate the etiology of ribosomopathies. The naturally duplicated ribosomal protein genes of haploid yeast cells provide us with the opportunity to use a pseudo-diploid model. One of the many defining characteristics that make yeast a model system is the ability to genetically manipulate the genome, generating yeast strains that contain single isoform knock out of ribosomal protein genes. This provided us a platform to investigate the effects of pseudo-haploinsufficiency of ribosomal proteins during translation.

Yeast ribosomal protein pseudo-haploinsufficient studies reveal defects in the translational machinery. Monitoring the translational fidelity of the ribosome via measuring translational recoding efficiencies, -1 PRF and +1 PRF efficiencies revealed isoform and sequence specific effects. However the major finding is that all of the pseudo-haploinsufficient ribosomes tested

exhibited increased stop codon readthrough. The largest effect of inhibited stop-codon recognition is evident during the GCN4 reporter assay which contains multiple uORFs. These results suggests an additive effect in stop codon readthrough efficiency of pseudo-haploinsufficient ribosomes. If the ribosome is directed to a premature termination codon, NMD–dependent mRNA degradation is contingent on stop codon recognition (215, 216). Probing the steady-state abundances of messages containing frameshift recoding elements (-1 and +1 PRF signals) revealed that pseudo-haploinsufficiency for RPS19 is unique in expressing a global decrease for all mRNA sequences, the extent of which is paralog-specific. Pseudo-haploinsufficiency for RPS0 and RPS14 exhibits a general decrease in mRNA abundance with the exception of a single mRNA, CDC13. The combination of the results from the dual luciferase reporter assays and the qRT-PCR assays, led us to the hypothesis that increased rates of stop codon readthrough increases the fraction of ribosomes that read through bona fide termination codons, leading to increased rates of NSD on all mRNAs. To test that hypothesis, we probed messages that contained uORfs that made the messages into substrates for NMD (GCN4, CPA1 and NMD4). We also investigated messages that were essential for cellular function but lacked elements that would make them targets for degradation (ACT1, BRR6, HOM3, PGK1, and TUB1). The results reveal that ribosomal protein pseudo-haploinsufficiency confers sequence and paralog specific effects on mRNA abundance. This is suggestive of a selective translational apparatus, a

property that is predicted to be associated with ‘specialized’ ribosomes. In support of this, preliminary results suggest that the translational fidelity defects exhibited by the ribosomal protein pseudo-haploinsufficiency are at least partially reproducible in the mammalian system. Specifically, our collaborator was able to generate a single copy knockout of RPS19 in HEK cells by using the CRISPR-Cas9 system. Mammalian cells containing a single copy of RPS19 exhibited increased stop codon readthrough rates.

The nature of ribosomopathies and the observations in pseudo-haploinsufficient yeast cells challenges our current understanding of the ribosome. Historically, the ribosome has been thought to be monolithic in nature, a singular and precise nanomachine capable of performing all translational functions perfectly. The observation that single ribosomal protein gene deletions in yeast exhibits idiosyncratic effects suggests that this is not necessarily the case. This indicates that each RP gene paralog represents a potential source of heterogeneity. It also forces the question, which is more plausible: that nature would select for n unique and functionally maximized machine with the ability to translate infinite mRNAs in response to an infinite number of stimuli? Or a system with the capacity to generate an infinite set of variations of the same machine, each endowed with its own idiosyncratic properties? Consider that within this heterogeneous population of ribosomes, there exists a minimum of 2^{78} variations, as eukaryotic genomes contain two copies of 78 protein genes, and each of the 4 rRNAs contain 212 potentially modified bases (212!). The two combined generates a potentially infinite

number of different ribosomal compositions and each with its own idiosyncratic property. Supposing that it is the latter, there are three implications. First, ribosomal factor haploinsufficiency leads to the unique functional loss for that the ribosomal factor would have otherwise served. Second, the subset of ribosomes that are missing the ribosomal factor or possesses a mutated form of it are translationally dysfunctional and the altered translational fidelity of these ribosomes will disrupt normal decay mechanisms that will result in differential gene expression. Finally, the differential gene expression begins a domino effect in the cell which ultimately leads to the clinical presentation of the ribosomopathy associated to the initial ribosomal factor gene. Hematopoiesis and neuronal tissue differentiation relies on gene expression to regulate tissue proliferation and differentiation, processes that are wholly contingent on ribosomal translational fidelity and mRNA decay mechanisms (153, 237). Our argument posits that specific tissues require ribosomes capable of specific translational patterns in order to regulate gene expression to promote cellular differentiation. When genes that encode ribosomal factors capable of regulating gene expression are missing or mutated, these tissues cannot sufficiently differentiate or develop into adult cells. As applied to more complex organisms, the hypothesis that differential ribosomal composition is required to promote tissue specific cell differentiation, it also provides a medium upon which selective processes can work.

Environmental conditions can exert influence on cellular gene expression. Ribosomal assembly is an energetically expensive process under normal conditions and can be influenced by cellular stress conditions as a response to maintain cellular homeostasis. In the monolithic ribosomal model, in order to respond to changes in environmental factors, another layer of interaction and complexity is required to force changes in the ribosome. This additional step would need to be able to provide for a specific translational pattern in order to result in a specific differential gene expression that would accommodate the cell's needs in response to the stressor. In contrast, a heterogeneous population of ribosomes model presents an alternate solution for regulating translation patterns without (or bypassing) the extra layer of complexity. The heterogeneous ribosome model provides a reductionist mechanism to fit (accommodate) the cell's translational needs in order to maintain/ensure essential cellular functions to promote optimal adaptability in response to environmental stimuli. The heterogeneous ribosome model also provides an additional mechanism for epigenetics, where external factors may influence gene expression, for "increased genetic adaptability" beyond the rate of natural selection/evolution, promoting beneficial inheritable genetic traits. Ribosomal protein gene haploinsufficiency has been shown to induce the p53 pathway, a response reserved for ribosomal and cellular stress. Diamond Blackfan Anemia patients with mutations of RPS19 and 5q- syndrome patients express increased activation of the p53 pathway in response to ribosomal dysfunction (238).

The idea of a heterogeneous population of ribosomes is consistent with the selective translating behavior of ‘specialized’ ribosomes. The heterogeneous ribosome model is similar to the viral quasispecies model, proposed by Eigen and Schuster (239). Eigen and Schuster determined that in an environment of high mutation rate and thermodynamic conditions far from equilibrium, the original self-replicating entity reaches a maximum reproductive fitness and this self-replicating entity was represented as a “clan” and not as a single molecule (239). This “clan” would consist of a distribution heterogeneous population of viruses and this distribution was then referred as “quasispecies”. This theory links Darwinian evolution and chemical thermodynamics and kinetics. In the context of chemical thermodynamics and kinetics, viral genomes that are thermodynamically cheaper would always exist and accumulate in greater number relative to those that are more thermodynamically expensive. This creates a “thermodynamic” selective pressure. This is akin to Darwinian selective pressure that, in a non-equilibrium scenario involving self-reproduction, mutation and degradation of the viral genome, will select certain genotypes and regulate the abundance of viral particles. Only viral variants nearest to the optimal fitness are capable of surviving this selective process. According to the quasispecies model, selection is based on the competition between phenotypes (in response or adaptation to environmental conditions) or the ability to produce progenies.

We developed a new model for ribosomes, the ribosomal quasispecies model. In this model, we propose that ribosomes exists in a distribution of

heterogeneous variants. Cellular chemical thermodynamics and kinetics dictates the presence of a habitable zone. There exists a need for a minimum and maximum in the accuracy and speed of translation, e.g. K_D of tRNAs an K_{cat} of protein formation, to maintain cellular homeostasis (Figure 32). A even distribution of ribosomes that exists within these boundaries serve as a buffering zone; a system of checks and balances where each ribosomal variant will translate each message uniquely in respect to elements that can destabilize the message. Some ribosomes will be redirected by the recoding element and lead to a premature termination codon and initiate the NMD-dependent pathway. Other ribosomes may not be redirected by the same recoding element and the message will remain intact for another round of translation. This allows the transcriptome to maintain homeostasis, to exist between a minimum for cellular survival and a maximum before deleterious effects occur. The ribosomal assembly is dictated by thermodynamic cost. Thus in non-equilibrium scenarios, e.g. development of precursor red blood cells into adult red blood cells or in cell stress conditions, the distribution of ribosomal variants shifts to those that are thermodynamically essential to maintain cellular homeostasis (Figure 32). Ribosomopathies by haploinsufficiency of ribosomal protein eliminates this subset of ribosomal variant and forces the distribution of ribosomes to beyond the boundaries of the habitable zone (Figure 32). Those that exist within the habitable zone exhibit translational patterns unique to non-equilibrium cellular conditions such as cellular/tissue differentiation or a stress response. Diamond Blackfan

Anemia, 5q- syndrome and ICA are all ribosomopathies that may exhibit ribosomal distributions that are synonymous with tissue development defects.

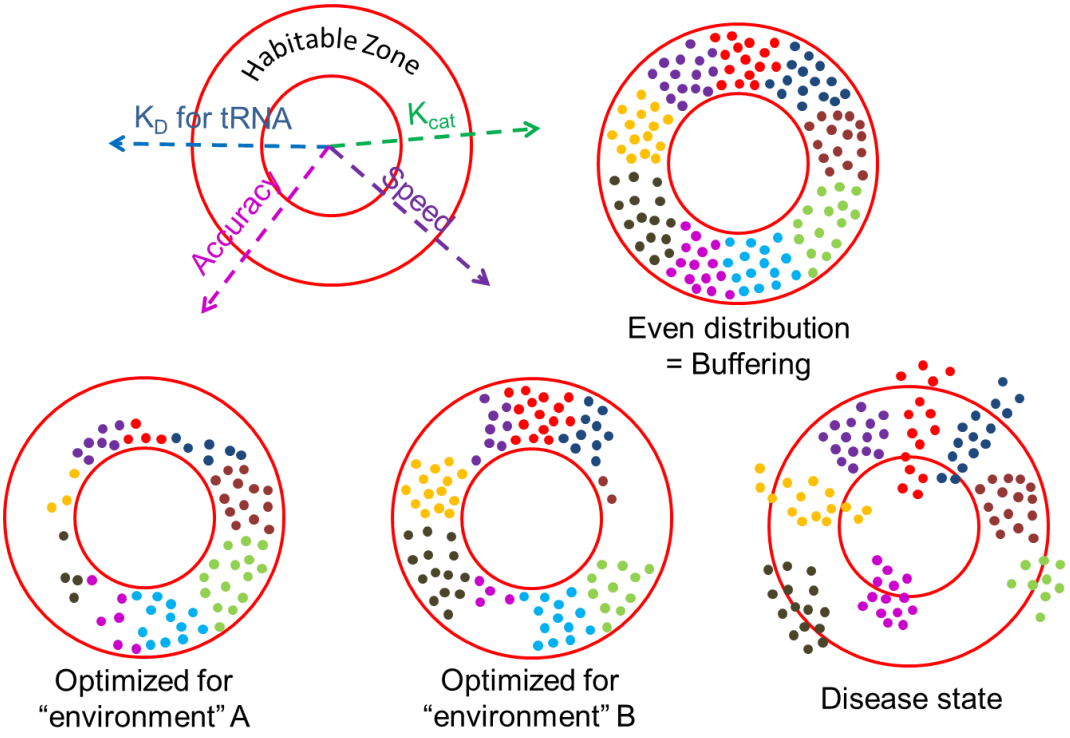

Figure 32: The ribosome quasispecies model and implications.
All cells at equilibrium contain a habitable zone, a range in which ribosomes must translate in order to maintain cellular homeostasis. The variety of ribosomes and their inherent idiosyncratic translating properties generate a buffering zone that ensures optimal cellular functions. In scenarios where an even distribution of ribosomes is thermodynamically costly, only the essential ribosomal variants are produced and are able to maintain homeostasis. Ribosomopathies, a diseased state, forces these ribosomes variants exist and translate outside the habitable zone and their subtle translational defects accumulate to present the corresponding phenotype.

There are two challenges that need to be overcome for further studies. First, how to biochemically isolate a “specialized” ribosome and test its activity and second, how to resolve individual ribosomes from homogenous ribosomes. The means to study of an individual ribosome are currently unknown, however, probing for ribosomal variation within a population is possible. Deep sequencing of ribosomal RNA in wild-type isogenic embryonic

stem cells and patient cells to distinguish post-transcriptional modification patterns at each stage of tissue development for “hits” at sites known to be modified is a potential method to identify heterogeneity of ribosomes. While it does not identify or isolate individual ribosomes, ribosomes may exhibit differential post-transcriptional modification patterns (via pseudo-uridylation/methylation) at different stages of cellular/tissue differentiation. This may provide a means to recognize the influences in translational patterns that heterogeneously composed ribosomes have in cellular functions/differentiation.

This paradigm shift in understanding ribosomes offers a fresh insight into the mechanistic nature of ribosomes under duress by internal or external factors.

Chapter 4: Materials and Methods

Experimental Procedures

Dual Luciferase Assays

Dual luciferase assays were performed using a Turner Biosystems GloMax-Multi Microplate Multimode Reader and Dual Luciferase Reagent Kit from Promega. Data analysis were performed as described in ***(240)***.

The dual luciferase reporter plasmids pYDL-control, pYDL-LA, pYDL-CDC13, pYDL-EST1, pYDL-EST2, pYDL-STN1, pYDL-OAZ1, pYDL-Ty*1*, pYDL-GCN4, pYDL-UAA , pYDL-UAG, pYDL-UGA, and pYDL-AGC_{218} and pYDL-TCT_{218} were employed to quantitatively monitor programmed -1 ribosomal frameshifting, programmed +1 ribosomal frameshifting, suppression of UAA, UGA, UAG codons, and suppression of an AGC near-cognate serine codon and a TCT non-cognate serine codon in place of the cognate AGA codon in the firefly luciferase catalytic site, respectively (241, 242).

The reporters were expressed from high-copy *URA3*-based plasmids (pJD375, pJD376, pJD1803, pJD1019, pJD1039, pJD1041, pJD1943, pJD377, pJD1982, pJD1983, pJD431, pJD432, pJD433, pJD642, pJD643 respectively) Assays were performed as previously described (240).

Yeast cells were grown to mid-log phase before analysis. The cells were lysed using glass beads in a PBS buffered lysis solution containing a protease inhibitor cocktail. The lysates were diluted to a 1:2 – 1:10 ratio;

dilutions were depending on the cell culture volume. The lysates were then aliquoted in an initial volume of 50 µl (as compared to suggested 100 µl) into each well of the 96 well plates and each Renilla and Firefly luciferase substrates were measured in the luminometer. All assays were repeated at least 4 times.

Quantitative Real Time Reverse Transcriptase Polymerase Chain Reaction (qRT-PCR)

Yeast cells were grown to mid-log phase and RNA samples were isolated using Trizol Reagent protocol DNAse digestion was performed using the RNA Microaqueous kit from Ambion (Life Technologies). The RNA samples were then assayed for contamination using RNAse-free agarose gel electrophoresis and $OD_{260/280}$ measurements. The pure RNA samples were reverse transcribed to generate cDNA by using the iScript cDNA synthesis kit from Bio-Rad. cDNA was diluted 1:100 – 1:10,000 depending the RNA concentration. Reactions were performed using the iTaq Universal SYBR green mix from Bio-Rad. Reactions were amplified using the Bio-Rad CFX 96 thermocycler as follows: 25˚C for 10 seconds, 95˚C for 5 min, followed by 45-60 cycles of 95˚C for 10 seconds, 48˚C for 15 seconds, and 72˚C for 15 seconds. Melting curves were monitored by taking readings every 0.5˚C from 55-95˚C. U3 snoRNA was used as loading control.

Transformations

Bacterial Transformations

Transformations using the bacterial strain DH5α were performed as described in (243).

Yeast Transformations

Yeast strains were transformed using modified alkali cation method as described in (244). Yeast cells were grown in mid-log phase in YPAD or the appropriate selective media. Transformations were performed using 0.1 M LiOAc/TE and excess (400 µl) PEG/LiOAc/TE buffers. Approximately double amount of ssDNA was used. The sample were incubated at 30°C for 30-90 minutes (approximately double time recommended incubation time). The cells were heat shocked at 42°C for 15 minutes before spinning the samples down, removing the supernatant and resuspending the pellet in approximately 60-100 µl nuclease-free water solution. The resulting solution were then spread onto petri dishes containing the appropriate selective media.

Statistical Analysis

Student's t test for two-tailed *p*-value calculations was used throughout. Data analysis of dual-luciferase assays was carried out as described (240).

Appendix 1: Yeast Strains Used

Strain number	Phenotype	Purpose
yJD1158	BY4742 MATα his3Δ1 leu2Δ0 lys2Δ0 ura3Δ0	WT strain for steady states assays and frameshifting
yJD1573	MAT α his3-1; leu2-0; lys2-0; ura3-0; YGR214W::KanR	rpS0A deletion
yJD1574	MAT α his3-1; leu2-0; lys2-0; ura3-0; YLR048W::KanR	rpS0B deletion
yJD1575	MAT α his3-1; leu2-0; lys2-0; ura3-0; YCR031C::KanR	rpS14A deletion
yJD1577	MAT α his3-1; leu2-0; lys2-0; ura3-0; YOL121C::KanR	rpS19A deletion
yJD1578	MAT α his3-1; leu2-0; lys2-0; ura3-0; YNL302C::KanR	rpS19B deletion
yJD1589	MAT a his3-1; leu2-0; lys2-0; met15-0; ura3-0; YJL191W::G418R	rpS14B deletion

Obtaining Knock Out Yeast Strains

Gene knockout yeast strains were purchased from Invitrogen's *Saccharomyces* Genome Deletion Project. Targeted gene knockouts were verified via PCR amplification.

Appendix 2: Yeast based plasmids

Plasmid Number	Backbone Plasmid	Description/Purpose
pJD0375	pRS316	Dual luciferase cassette in pRS316, genomic context
pJD0376	pJD375	LA frameshift signal sequence inserted in dual luciferase reporter, viral context
pJD0377	pJD375	Tyl frameshift signal sequence inserted in dual luciferase reporter, viral context
pJD0431	pJD375	In-frame UAA stop codon sequence inserted downstream of Renilla in dual luciferase reporter
pJD0432	pJD375	In-frame UAG stop codon sequence inserted downstream of Renilla in dual luciferase reporter
pJD0433	pJD375	In-frame UGA stop codon sequence inserted downstream of Renilla in dual luciferase reporter
pJD0521	pJD375	EST2 PRF sequence at 1653 inserted in dual luciferase reporter, viral context
pJD0642	pJD375	In-frame non-cognate TCT R218S mutation in firefly sequence of dual luciferase reporter
pJD0643	pJD375	In-frame near-cognate AGC R218S mutation in firefly sequence of dual luciferase reporter
pJD0753	pJD0741	Readthrough containing small amounts of Renilla and Firefly in PGK1 reporter
pJD0828	pJD753	Premature termination codon in PGK1 reporter
pJD1018	pJD375	EST2 PRF sequence at 1215 inserted in dual luciferase reporter, viral context
pJD1019	pJD375	EST2 PRF sequence at 1326 inserted in dual luciferase reporter, viral context
pJD1038	pJD375	STN1 PRF sequence at 885 inserted in dual luciferase reporter, viral context
pJD1039	pJD375	STN1 PRF sequence at 1203 inserted in dual luciferase reporter, viral context
pJD1041	pJD375	EST1 PRF sequence at 1272 inserted in dual luciferase reporter, viral context
pJD1803	pJD375	CDC13 PRF sequence at 1272 inserted in dual luciferase reporter, viral context
pJD1943	pJD375	OAZ1 PRF signal inserted in dual luciferase reporter, viral context
pJD1982	pJD375	In-frame GCN4 readthrough control sequence in dual luciferase reporter
pJD1983	pJD375	In-frame GCN4 uORF sequence inserted in dual luciferase reporter

Appendix 3: Oligos used for qPCR

Name	Template	Sequence
yEST2 Fwd	Yeast cDNA	5'-TGG TCG GTA CAT ACG CAT TC-3'
yEST2 Rev	Yeast cDNA	5'-CGG CAG ATG AGG TTC GTT AC-3'
yEST1 Fwd	Yeast cDNA	5'-ATT CCG TGA TAC CAT TGG TTC-3'
yEST1 Rev	Yeast cDNA	5'-CTT TCT TCT GTT ACT TAG TCG CA-3'
ySTN1 Fwd	Yeast cDNA	5'-ACA GCA AAT ACA CCT TAT TGG C-3'
ySTN1 Rev	Yeast cDNA	5'-ACC AAT GAA GAG TCT GAA GTA CA-3'
yCDC13 Fwd	Yeast cDNA	5'-TGG TAA GTG TGA TAA GCA CC-3'
yCDC13 Rev	Yeast cDNA	5'-AGA TAT CCA CAA GTG AGT TGT-3'
yPGK1-DLR Rev	Exogenous PGK1	5'-GTT CGT TGA GCG AGT TCT CA-3'
yPGK1-DLR Fwd	Exogenous PGK1	5'-GGT ACC GGC GTC TTC CAT-3'
U3 Forward	Yeast cDNA	5'-TCC AAC TTG GTT GAT GAG TCC-3'
U3 Reverse	Yeast cDNA	5'-CGA ACC GCT AAG GAT TGC-3'
yCCR4 Fwd	Yeast cDNA	5'-AGC AAT CTC ACA TTG CAG AAG C-3'
yCCR4 Rev	Yeast cDNA	5'-CGT AGG TTG TTG TTT CTT TGC T-3'
yGCN4 Fwd	Yeast cDNA	5'-ACA TTC CAG TTA CCA CTG ACG ATG T-3'
yGCN4 Rev	Yeast cDNA	5'-GGG TAA GAA TGA AGT TGT CGA GAC TTC-3'
yTel Fwd	Yeast gDNA	5'-CAGTGGTGTGGG TGT GCATGGTGGTGTGGGTGTGTGG-3'
yTel Rev	Yeast gDNA	5'-GCCCACAACCACACCCAACACATCCCACACCACCCAC-3'
yHOM3 Fwd	Yeast cDNA	5'-CTA AAC CTG ACG GCC CAA AC-3'
yHOM3 Rev	Yeast cDNA	5'-GAA ATT CAG ATT CTT GCG AAG C-3'
yADE4 Fwd	Yeast cDNA	5'-ATT AGC AAA CCA AAC CAC TCC AG-3'
yADE4 Rev	Yeast cDNA	5'-CGT CAC GAG CCA TAC CAT TAC-3'
yLUC7 Fwd	Yeast cDNA	5'-ACG CAA ACT CGT CGA ACA G-3'
yLUC7 Rev	Yeast cDNA	5'-GCA CTC GCC AAC AAG GTA TG-3'
yBRR6 Fwd	Yeast cDNA	5'-CTA GAC AGC CTG ATG GCA TAC-3'
yBRR6 Rev	Yeast cDNA	5'-GCA ATT AAA CTT GGG CTC AAC C-3'
yPRP8 Fwd	Yeast cDNA	5'-TTG AAG AGG ACA GCG ACT TAG-3'
yPRP8 Rev	Yeast cDNA	5'-GTG GAG GCG GAA GGA ATG TAT C-3'
yACT1 Fwd	Yeast cDNA	5'-GGT TGC TGC TTT GGT TAT TG-3'
yACT1 Rev	Yeast cDNA	5'-TTT GAC CCA TAC CGA CCA TGA TAC-3'
yTUB1 Fwd	Yeast cDNA	5'-GCT GGT TGT CAG ATT GGT AAT G-3'
yTUB1 Rev	Yeast cDNA	5'-GAA ACC CTC TTC TCC TCC CTT CG-3'
yRPS0 Fwd	Yeast cDNA	5'-GTT GTT GCC ATC TCT TCC AG-3'
yRPS0 Rev	Yeast cDNA	5'-GTG AAA GAA CCT GGA GTG AAT C-3'
yRPS14 Fwd	Yeast cDNA	5'-TGT TAC CGA TTT ATC TGG TAA GG-3'
yRPS14 Rev	Yeast cDNA	5'-TTA CAC TTA GCG GCA ACA TC-3'
yRPS19 Fwd	Yeast cDNA	5'-TGC TTA CGC TTC TTT CTT GC-3'
yRPS19 Rev	Yeast cDNA	5'-CGC TTG TAG AAC CAA CCT TC-3'

Chapter 5: Supplementary Data

Supplementary Table 1: Dual Luciferase Reporter Assay – Translational Recoding Rates

The following table presents Translational Fidelity efficiencies as calculated by the following formula:

$$\%\ \boldsymbol{Recoding} = \frac{\frac{\boldsymbol{Firefly_{exp}}}{\boldsymbol{Renilla_{exp}}}}{\frac{\boldsymbol{Firefly_{control}}}{\boldsymbol{Renilla_{control}}}}\ \boldsymbol{x\ 100}$$

This table contains dual luciferase translational efficiencies from 5 reporters that measure -1 PRF rates, 4 reporters that measure stop codon read through rates, 2 reporters that measure missense incorporation rates and 1 reporters that measure +1 PRF rates.

	WT	**S0AΔ**	**S0BΔ**	**S14AΔ**	**S14BΔ**	**S19AΔ**	**S19BΔ**
-1 PRF							
LA	6.98% ± 0.29%	9.53% ± 0.94%	7.32% ± 0.67%	7.11% ± 0.58%	9.34% ± 0.88%	7.61% ± 0.71%	10.98% ± 0.87%
CDC13	1.80% ± 0.09%	3.09% ± 0.38%	1.09% ± 0.10%	0.84% ± 0.05%	2.09% ± 0.78%	1.62% ± 0.13%	1.83% ± 0.08%
EST1	0.22% ± 0.01%	0.27% ± 0.02%	0.25% ± 0.01%	0.81% ± 0.10%	0.49% ± 0.09%	0.17% ± 0.01%	0.36% ± 0.03%
EST2	1.62% ± 0.06%	1.58% ± 0.08%	1.53% ± 0.13%	0.95% ± 0.08%	1.78% ± 0.06%	1.38% ± 0.08%	1.81% ± 0.17%
STN1	2.58% ± 0.14%	2.68% ± 0.26%	4.71% ± 0.48%	2.63% ± 0.14%	1.61% ± 0.23%	3.89% ± 0.42%	7.88% ± 0.43%
Stop Codon Readthrough							
GCN4	1.32% ± 0.18%	5.13% ± 0.58%	2.53% ± 0.63%	4.75% ± 1.22%	7.85% ± 1.92%	7.28% ± 1.08%	3.15% ± 0.39%
UAA	0.21% ± 0.01%	0.32% ± 0.04%	0.41% ± 0.04%	0.32% ± 0.02%	0.30% ± 0.03%	0.58% ± 0.05%	0.84% ± 0.06%
UAG	0.22% ± 0.01%	0.57% ± 0.06%	0.33% ± 0.03%	0.32% ± 0.02%	0.29% ± 0.03%	0.47% ± 0.04%	0.53% ± 0.03%
UGA	0.46% ± 0.02%	1.38% ± 0.12%	0.83% ± 0.06%	0.76% ± 0.09%	0.60% ± 0.07%	0.64% ± 0.14%	2.47% ± 0.23%
Missense Incorporation							
Non C	0.06% ± 0.004%	0.08% ± 0.002%	0.06% ± 0.002%	0.04% ± 0.001%	0.05% ± 0.001%	0.11% ± 0.004%	0.06% ± 0.002%
Near C	0.14% ± 0.012%	0.18% ± 0.004%	0.13% ± 0.006%	0.13% ± 0.004%	0.14% ± 0.003%	0.15% ± 0.006%	0.26% ± 0.005%
+1 PRF							
OAZ1	0.23% ± 0.01%	0.51% ± 0.02%	0.39% ± 0.03%	0.21% ± 0.01%	0.21% ± 0.03%	0.23% ± 0.01%	0.26% ± 0.02%
Ty1	13.99% ± 0.80%	20.46% ± 1.80%	11.73% ± 1.29%	12.56% ± 1.44%	11.20% ± 0.97%	18.92% ± 1.23%	24.56% ± 2.77%

Supplementary Table 2: Dual Luciferase Reporter Assay, Fold Wild-type Translational Recoding Rates

This table presents the values obtained by comparing the translational recoding rates of the mutant yeast strains to that of the wild-type control strain. Fold wild-type is calculated by the following formula:

$$\frac{\%\ \boldsymbol{translational\ recoding\ rate_{mutant}}}{\%\ \boldsymbol{translational\ recoding\ rate_{wild-type}}}$$

	WT	S0AΔ	S0BΔ	S14AΔ	S14BΔ	S19AΔ	S19BΔ
-1 PRF							
LA	1.00	1.37	1.05	1.02	1.34	1.09	1.57
CDC13	1.00	1.71	0.60	0.46	1.16	0.90	1.02
EST1	1.00	1.20	1.10	3.65	2.21	0.77	1.61
EST2	1.00	0.97	0.94	0.58	1.09	0.85	1.12
STN1	1.00	1.04	1.83	1.02	0.62	1.51	3.06
Stop Codon Readthrough							
GCN4	1.00	3.89	1.92	3.60	5.94	5.52	2.39
UAA	1.00	1.55	1.99	1.53	1.47	2.82	4.06
UAG	1.00	2.58	1.49	1.46	1.32	2.14	2.37
UGA	1.00	3.03	1.82	1.66	1.32	1.41	5.41
Missense Incorporation							
Non C	1.00	1.41	0.96	0.64	0.87	1.87	1.04
Near C	1.00	1.29	0.95	0.94	1.02	1.05	1.83
+1 PRF							
OAZ1	1.00	2.20	1.68	0.88	0.91	0.99	1.11
Ty1	1.00	1.46	0.84	0.90	0.80	1.35	1.76

Supplementary Table 3: Number of biological samples used per Dual Luciferase assay

The table below contains the total number of biological samples used to obtain statistical values.

	WT	S0AΔ	S0BΔ	S14AΔ	S14BΔ	S19AΔ	S19BΔ
Control							
RT	53	22	20	17	14	29	19
-1 PRF							
LA	18	4	3	4	3	5	4
CDC13	18	6	4	3	3	4	3
EST1	16	4	3	5	3	4	5
EST2	21	3	3	5	3	6	6
STN1	20	4	4	3	4	5	4
Stop Codon Readthrough							
RT GCN4	14	4	5	4	4	10	10
GCN4	7	7	8	7	7	11	4
UAA	22	4	5	4	4	8	9
UAG	23	3	3	3	5	7	6
UGA	26	4	4	4	4	10	9
Missense Incorporation							
Non C	10	3	5	3	4	4	4
Near C	7	3	3	3	3	3	3
+1 PRF							
OAZ1	19	3	3	3	4	6	4
Ty1	11	4	4	4	4	4	5

	LA	CDC13	EST1	EST2	STN1	GCN4	UAA	UAG	UGA	Non Cognate	Near Cognate	OAZ1	Ty1
S0AΔ	4.90E-02	7.30E-03	1.58E-01	8.06E-01	7.67E-01	2.99E-06	2.03E-02	2.00E-03	7.67E-05	6.21E-02	7.65E-02	1.76E-04	1.83E-02
S0BΔ	7.72E-01	6.57E-04	5.35E-01	6.95E-01	9.51E-03	5.30E-02	1.52E-03	5.96E-02	4.70E-03	7.88E-01	7.74E-01	2.70E-02	2.76E-01
S0AΔ	**	***	ns	ns	ns	***	**	***	***	ns	ns	***	**
S0BΔ	ns	***	ns	ns	***	ns	***	ns	***	ns	ns	**	ns
S14AΔ	8.71E-01	5.64E-09	2.41E-04	7.99E-06	8.69E-01	5.05E-03	6.31E-03	1.96E-02	1.43E-02	2.43E-03	7.16E-01	2.83E-01	4.70E-01
S14BΔ	5.17E-02	7.29E-01	1.83E-02	2.68E-01	3.37E-03	1.86E-03	1.91E-02	4.26E-02	9.19E-02	3.17E-01	9.15E-01	4.86E-01	7.66E-02
S14AΔ	ns	***	***	***	ns	***	***	**	**	***	ns	ns	ns
S14BΔ	ns	ns	**	ns	***	***	**	**	ns	ns	ns	ns	ns
S19AΔ	5.35E-01	4.33E-01	5.46E-02	1.12E-01	2.90E-02	3.91E-06	1.69E-06	5.03E-05	5.31E-01	2.43E-02	8.04E-01	9.41E-01	5.18E-02
S19BΔ	6.67E-03	8.97E-01	4.81E-03	3.80E-01	1.09E-05	6.46E-03	1.22E-09	4.01E-06	2.47E-08	8.25E-01	1.67E-02	3.94E-01	5.88E-03
S19AΔ	ns	ns	ns	ns	**	***	***	***	ns	**	ns	ns	ns
S19BΔ	***	ns	***	ns	***	***	***	***	***	ns	**	ns	***

Supplementary Table 4: Dual Luciferase Reporter Assay – Translational Recoding calculated p-values

p-values in this table were calculated as described (240). Each reporter of the dual luciferase assays measuring translational recoding rates is presented in two forms; the numerical p-value and the asterisk system denoting its corresponding p-value. The relationship between the numerical value and the asterisks are shown in the legend below

P > 0.05	P ≤ 0.05	P ≤ 0.01	P ≤ 0.001	P ≤ 0.0001
Not significant (ns)	*	**	***	****

Supplementary Table 5: quantitative Real Time PCR – Steady state mRNA abundance Fold Wild-type

Steady state mRNA abundances were measured by qualitative Real Time PCR. The mRNA abundances of each probe was normalized to U3, a stable non-coding RNA message. The abundance of the probe in a mutant yeast strain is the compared to the abundance of the same message in the wild-type control yeast strain. The calculations can be visualized by the following formula:

$$\frac{\left(\frac{abundance\ of\ target\ message}{abundance\ of\ U3\ message}\right)_{mutant}}{\left(\frac{abundance\ of\ target\ message}{abundance\ of\ U3\ message}\right)_{wild-type\ control}}$$

The table below contains steady state mRNA abundances fold wild-type for messages that contain a -1 PRF signal, a message that contains multiple uORFs (GCN4), messages that contains a +1 PRF signal, messages that are substrates for mRNA decay, messages that encode for housekeeping proteins, messages that encode for ribosomal proteins and, messages that are regulated during cellular stress and/or increased ribosomal turnover.

	WT	S0AΔ	S0BΔ	S14AΔ	S14BΔ	S19AΔ	S19BΔ
-1 PRF							
CDC13	1.00	2.45 ± 0.42	2.31 ± 0.30	3.82 ± 0.78	5.57 ± 0.57	0.40 ± 0.16	0.16 ± 0.06
EST1	1.00	0.46 ± 0.04	0.43 ± 0.08	0.77 ± 0.21	1.16 ± 0.21	0.62 ± 0.22	0.22 ± 0.06
EST2	1.00	0.48 ± 0.08	0.47 ± 0.09	0.80 ± 0.11	0.98 ± 0.28	0.51 ± 0.15	0.17 ± 0.06
STN1	1.00	0.36 ± 0.06	0.39 ± 0.07	0.58 ± 0.10	0.72 ± 0.25	0.48 ± 0.17	0.20 ± 0.07
+1 PRF							
EST3	1.00	0.22 ± 0.04	0.19 ± 0.01	0.35 ± 0.05	0.43 ± 0.19	0.74 ± 0.08	0.25 ± 0.05
OAZ1	1.00	0.48 ± 0.05	0.54 ± 0.08	0.69 ± 0.20	0.99 ± 0.31	0.41 ± 0.15	0.13 ± 0.04
Substrates for NMD							
GCN4	1.00	0.24 ± 0.06	0.23 ± 0.07	0.32 ± 0.07	0.38 ± 0.11	0.60 ± 0.21	0.27 ± 0.07
CPA1	1.00	0.31 ± 0.08	0.43 ± 0.001	0.48 ± 0.03	0.87 ± 0.22	0.58 ± 0.004	0.16 ± 0.02
NMD4	1.00	0.30 ± 0.10	0.35 ± 0.08	0.46 ± 0.05	0.57 ± 0.19	0.49 ± 0.10	0.19 ± 0.02
Housekeeping genes							
ACT1	1.00	0.57 ± 0.07	0.41 ± 0.09	0.96 ± 0.23	0.72 ± 0.24	0.52 ± 0.01	0.41 ± 0.01
BRR6	1.00	0.51 ± 0.05	0.50 ± 0.07	0.60 ± 0.12	0.66 ± 0.10	0.58 ± 0.02	0.27 ± 0.08
HOM3	1.00	0.43 ± 0.11	0.67 ± 0.29	0.68 ± 0.12	1.44 ± 0.21	0.53 ± 0.03	0.22 ± 0.06
PGK1	1.00	0.22 ± 0.03	0.17 ± 0.06	0.50 ± 0.02	0.84 ± 0.04	0.37 ± 0.16	0.26 ± 0.06
TUB1	1.00	1.34 ± 0.20	1.02 ± 0.13	2.64 ± 0.25	3.18 ± 1.36	0.49 ± 0.11	0.23 ± 0.01
Ribosomal Proteins							
S0	1.00	0.20 ± 0.02	0.15 ± 0.02	0.46 ± 0.07	0.52 ± 0.16	0.82 ± 0.07	0.42 ± 0.03
S14	1.00	0.26 ± 0.05	0.22 ± 0.01	0.22 ± 0.04	0.36 ± 0.10	0.75 ± 0.04	0.37 ± 0.01
S19	1.00	0.26 ± 0.03	0.21 ± 0.03	0.36 ± 0.06	0.35 ± 0.10	0.73 ± 0.02	0.02 ± 0.004
Cellular Stress/Ribosomal Turnover							
ADE4	1.00	3.81 ± 0.86	2.38 ± 0.29	7.79 ± 2.06	7.42 ± 1.61	0.50 ± 0.18	0.19 ± 0.02
CCR4	1.00	4.84 ± 1.17	4.19 ± 0.70	5.47 ± 0.78	6.49 ± 1.02	0.50 ± 0.03	0.12 ± 0.02
HAC1	1.00	1.11 ± 0.18	1.45 ± 0.24	1.81 ± 0.43	1.86 ± 0.65	0.33 ± 0.06	0.12 ± 0.001
LUC7	1.00	0.92 ± 0.18	0.83 ± 0.04	1.22 ± 0.16	1.57 ± 0.34	0.41 ± 0.07	0.17 ± 0.04
PRP8	1.00	4.15 ± 0.25	3.69 ± 0.21	7.32 ± 1.74	8.02 ± 2.35	0.26 ± 0.10	0.13 ± 0.06

Supplementary Table 6: Number of biological samples used per quantitative Real Time PCR assay

The table below contains the total number of biological samples used to obtain statistical values.

Student's t-test	S0AΔ	S0BΔ	S14AΔ	S14BΔ	S19AΔ	S19BΔ
-1 PRF						
CDC13	3	3	3	3	4	3
EST1	3	3	3	3	4	3
EST2	5	4	4	3	5	4
STN1	3	3	5	3	4	3
+1 PRF						
EST3	3	3	3	3	4	3
OAZ1	3	4	5	3	3	3
Substrates for NMD						
GCN4	3	3	3	3	5	3
CPA1	3	3	3	3	3	3
NMD4	3	3	3	3	4	3
Housekeeping genes						
ACT1	4	5	5	3	3	3
BRR6	3	3	3	3	3	3
HOM3	4	3	3	3	3	3
PGK1	3	3	3	3	3	3
TUB1	4	4	4	3	5	3
Ribosomal Proteins						
S0	3	3	3	3	5	4
S14	3	3	3	3	4	4
S19	3	3	3	3	5	4
Cellular Stress Ribosomal Turnover						
ADE4	4	4	4	3	3	3
CCR4	3	3	3	2	3	3
HAC1	3	3	3	3	3	3
LUC7	4	3	3	3	3	3
PRP8	4	3	3	4	3	3

Supplementary Table 7: quantitative Real Time PCR – Steady state mRNA abundance Student's t-test calculations

The table below contains the calculated probabilities associated with a Student's t-Test.

Student's t-test	S0AΔ	S0BΔ	S14AΔ	S14BΔ	S19AΔ	S19BΔ
-1 PRF						
CDC13	1.34E-02	8.53E-03	1.23E-02	2.53E-03	1.16E-02	9.44E-04
EST1	9.25E-04	3.01E-03	7.58E-04	1.56E-01	4.63E-02	9.21E-04
EST2	3.77E-03	4.47E-03	4.26E-02	4.47E-01	1.49E-02	9.23E-04
STN1	1.55E-03	2.39E-03	1.01E-02	3.08E-03	1.62E-02	1.38E-03
+1 PRF						
EST3	4.67E-04	3.02E-05	9.22E-04	1.75E-02	5.42E-02	7.23E-04
OAZ1	1.42E-03	5.15E-03	5.90E-02	1.46E-02	1.02E-02	4.27E-04
Substrates for NMD						
GCN4	9.09E-04	1.49E-03	1.86E-03	5.44E-03	4.10E-02	1.55E-03
CPA1	2.34E-03	1.04E-06	6.44E-04	2.14E-01	1.68E-05	1.09E-04
NMD4	3.24E-03	2.46E-03	1.40E-03	2.93E-02	8.48E-03	6.61E-05
Housekeeping genes						
ACT1	6.22E-04	5.77E-05	3.64E-01	9.01E-02	9.91E-05	7.81E-05
BRR6	6.47E-04	3.64E-03	3.14E-03	2.22E-03	2.88E-04	1.87E-03
HOM3	9.03E-04	9.50E-02	6.02E-03	3.39E-02	5.82E-04	9.72E-04
PGK1	3.07E-04	9.26E-04	2.65E-04	1.48E-03	1.05E-02	1.10E-03
TUB1	2.13E-02	3.64E-01	2.68E-03	5.43E-02	2.15E-04	4.37E-05
Ribosomal Proteins						
S0	9.24E-05	8.61E-05	2.48E-03	1.70E-02	2.34E-02	1.01E-04
S14	8.91E-04	9.39E-06	4.64E-04	3.71E-03	4.98E-03	3.45E-05
S19	2.11E-04	2.83E-04	1.42E-03	3.67E-03	7.93E-04	1.29E-08
Cellular Stress Ribosomal Turnover						
ADE4	3.69E-03	1.27E-03	3.56E-03	9.00E-04	1.96E-02	9.52E-05
CCR4	1.49E-02	7.79E-03	5.06E-03	5.64E-03	4.29E-04	6.19E-05
HAC1	2.01E-01	4.25E-02	3.17E-02	7.42E-02	1.13E-03	9.47E-04
LUC7	3.33E-01	1.08E-02	3.65E-02	2.20E-02	2.10E-03	4.65E-04
PRP8	6.64E-05	1.01E-03	2.68E-03	4.72E-03	2.77E-03	7.90E-04

Bibliography

1. Planta RJ, Mager WH (1998) The list of cytoplasmic ribosomal proteins of Saccharomyces cerevisiae. *Yeast Chichester Engl* 14(5):471–477.

2. Ben-Shem A, Jenner L, Yusupova G, Yusupov M (2010) Crystal Structure of the Eukaryotic Ribosome. *Science* 330(6008):1203 –1209.

3. Giegé R, Sissler M, Florentz C (1998) Universal rules and idiosyncratic features in tRNA identity. *Nucleic Acids Res* 26(22):5017–5035.

4. Noller HF (2005) RNA Structure: Reading the Ribosome. *Science* 309(5740):1508–1514.

5. Moore PB (1999) Structural motifs in RNA. *Annu Rev Biochem* 68:287–300.

6. Schulze H, Nierhaus KH (1982) Minimal set of ribosomal components for reconstitution of the peptidyltransferase activity. *EMBO J* 1(5):609–613.

7. Wilson DN, Nierhaus KH (2005) Ribosomal proteins in the spotlight. *Crit Rev Biochem Mol Biol* 40(5):243–267.

8. DeLano WL (2002) The PyMOL molecular graphics system.

9. Ben-Shem A, et al. (2011) The Structure of the Eukaryotic Ribosome at 3.0 Å Resolution. *Science*. doi:10.1126/science.1212642.

10. Griffiths-Jones S, et al. (2005) Rfam: annotating non-coding RNAs in complete genomes. *Nucleic Acids Res* 33(Database issue):D121–124.

11. Warner JR (1999) The economics of ribosome biosynthesis in yeast. *Trends Biochem Sci* 24(11):437–440.

12. Kressler D, Hurt E, Baβler J (2010) Driving ribosome assembly. *Biochim Biophys Acta BBA - Mol Cell Res* 1803(6):673–683.

13. Fromont-Racine M, Senger B, Saveanu C, Fasiolo F (2003) Ribosome assembly in eukaryotes. *Gene* 313:17–42.

14. Kressler D, Linder P, de La Cruz J (1999) Protein trans-acting factors involved in ribosome biogenesis in Saccharomyces cerevisiae. *Mol Cell Biol* 19(12):7897–7912.

15. Mélèse T, Xue Z (1995) The nucleolus: an organelle formed by the act of building a ribosome. *Curr Opin Cell Biol* 7(3):319–324.

16. Scheer U, Hock R (1999) Structure and function of the nucleolus. *Curr Opin Cell Biol* 11(3):385–390.

17. Decatur WA, Fournier MJ (2002) rRNA modifications and ribosome function. *Trends Biochem Sci* 27(7):344–351.

18. Woolford JL, Baserga SJ (2013) Ribosome biogenesis in the yeast Saccharomyces cerevisiae. *Genetics* 195(3):643–681.

19. Warner JR, Mitra G, Schwindinger WF, Studeny M, Fried HM (1985) Saccharomyces cerevisiae coordinates accumulation of yeast ribosomal proteins by modulating mRNA splicing, translational initiation, and protein turnover. *Mol Cell Biol* 5(6):1512–1521.

20. Xue S, Barna M (2012) Specialized ribosomes: a new frontier in gene regulation and organismal biology. *Nat Rev Mol Cell Biol* 13(6):355–369.

21. Zaher HS, Green R (2009) Fidelity at the Molecular Level: Lessons from Protein Synthesis. *Cell* 136(4):746–762.

22. Sonenberg N, Hinnebusch AG (2009) Regulation of translation initiation in eukaryotes: mechanisms and biological targets. *Cell* 136(4):731–745.

23. Rabl J, Leibundgut M, Ataide SF, Haag A, Ban N (2011) Crystal Structure of the Eukaryotic 40S Ribosomal Subunit in Complex with Initiation Factor 1. *Science* 331(6018):730 –736.

24. Asano K, Clayton J, Shalev A, Hinnebusch AG (2000) A multifactor complex of eukaryotic initiation factors, eIF1, eIF2, eIF3, eIF5, and initiator tRNA(Met) is an important translation initiation intermediate in vivo. *Genes Dev* 14(19):2534–2546.

25. Gingras AC, Raught B, Sonenberg N (1999) eIF4 initiation factors: effectors of mRNA recruitment to ribosomes and regulators of translation. *Annu Rev Biochem* 68:913–963.

26. Hinnebusch AG (2014) The scanning mechanism of eukaryotic translation initiation. *Annu Rev Biochem* 83:779–812.

27. Boeke JD, Garfinkel DJ, Styles CA, Fink GR (1985) Ty elements transpose through an RNA intermediate. *Cell* 40(3):491–500.

28. Belcourt MF, Farabaugh PJ (1990) Ribosomal frameshifting in the yeast retrotransposon Ty: tRNAs induce slippage on a 7 nucleotide minimal site. *Cell* 62(2):339–352.

29. Kawakami K, et al. (1993) A rare tRNA-Arg(CCU) that regulates Ty1 element ribosomal frameshifting is essential for Ty1 retrotransposition in Saccharomyces cerevisiae. *Genetics* 135(2):309–320.

30. Hinnebusch AG (2011) Molecular mechanism of scanning and start codon selection in eukaryotes. *Microbiol Mol Biol Rev MMBR* 75(3):434–467, first page of table of contents.

31. Dias A, et al. (2009) The cap-snatching endonuclease of influenza virus polymerase resides in the PA subunit. *Nature* 458(7240):914–918.

32. Goodfellow I, et al. (2000) Identification of a cis-acting replication element within the poliovirus coding region. *J Virol* 74(10):4590–4600.

33. Flanegan JB, Petterson RF, Ambros V, Hewlett NJ, Baltimore D (1977) Covalent linkage of a protein to a defined nucleotide sequence at the 5'-terminus of virion and replicative intermediate RNAs of poliovirus. *Proc Natl Acad Sci U S A* 74(3):961–965.

34. Thompson SR (2012) Tricks an IRES uses to enslave ribosomes. *Trends Microbiol* 20(11):558–566.

35. Costantino DA, Pfingsten JS, Rambo RP, Kieft JS (2008) tRNA-mRNA mimicry drives translation initiation from a viral IRES. *Nat Struct Mol Biol* 15(1):57–64.

36. Thompson SR, Gulyas KD, Sarnow P (2001) Internal initiation in Saccharomyces cerevisiae mediated by an initiator tRNA/eIF2-independent internal ribosome entry site element. *Proc Natl Acad Sci U S A* 98(23):12972–12977.

37. Hellen CU, Sarnow P (2001) Internal ribosome entry sites in eukaryotic mRNA molecules. *Genes Dev* 15(13):1593–1612.

38. López-Lastra M, Rivas A, Barría MI (2005) Protein synthesis in eukaryotes: the growing biological relevance of cap-independent translation initiation. *Biol Res* 38(2-3):121–146.

39. Thakor N, Holcik M (2012) IRES-mediated translation of cellular messenger RNA operates in eIF2α- independent manner during stress. *Nucleic Acids Res* 40(2):541–552.

40. Rodnina MV, Wintermeyer W (2001) Fidelity of aminoacyl-tRNA selection on the ribosome: kinetic and structural mechanisms. *Annu Rev Biochem* 70:415–435.

41. Rodnina MV, Gromadski KB, Kothe U, Wieden H-J (2005) Recognition and selection of tRNA in translation. *FEBS Lett* 579(4):938–942.

42. Valle M, et al. (2002) Cryo-EM reveals an active role for aminoacyl-tRNA in the accommodation process. *EMBO J* 21(13):3557–3567.

43. Ogle JM, et al. (2001) Recognition of cognate transfer RNA by the 30S ribosomal subunit. *Science* 292(5518):897–902.

44. Schmeing TM, Ramakrishnan V (2009) What recent ribosome structures have revealed about the mechanism of translation. *Nature* 461(7268):1234–42.

45. Schuette J-C, et al. (2009) GTPase activation of elongation factor EF-Tu by the ribosome during decoding. *EMBO J* 28(6):755–765.

46. Pape T, Wintermeyer W, Rodnina MV (1998) Complete kinetic mechanism of elongation factor Tu-dependent binding of aminoacyl-tRNA to the A site of the E. coli ribosome. *EMBO J* 17(24):7490–7497.

47. Rodnina MV (2009) Long-range signalling in activation of the translational GTPase EF-Tu. *EMBO J* 28(6):619–620.

48. Gromadski KB, Daviter T, Rodnina MV (2006) A uniform response to mismatches in codon-anticodon complexes ensures ribosomal fidelity. *Mol Cell* 21(3):369–377.

49. Gromadski KB, Rodnina MV (2004) Kinetic determinants of high-fidelity tRNA discrimination on the ribosome. *Mol Cell* 13(2):191–200.

50. Mittelstaet J, Konevega AL, Rodnina MV (2011) Distortion of tRNA upon Near-cognate Codon Recognition on the Ribosome. *J Biol Chem* 286(10):8158 –8164.

51. Demeshkina N, Jenner L, Westhof E, Yusupov M, Yusupova G (2012) A new understanding of the decoding principle on the ribosome. *Nature* 484(7393):256–259.

52. Ogle JM, Ramakrishnan V (2005) Structural insights into translational fidelity. *Annu Rev Biochem* 74:129–177.

53. Pape T, Wintermeyer W, Rodnina M (1999) Induced fit in initial selection and proofreading of aminoacyl-tRNA on the ribosome. *EMBO J* 18(13):3800–3807.

54. Schmeing TM, Huang KS, Strobel SA, Steitz TA (2005) An induced-fit mechanism to promote peptide bond formation and exclude hydrolysis of peptidyl-tRNA. *Nature* 438(7067):520–524.

55. Sievers A, Beringer M, Rodnina MV, Wolfenden R (2004) The ribosome as an entropy trap. *Proc Natl Acad Sci U S A* 101(21):7897–7901.

56. Trobro S, Aqvist J (2005) Mechanism of peptide bond synthesis on the ribosome. *Proc Natl Acad Sci U S A* 102(35):12395–12400.

57. Rodnina MV, Beringer M, Wintermeyer W (2007) How ribosomes make peptide bonds. *Trends Biochem Sci* 32(1):20–26.

58. Zavialov AV, Mora L, Buckingham RH, Ehrenberg M (2002) Release of peptide promoted by the GGQ motif of class 1 release factors regulates the GTPase activity of RF3. *Mol Cell* 10(4):789–798.

59. Frolova LY, et al. (1999) Mutations in the highly conserved GGQ motif of class 1 polypeptide release factors abolish ability of human eRF1 to trigger peptidyl-tRNA hydrolysis. *RNA N Y N* 5(8):1014–1020.

60. Seit-Nebi A, Frolova L, Justesen J, Kisselev L (2001) Class-1 translation termination factors: invariant GGQ minidomain is essential for release activity and ribosome binding but not for stop codon recognition. *Nucleic Acids Res* 29(19):3982–3987.

61. Valle M, et al. (2003) Locking and Unlocking of Ribosomal Motions. *Cell* 114(1):123–134.

62. Agirrezabala X, Frank J (2009) Elongation in translation as a dynamic interaction among the ribosome, tRNA, and elongation factors EF-G and EF-Tu. *Q Rev Biophys* 42(3):159–200.

63. Spahn CM, et al. (2004) Domain movements of elongation factor eEF2 and the eukaryotic 80S ribosome facilitate tRNA translocation. *EMBO J* 23(5):1008–1019.

64. Frank J, Gao H, Sengupta J, Gao N, Taylor DJ (2007) The process of mRNA–tRNA translocation. *Proc Natl Acad Sci* 104(50):19671 –19678.

65. Noller HF, Yusupov MM, Yusupova GZ, Baucom A, Cate J (2002) Translocation of tRNA during protein synthesis. *FEBS Lett* 514(1):11–16.

66. Frank J, Agrawal RK (2000) A ratchet-like inter-subunit reorganization of the ribosome during translocation. *Nature* 406(6793):318–322.

67. Taylor DJ, et al. (2009) Comprehensive Molecular Structure of the Eukaryotic Ribosome. *Structure* 17(12):1591–1604.

68. Zhang W, Dunkle JA, Cate JHD (2009) Structures of the Ribosome in Intermediate States of Ratcheting. *Science* 325(5943):1014 –1017.

69. Dunkle JA, et al. (2011) Structures of the bacterial ribosome in classical and hybrid states of tRNA binding. *Science* 332(6032):981–984.

70. Kisselev LL, Buckingham RH (2000) Translational termination comes of age. *Trends Biochem Sci* 25(11):561–566.

71. Song H, et al. (2000) The crystal structure of human eukaryotic release factor eRF1--mechanism of stop codon recognition and peptidyl-tRNA hydrolysis. *Cell* 100(3):311–321.

72. Zhouravleva G, et al. (1995) Termination of translation in eukaryotes is governed by two interacting polypeptide chain release factors, eRF1 and eRF3. *EMBO J* 14(16):4065–4072.

73. Frolova LY, Merkulova TI, Kisselev LL (2000) Translation termination in eukaryotes: polypeptide release factor eRF1 is composed of functionally and structurally distinct domains. *RNA N Y N* 6(3):381–390.

74. Merkulova TI, Frolova LY, Lazar M, Camonis J, Kisselev LL (1999) C-terminal domains of human translation termination factors eRF1 and eRF3 mediate their in vivo interaction. *FEBS Lett* 443(1):41–47.

75. Mora L, et al. (2003) The essential role of the invariant GGQ motif in the function and stability in vivo of bacterial release factors RF1 and RF2. *Mol Microbiol* 47(1):267–275.

76. Nakamura Y, Ito K (2011) tRNA mimicry in translation termination and beyond. *Wiley Interdiscip Rev RNA* 2(5):647–668.

77. Pisarev AV, et al. (2010) The role of ABCE1 in eukaryotic posttermination ribosomal recycling. *Mol Cell* 37(2):196–210.

78. Eyler DE, Green R (2011) Distinct response of yeast ribosomes to a miscoding event during translation. *RNA*. doi:10.1261/rna.2623711.

79. Dinman JD (2006) Programmed Ribosomal Frameshifting Goes Beyond Viruses: Organisms from all three kingdoms use frameshifting to regulate gene expression, perhaps signaling a paradigm shift. *Microbe Wash DC* 1(11):521–527.

80. Jacks T, Varmus HE (1985) Expression of the Rous sarcoma virus pol gene by ribosomal frameshifting. *Science* 230(4731):1237–1242.

81. Firth AE, Chung BY, Fleeton MN, Atkins JF (2008) Discovery of frameshifting in Alphavirus 6K resolves a 20-year enigma. *Virol J* 5:108.

82. Lewis TL, Matsui SM (1997) Studies of the astrovirus signal that induces (-1) ribosomal frameshifting. *Adv Exp Med Biol* 412:323–330.

83. Marra MA, et al. (2003) The Genome Sequence of the SARS-Associated Coronavirus. *Science* 300(5624):1399–1404.

84. Plant EP, Rakauskaite R, Taylor DR, Dinman JD (2010) Achieving a golden mean: mechanisms by which coronaviruses ensure synthesis of the correct stoichiometric ratios of viral proteins. *J Virol* 84(9):4330–4340.

85. Bekaert M, et al. (2010) Recode-2: new design, new search tools, and many more genes. *Nucleic Acids Res* 38(Database issue):D69–D74.

86. Brierley I, Digard P, Inglis SC (1989) Characterization of an efficient coronavirus ribosomal frameshifting signal: requirement for an RNA pseudoknot. *Cell* 57(4):537–547.

87. Harger JW, Meskauskas A, Dinman JD (2002) An "integrated model" of programmed ribosomal frameshifting. *Trends Biochem Sci* 27(9):448–454.

88. Lopinski JD, Dinman JD, Bruenn JA (2000) Kinetics of ribosomal pausing during programmed -1 translational frameshifting. *Mol Cell Biol* 20(4):1095–1103.

89. Plant EP, et al. (2003) The 9-A solution: how mRNA pseudoknots promote efficient programmed -1 ribosomal frameshifting. *RNA N Y N* 9(2):168–174.

90. Brierley I, Jenner AJ, Inglis SC (1992) Mutational analysis of the "slippery-sequence" component of a coronavirus ribosomal frameshifting signal. *J Mol Biol* 227(2):463–479.

91. Dinman JD (2012) Mechanisms and implications of programmed translational frameshifting. *Wiley Interdiscip Rev RNA* 3(5):661–673.

92. Jacks T, Madhani HD, Masiarz FR, Varmus HE (1988) Signals for ribosomal frameshifting in the Rous sarcoma virus gag-pol region. *Cell* 55(3):447–458.

93. Marczinke B, Hagervall T, Brierley I (2000) The Q-base of asparaginyl-tRNA is dispensable for efficient -1 ribosomal frameshifting in eukaryotes. *J Mol Biol* 295(2):179–191.

94. Dulude D, Baril M, Brakier-Gingras L (2002) Characterization of the frameshift stimulatory signal controlling a programmed -1 ribosomal frameshift in the human immunodeficiency virus type 1. *Nucleic Acids Res* 30(23):5094–5102.

95. Farabaugh PJ (2000) Translational frameshifting: implications for the mechanism of translational frame maintenance. *Prog Nucleic Acid Res Mol Biol* 64:131–170.

96. Cho C-P, Lin S-C, Chou M-Y, Hsu H-T, Chang K-Y (2013) Regulation of programmed ribosomal frameshifting by co-translational refolding RNA hairpins. *PloS One* 8(4):e62283.

97. Liao P-Y, Choi YS, Dinman JD, Lee KH (2011) The many paths to frameshifting: kinetic modelling and analysis of the effects of different elongation steps on programmed -1 ribosomal frameshifting. *Nucleic Acids Res* 39(1):300–312.

98. Belew AT, Dinman JD (2015) Cell cycle control (and more) by programmed −1 ribosomal frameshifting: implications for disease and therapeutics. *Cell Cycle* 14(2):172–178.

99. Dinman JD, Wickner RB (1992) Ribosomal frameshifting efficiency and gag/gag-pol ratio are critical for yeast M1 double-stranded RNA virus propagation. *J Virol* 66(6):3669–3676.

100. Advani VM, Belew AT, Dinman JD (2013) Yeast telomere maintenance is globally controlled by programmed ribosomal frameshifting and the nonsense-mediated mRNA decay pathway. *Translation* 1(1):e24418.

101. Belew AT, Hepler NL, Jacobs JL, Dinman JD (2008) PRFdb: a database of computationally predicted eukaryotic programmed -1 ribosomal frameshift signals. *BMC Genomics* 9:339.

102. Jacobs JL, Belew AT, Rakauskaite R, Dinman JD (2007) Identification of functional, endogenous programmed -1 ribosomal frameshift signals in the genome of Saccharomyces cerevisiae. *Nucleic Acids Res* 35(1):165–174.

103. Manktelow E, Shigemoto K, Brierley I (2005) Characterization of the frameshift signal of Edr, a mammalian example of programmed -1 ribosomal frameshifting. *Nucleic Acids Res* 33(5):1553–1563.

104. Wills NM, Moore B, Hammer A, Gesteland RF, Atkins JF (2006) A functional -1 ribosomal frameshift signal in the human paraneoplastic Ma3 gene. *J Biol Chem* 281(11):7082–7088.

105. Plant EP, Wang P, Jacobs JL, Dinman JD (2004) A programmed -1 ribosomal frameshift signal can function as a cis-acting mRNA destabilizing element. *Nucleic Acids Res* 32(2):784–790.

106. Belew AT, Advani VM, Dinman JD (2011) Endogenous ribosomal frameshift signals operate as mRNA destabilizing elements through at least two molecular pathways in yeast. *Nucleic Acids Res* 39(7):2799–2808.

107. Craigen WJ, Caskey CT (1986) Expression of peptide chain release factor 2 requires high-efficiency frameshift. *Nature* 322(6076):273–275.

108. Matsufuji S, et al. (1995) Autoregulatory frameshifting in decoding mammalian ornithine decarboxylase antizyme. *Cell* 80(1):51–60.

109. Farabaugh PJ, Zhao H, Vimaladithan A (1993) A novel programed frameshift expresses the POL3 gene of retrotransposon Ty3 of yeast: frameshifting without tRNA slippage. *Cell* 74(1):93–103.

110. Clare J, Farabaugh P (1985) Nucleotide sequence of a yeast Ty element: evidence for an unusual mechanism of gene expression. *Proc Natl Acad Sci U S A* 82(9):2829–2833.

111. Adamski FM, Donly BC, Tate WP (1993) Competition between frameshifting, termination and suppression at the frameshift site in the Escherichia coli release factor-2 mRNA. *Nucleic Acids Res* 21(22):5074–5078.

112. Morris DK, Lundblad V (1997) Programmed translational frameshifting in a gene required for yeast telomere replication. *Curr Biol CB* 7(12):969–976.

113. Namy O, Rousset J-P, Napthine S, Brierley I (2004) Reprogrammed genetic decoding in cellular gene expression. *Mol Cell* 13(2):157–168.

114. Pegg AE (1986) Recent advances in the biochemistry of polyamines in eukaryotes. *Biochem J* 234(2):249–262.

115. Ivanov IP, Matsufuji S, Murakami Y, Gesteland RF, Atkins JF (2000) Conservation of polyamine regulation by translational frameshifting from yeast to mammals. *EMBO J* 19(8):1907–1917.

116. Balasundaram D, Dinman JD, Tabor CW, Tabor H (1994) SPE1 and SPE2: two essential genes in the biosynthesis of polyamines that modulate +1 ribosomal frameshifting in Saccharomyces cerevisiae. *J Bacteriol* 176(22):7126–7128.

117. Beier H, Grimm M (2001) Misreading of termination codons in eukaryotes by natural nonsense suppressor tRNAs. *Nucleic Acids Res* 29(23):4767–4782.

118. Wills NM, Gesteland RF, Atkins JF (1991) Evidence that a downstream pseudoknot is required for translational read-through of the Moloney murine leukemia virus gag stop codon. *Proc Natl Acad Sci U S A* 88(16):6991–6995.

119. Yoshinaka Y, Katoh I, Copeland TD, Oroszlan S (1985) Murine leukemia virus protease is encoded by the gag-pol gene and is synthesized through suppression of an amber termination codon. *Proc Natl Acad Sci U S A* 82(6):1618–1622.

120. Hoffmann PR, Berry MJ (2005) Selenoprotein synthesis: a unique translational mechanism used by a diverse family of proteins. *Thyroid Off J Am Thyroid Assoc* 15(8):769–775.

121. Hatfield DL, Gladyshev VN (2002) How selenium has altered our understanding of the genetic code. *Mol Cell Biol* 22(11):3565–3576.

122. Tujebajeva RM, et al. (2000) Decoding apparatus for eukaryotic selenocysteine insertion. *EMBO Rep* 1(2):158–163.

123. Wills NM, Gesteland RF, Atkins JF (1994) Pseudoknot-dependent read-through of retroviral gag termination codons: importance of sequences in the spacer and loop 2. *EMBO J* 13(17):4137–44.

124. Alam SL, Wills NM, Ingram JA, Atkins JF, Gesteland RF (1999) Structural studies of the RNA pseudoknot required for readthrough of the gag-termination codon of murine leukemia virus. *J Mol Biol* 288(5):837–852.

125. Goff SP (2004) Retrovirus restriction factors. *Mol Cell* 16(6):849–59.

126. Eswarappa SM, et al. (2014) Programmed Translational Readthrough Generates Antiangiogenic VEGF-Ax. *Cell* 157(7):1605–1618.

127. Maquat LE (1995) When cells stop making sense: effects of nonsense codons on RNA metabolism in vertebrate cells. *RNA N Y N* 1(5):453–465.

128. Culbertson MR, Leeds PF (2003) Looking at mRNA decay pathways through the window of molecular evolution. *Curr Opin Genet Dev* 13(2):207–214.

129. Lykke-Andersen J (2001) mRNA quality control: Marking the message for life or death. *Curr Biol CB* 11(3):R88–91.

130. Hilleren P, Parker R (1999) Mechanisms of mRNA surveillance in eukaryotes. *Annu Rev Genet* 33:229–260.

131. Bühler M, Steiner S, Mohn F, Paillusson A, Mühlemann O (2006) EJC-independent degradation of nonsense immunoglobulin-mu mRNA depends on 3’ UTR length. *Nat Struct Mol Biol* 13(5):462–464.

132. Amrani N, et al. (2004) A faux 3’-UTR promotes aberrant termination and triggers nonsense-mediated mRNA decay. *Nature* 432(7013):112–118.

133. Hogg JR, Goff SP (2010) Upf1 senses 3’UTR length to potentiate mRNA decay. *Cell* 143(3):379–389.

134. Leeds P, Wood JM, Lee BS, Culbertson MR (1992) Gene products that promote mRNA turnover in Saccharomyces cerevisiae. *Mol Cell Biol* 12(5):2165–2177.

135. Czaplinski K, et al. (1998) The surveillance complex interacts with the translation release factors to enhance termination and degrade aberrant mRNAs. *Genes Dev* 12(11):1665–1677.

136. Min EE, Roy B, Amrani N, He F, Jacobson A (2013) Yeast Upf1 CH domain interacts with Rps26 of the 40S ribosomal subunit. *RNA N Y N* 19(8):1105–1115.

137. Celik A, Kervestin S, Jacobson A (2015) NMD: At the crossroads between translation termination and ribosome recycling. *Biochimie* 114:2–9.

138. Mitchell P, Tollervey D (2003) An NMD pathway in yeast involving accelerated deadenylation and exosome-mediated 3'-->5' degradation. *Mol Cell* 11(5):1405–1413.

139. Belew AT, et al. (2014) Ribosomal frameshifting in the CCR5 mRNA is regulated by miRNAs and the NMD pathway. *Nature* 512(7514):265–269.

140. Doma MK, Parker R (2006) Endonucleolytic cleavage of eukaryotic mRNAs with stalls in translation elongation. *Nature* 440(7083):561–564.

141. Tsuboi T, et al. (2012) Dom34:hbs1 plays a general role in quality-control systems by dissociation of a stalled ribosome at the 3' end of aberrant mRNA. *Mol Cell* 46(4):518–529.

142. Chen L, et al. (2010) Structure of the Dom34-Hbs1 complex and implications for no-go decay. *Nat Struct Mol Biol* 17(10):1233–+.

143. Van den Elzen AMG, et al. (2010) Dissection of Dom34-Hbs1 reveals independent functions in two RNA quality control pathways. *Nat Struct Mol Biol* 17(12):1446–U74.

144. Frischmeyer PA, et al. (2002) An mRNA surveillance mechanism that eliminates transcripts lacking termination codons. *Science* 295(5563):2258–2261.

145. Van Hoof A, Frischmeyer PA, Dietz HC, Parker R (2002) Exosome-mediated recognition and degradation of mRNAs lacking a termination codon. *Science* 295(5563):2262–2264.

146. Araki Y, et al. (2001) Ski7p G protein interacts with the exosome and the Ski complex for 3′-to-5′ mRNA decay in yeast. *EMBO J* 20(17):4684–4693.

147. Inada T, Aiba H (2005) Translation of aberrant mRNAs lacking a termination codon or with a shortened 3′-UTR is repressed after initiation in yeast. *EMBO J* 24(8):1584–1595.

148. Wilson MA, Meaux S, van Hoof A (2007) A genomic screen in yeast reveals novel aspects of nonstop mRNA metabolism. *Genetics* 177(2):773–784.

149. Nakhoul H, et al. (2014) Ribosomopathies: mechanisms of disease. *Clin Med Insights Blood Disord* 7:7–16.

150. Gilbert B, et al. (2002) Familial isolated congenital asplenia: a rare, frequently hereditary dominant condition, often detected too late as a cause of overwhelming pneumococcal sepsis. Report of a new case and review of 31 others. *Eur J Pediatr* 161(7):368–372.

151. Heiss NS, et al. (1998) X-linked dyskeratosis congenita is caused by mutations in a highly conserved gene with putative nucleolar functions. *Nat Genet* 19(1):32–38.

152. Léger-Silvestre I, et al. (2005) Specific Role for Yeast Homologs of the Diamond Blackfan Anemia-associated Rps19 Protein in Ribosome Synthesis. *J Biol Chem* 280(46):38177–38185.

153. Weischenfeldt J, et al. (2008) NMD is essential for hematopoietic stem and progenitor cells and for eliminating by-products of programmed DNA rearrangements. *Genes Dev* 22(10):1381–1396.

154. Karam R, Wilkinson M (2012) A conserved microRNA/NMD regulatory circuit controls gene expression. *RNA Biol* 9(1):22–26.

155. Dinman JD (2012) Control of gene expression by translational recoding. *Adv Protein Chem Struct Biol* 86:129–149.

156. Musalgaonkar S, Moomau CA, Dinman JD (2014) Ribosomes in the balance: structural equilibrium ensures translational fidelity and proper gene expression. *Nucleic Acids Res* 42(21):13384–13392.

157. Sulima SO, et al. (2014) Eukaryotic rpL10 drives ribosomal rotation. *Nucleic Acids Res* 42(3):2049–2063.

158. Rhodin MHJ, Rakauskaitė R, Dinman JD (2011) The central core region of yeast ribosomal protein L11 is important for subunit joining and translational fidelity. *Mol Genet Genomics*. doi:10.1007/s00438-011-0623-2.

159. Jack K, et al. (2011) rRNA Pseudouridylation Defects Affect Ribosomal Ligand Binding and Translational Fidelity from Yeast to Human Cells. *Mol Cell* 44(4):660–666.

160. Lindström MS (2009) Emerging functions of ribosomal proteins in gene-specific transcription and translation. *Biochem Biophys Res Commun* 379(2):167–170.

161. Ruggero D, Pandolfi PP (2003) Does the ribosome translate cancer? *Nat Rev Cancer* 3(3):179–192.

162. Vlachos A, et al. (2008) Diagnosing and treating Diamond Blackfan anaemia: results of an international clinical consensus conference. *Br J Haematol* 142(6):859–876.

163. Lipton JM, Atsidaftos E, Zyskind I, Vlachos A (2006) Improving clinical care and elucidating the pathophysiology of Diamond Blackfan anemia: an update from the Diamond Blackfan Anemia Registry. *Pediatr Blood Cancer* 46(5):558–564.

164. Janov AJ, Leong T, Nathan DG, Guinan EC (1996) Diamond-Blackfan anemia. Natural history and sequelae of treatment. *Medicine (Baltimore)* 75(2):77–78.

165. Lipton JM, et al. (2001) Osteogenic sarcoma associated with Diamond-Blackfan anemia: a report from the Diamond-Blackfan Anemia Registry. *J Pediatr Hematol Oncol* 23(1):39–44.

166. Draptchinskaia N, et al. (1999) The gene encoding ribosomal protein S19 is mutated in Diamond-Blackfan anaemia. *Nat Genet* 21(2):169–175.

167. Campagnoli MF, et al. (2008) RPS19 mutations in patients with Diamond-Blackfan anemia. *Hum Mutat* 29(7):911–920.

168. Willig TN, et al. (1999) Mutations in ribosomal protein S19 gene and diamond blackfan anemia: wide variations in phenotypic expression. *Blood* 94(12):4294–4306.

169. Doherty L, et al. (2010) Ribosomal protein genes RPS10 and RPS26 are commonly mutated in Diamond-Blackfan anemia. *Am J Hum Genet* 86(2):222–228.

170. Cmejla R, Cmejlova J, Handrkova H, Petrak J, Pospisilova D (2007) Ribosomal protein S17 gene (RPS17) is mutated in Diamond-Blackfan anemia. *Hum Mutat* 28(12):1178–1182.

171. Farrar JE, et al. (2008) Abnormalities of the large ribosomal subunit protein, Rpl35a, in Diamond-Blackfan anemia. *Blood* 112(5):1582–1592.

172. Gazda HT, et al. (2006) Ribosomal protein S24 gene is mutated in Diamond-Blackfan anemia. *Am J Hum Genet* 79(6):1110–1118.

173. Gazda HT, et al. (2008) Ribosomal protein L5 and L11 mutations are associated with cleft palate and abnormal thumbs in Diamond-Blackfan anemia patients. *Am J Hum Genet* 83(6):769–780.

174. Peng W-T, et al. (2003) A Panoramic View of Yeast Noncoding RNA Processing. *Cell* 113(7):919–933.

175. Gripp KW, et al. (2014) Diamond-Blackfan anemia with mandibulofacial dystostosis is heterogeneous, including the novel DBA genes TSR2 and RPS28. *Am J Med Genet A* 164A(9):2240–2249.

176. Caiulo A, et al. (1991) Mapping the gene encoding the human erythroid transcriptional factor NFE1-GF1 to Xp11.23. *Hum Genet* 86(4):388–390.

177. Hamaguchi I, et al. (2002) Gene transfer improves erythroid development in ribosomal protein S19-deficient Diamond-Blackfan anemia. *Blood* 100(8):2724–2731.

178. Jaako P, et al. (2014) Gene therapy cures the anemia and lethal bone marrow failure in a mouse model of RPS19-deficient Diamond-Blackfan anemia. *Haematologica* 99(12):1792–1798.

179. Liu JM, Ellis SR (2006) Ribosomes and marrow failure: coincidental association or molecular paradigm? *Blood* 107(12):4583–4588.

180. Ganapathi KA, Shimamura A (2008) Ribosomal dysfunction and inherited marrow failure. *Br J Haematol* 141(3):376–387.

181. Altschul SF, Gish W, Miller W, Myers EW, Lipman DJ (1990) Basic local alignment search tool. *J Mol Biol* 215(3):403–410.

182. Warner JR, Kumar A, Udem SA, Wu RS (1973) Ribosomal proteins and the assembly of ribosomes in eukaryotes. *Biochem Soc Symp* 37(0):3–22.

183. Fatica A, Tollervey D (2002) Making ribosomes. *Curr Opin Cell Biol* 14(3):313–318.

184. Chen W, Bucaria J, Band DA, Sutton A, Sternglanz R (2003) Enp1, a yeast protein associated with U3 and U14 snoRNAs, is required for pre-rRNA processing and 40S subunit synthesis. *Nucleic Acids Res* 31(2):690–699.

185. Gelperin D, Horton L, Beckman J, Hensold J, Lemmon SK (2001) Bms1p, a novel GTP-binding protein, and the related Tsr1p are required for distinct steps of 40S ribosome biogenesis in yeast. *RNA N Y N* 7(9):1268–1283.

186. Geerlings TH, Faber AW, Bister MD, Vos JC, Raué HA (2003) Rio2p, an evolutionarily conserved, low abundant protein kinase essential for processing of 20 S Pre-rRNA in Saccharomyces cerevisiae. *J Biol Chem* 278(25):22537–22545.

187. Choesmel V, et al. (2007) Impaired ribosome biogenesis in Diamond-Blackfan anemia. *Blood* 109(3):1275–1283.

188. Flygare J, et al. (2007) Human RPS19, the gene mutated in Diamond-Blackfan anemia, encodes a ribosomal protein required for the maturation of 40S ribosomal subunits. *Blood* 109(3):980–986.

189. Da Costa L, et al. (2003) Nucleolar localization of RPS19 protein in normal cells and mislocalization due to mutations in the nucleolar localization signals

in 2 Diamond-Blackfan anemia patients: potential insights into pathophysiology. *Blood* 101(12):5039–5045.

190. Angelini M, et al. (2007) Missense mutations associated with Diamond-Blackfan anemia affect the assembly of ribosomal protein S19 into the ribosome. *Hum Mol Genet* 16(14):1720–1727.

191. Chiocchetti A, et al. (2005) Interactions between RPS19, mutated in Diamond-Blackfan anemia, and the PIM-1 oncoprotein. *Haematologica* 90(11):1453–1462.

192. Mahlaoui N, et al. (2011) Isolated congenital asplenia: a French nationwide retrospective survey of 20 cases. *J Pediatr* 158(1):142–148, 148.e1.

193. Bolze A, et al. (2013) Ribosomal Protein SA Haploinsufficiency in Humans with Isolated Congenital Asplenia. *Science* 340(6135):976–978.

194. Shachor-Meyouhas Y, Sprecher H, Kassis I (2010) [Isolated congenital asplenia--a rare cause of severe pneumococcal sepsis]. *Harefuah* 149(8):486–489, 552.

195. Waldman JD, Rosenthal A, Smith AL, Shurin S, Nadas AS (1977) Sepsis and congenital asplenia. *J Pediatr* 90(4):555–559.

196. Brendolan A, Rosado MM, Carsetti R, Selleri L, Dear TN (2007) Development and function of the mammalian spleen. *Bioessays* 29(2):166–177.

197. Koss M, et al. (2012) Congenital Asplenia in Mice and Humans with Mutations in a Pbx/Nkx2-5/p15 Module. *Dev Cell* 22(5):913–926.

198. O'Donohue M-F, Choesmel V, Faubladier M, Fichant G, Gleizes P-E (2010) Functional dichotomy of ribosomal proteins during the synthesis of mammalian 40S ribosomal subunits. *J Cell Biol* 190(5):853–866.

199. Tabb-Massey A, et al. (2003) Ribosomal proteins Rps0 and Rps21 of Saccharomyces cerevisiae have overlapping functions in the maturation of the 3′ end of 18S rRNA. *Nucleic Acids Res* 31(23):6798–6805.

200. Ebert BL, et al. (2008) Identification of RPS14 as a 5q- syndrome gene by RNA interference screen. *Nature* 451(7176):335–339.

201. Ebert BL (2009) Deletion 5q in myelodysplastic syndrome: a paradigm for the study of hemizygous deletions in cancer. *Leukemia* 23(7):1252–1256.

202. Barlow JL, et al. (2010) A p53-dependent mechanism underlies macrocytic anemia in a mouse model of human 5q- syndrome. *Nat Med* 16(1):59–66.

203. Zhou X, Hao Q, Liao J, Zhang Q, Lu H (2013) Ribosomal protein S14 unties the MDM2-p53 loop upon ribosomal stress. *Oncogene* 32(3):388–396.

204. Zhou X, Hao Q, Liao J, Liao P, Lu H (2013) Ribosomal Protein S14 Negatively Regulates c-Myc Activity. *J Biol Chem* 288(30):21793–21801.

205. Ford CL, Randal-Whitis L, Ellis SR (1999) Yeast proteins related to the p40/laminin receptor precursor are required for 20S ribosomal RNA processing and the maturation of 40S ribosomal subunits. *Cancer Res* 59(3):704–710.

206. Jakovljevic J, et al. (2004) The carboxy-terminal extension of yeast ribosomal protein S14 is necessary for maturation of 43S preribosomes. *Mol Cell* 14(3):331–342.

207. Granneman S, Nandineni MR, Baserga SJ (2005) The putative NTPase Fap7 mediates cytoplasmic 20S pre-rRNA processing through a direct interaction with Rps14. *Mol Cell Biol* 25(23):10352–10364.

208. Ferreira-Cerca S, et al. (2007) Analysis of the in vivo assembly pathway of eukaryotic 40S ribosomal proteins. *Mol Cell* 28(3):446–457.

209. Soudet J, Gélugne J-P, Belhabich-Baumas K, Caizergues-Ferrer M, Mougin A (2010) Immature small ribosomal subunits can engage in translation initiation in Saccharomyces cerevisiae. *EMBO J* 29(1):80–92.

210. Wolfe KH, Shields DC (1997) Molecular evidence for an ancient duplication of the entire yeast genome. *Nature* 387(6634):708–713.

211. Dujon B, et al. (2004) Genome evolution in yeasts. *Nature* 430(6995):35–44.

212. Kellis M, Birren BW, Lander ES (2004) Proof and evolutionary analysis of ancient genome duplication in the yeast Saccharomyces cerevisiae. *Nature* 428(6983):617–624.

213. Ellenberger TE, Brandl CJ, Struhl K, Harrison SC (1992) The GCN4 basic region leucine zipper binds DNA as a dimer of uninterrupted alpha helices: crystal structure of the protein-DNA complex. *Cell* 71(7):1223–1237.

214. Hekman KE, et al. (2012) A conserved eEF2 coding variant in SCA26 leads to loss of translational fidelity and increased susceptibility to proteostatic insult. *Hum Mol Genet* 21(26):5472–5483.

215. Stansfield I, et al. (1995) The products of the SUP45 (eRF1) and SUP35 genes interact to mediate translation termination in Saccharomyces cerevisiae. *EMBO J* 14(17):4365–4373.

216. Keeling KM, et al. (2004) Leaky termination at premature stop codons antagonizes nonsense-mediated mRNA decay in S. cerevisiae. *RNA N Y N* 10(4):691–703.

217. Piérard A, Messenguy F, Feller A, Hilger F (1979) Dual regulation of the synthesis of the arginine pathway carbamoylphosphate synthase of Saccharomyces cerevisiae by specific and general controls of amino acid biosynthesis. *Mol Gen Genet MGG* 174(2):163–171.

218. He F, Jacobson A (1995) Identification of a novel component of the nonsense-mediated mRNA decay pathway by use of an interacting protein screen. *Genes Dev* 9(4):437–454.

219. Thireos G, Penn MD, Greer H (1984) 5’ untranslated sequences are required for the translational control of a yeast regulatory gene. *Proc Natl Acad Sci U S A* 81(16):5096–5100.

220. Guan Q, et al. (2006) Impact of Nonsense-Mediated mRNA Decay on the Global Expression Profile of Budding Yeast. *PLoS Genet* 2(11):e203.

221. Gaba A, Jacobson A, Sachs MS (2005) Ribosome occupancy of the yeast CPA1 upstream open reading frame termination codon modulates nonsense-mediated mRNA decay. *Mol Cell* 20(3):449–460.

222. Sun X, et al. (2001) Nonsense-mediated Decay of mRNA for the Selenoprotein Phospholipid Hydroperoxide Glutathione Peroxidase Is Detectable in Cultured Cells but Masked or Inhibited in Rat Tissues. *Mol Biol Cell* 12(4):1009–1017.

223. Dominguez R, Holmes KC (2011) Actin Structure and Function. *Annu Rev Biophys* 40(1):169–186.

224. De Bruyn Kops A, Guthrie C (2001) An essential nuclear envelope integral membrane protein, Brr6p, required for nuclear transport. *EMBO J* 20(15):4183–4193.

225. Rafalski JA, Falco SC (1990) Structure of the yeast HOM3 gene which encodes aspartokinase. *J Biol Chem* 265(25):15346.

226. Blake CC, Rice DW (1981) Phosphoglycerate kinase. *Philos Trans R Soc Lond B Biol Sci* 293(1063):93–104.

227. Schatz PJ, Pillus L, Grisafi P, Solomon F, Botstein D (1986) Two functional alpha-tubulin genes of the yeast Saccharomyces cerevisiae encode divergent proteins. *Mol Cell Biol* 6(11):3711–3721.

228. Woods RA, Roberts DG, Friedman T, Jolly D, Filpula D (1983) Hypoxanthine: guanine phosphoribosyltransferase mutants in Saccharomyces cerevisiae. *Mol Gen Genet MGG* 191(3):407–412.

229. Tucker M, et al. (2001) The transcription factor associated Ccr4 and Caf1 proteins are components of the major cytoplasmic mRNA deadenylase in Saccharomyces cerevisiae. *Cell* 104(3):377–386.

230. Guydosh NR, Green R (2014) Dom34 Rescues Ribosomes in 3´ Untranslated Regions. *Cell* 156(5):950–962.

231. Puig O, Bragado-Nilsson E, Koski T, Séraphin B (2007) The U1 snRNP-associated factor Luc7p affects 5' splice site selection in yeast and human. *Nucleic Acids Res* 35(17):5874–5885.

232. Fortes P, et al. (1999) Luc7p, a novel yeast U1 snRNP protein with a role in 5' splice site recognition. *Genes Dev* 13(18):2425–2438.

233. Umen JG, Guthrie C (1995) The second catalytic step of pre-mRNA splicing. *RNA N Y N* 1(9):869–885.

234. Stevens SW, Abelson J (1999) Purification of the yeast U4/U6.U5 small nuclear ribonucleoprotein particle and identification of its proteins. *Proc Natl Acad Sci U S A* 96(13):7226–7231.

235. Li X, et al. (2013) Comprehensive in vivo RNA-binding site analyses reveal a role of Prp8 in spliceosomal assembly. *Nucleic Acids Res* 41(6):3805–3818.

236. Atkins JF, Gesteland RF eds. (2010) *Recoding: Expansion of Decoding Rules Enriches Gene Expression* Available at: http://link.springer.com/book/10.1007%2F978-0-387-89382-2.

237. Lou CH, et al. (2014) Posttranscriptional Control of the Stem Cell and Neurogenic Programs by the Nonsense-Mediated RNA Decay Pathway. *Cell Rep* 6(4):748–764.

238. Dutt S, et al. (2011) Haploinsufficiency for ribosomal protein genes causes selective activation of p53 in human erythroid progenitor cells. *Blood* 117(9):2567–2576.

239. Eigen M, Schuster P (1977) The hypercycle. A principle of natural self-organization. Part A: Emergence of the hypercycle. *Naturwissenschaften* 64(11):541–565.

240. Jacobs JL, Dinman JD (2004) Systematic analysis of bicistronic reporter assay data. *Nucleic Acids Res* 32(20):e160.

241. HARGER JW, DINMAN JD (2003) An in vivo dual-luciferase assay system for studying translational recoding in the yeast Saccharomyces cerevisiae. *RNA* 9(8):1019 –1024.

242. Plant EP, et al. (2007) Differentiating between Near- and Non-Cognate Codons in Saccharomyces cerevisiae. *PLoS ONE* 2(6):e517.

243. Sambrook J, Russell DW (2001) *Molecular cloning: a laboratory manual* (Cold spring harbor laboratory press, Cold Spring Harbor, NY).

244. Ito H, Fukuda Y, Murata K, Kimura A (1983) Transformation of intact yeast cells treated with alkali cations. *J Bacteriol* 153(1):163–168.